

An Intelligent Algorithm for Smart Grid Protection Applications

PROEFSCHRIFT

ter verkrijging van de graad van doctor
aan de Technische Universiteit Delft,
op gezag van de Rector Magnificus, Prof. ir. K.C.A.M. Luyben,
voorzitter van het College voor Promoties,
in het openbaar te verdedigen op dinsdag 8 november 2011 om 10.00 uur
door

Ioanna XYNGI

Elektrotechnisch en Computer Ingenieur, Universiteit van Patras, Griekenland

geboren te Athene, Griekenland

Dit proefschrift is goedgekeurd door de promotor:

Prof. ir. L. van der Sluis

Samenstelling promotiecomissie:

Rector Magnificus, voorzitter

Prof. ir. L. van der Sluis, Technische Universiteit Delft, promotor

Dr. dipl.-ing. M. Popov, Technische Universiteit Delft, copromotor

Prof. ir. M.A.M.M. van der Meijden, Technische Universiteit Delft

Prof. dr. M. Zeman, Technische Universiteit Delft

Prof. dr. ir. J.G. Slootweg, Technische Universiteit Eindhoven

Prof. dr. V. Terzija, The University of Manchester

Dr. ir. O. Mansour, Locamation

Prof. dr. ir. J. J. Smit, reservelid, Technische Universiteit Delft

Dit onderzoek werd uitgevoerd in het kader van het onderzoeksprogramma “Innovatiegerichte Onderzoeksprogramma’s – Elektromagnetische Vermogenstechiek” (IOP-EMVT), dat financieel wordt ondersteund door SenterNovem, een agentschap van het Nederlandse Ministerie van Economische Zaken.

Printed by: Wöhrmann Print Service, Zutphen, the Netherlands

ISBN 978-94-6186-014-9

Copyright © 2011 by I. Xyngi

All rights reserved.

No part of the material protected by this copyright notice may be reproduced or utilized in any form or by any means, electronic or mechanical, including photocopying, recording or by any information storage and retrieval system, without permission from the publisher or authors.

“ Πάσα τε επιστήμη χωριζομένη δικαιοσύνης και της άλλης αρετής πανουργία, ου σοφία φαίνεται. ”

ΠΛΑΤΩΝΑΣ (Μενέξενος)

Summary

An Intelligent Algorithm for Smart Grid Protection Applications

Future distribution networks may include a massive penetration of distributed generation integrated in Medium Voltage grids. This future scenario will inevitably lead to a gradual transition from passive to active distribution networks. The integration of distributed generation changes totally the present-time well consolidated picture of passive distribution networks featuring unidirectional power flows. The incorporation of DG-units can significantly influence the power flow, the voltage profile and the operation of protection schemes in distribution grids. In this dissertation, an existing typical Dutch underground-cable distribution network has been investigated. The following aspects are addressed:

- the exploration of the issues driving the requirement for future fast and smart protection schemes,
- the demonstration of how recent technological advances revolutionize conventional protection strategies and permit the real implementation of fully centralized or distributed communication-aided protection schemes,
- the design and development of a protection strategy which can be applied on any arbitrary DG-supplied distribution grid. The innovative protection philosophy should guarantee the protection selectivity and enhance the DG during-fault availability.
- the application of the novel concept of a smart protection algorithm on an existing Dutch distribution network.

The influence of DG on protection of MV grids is analyzed and the needs as well as the arguments of migration towards intelligent protection strategies are addressed and justified. Therefore, the performance of conventional definite and inverse-time protection schemes are evaluated for an existing Dutch distribution grid for two different DG penetration levels. In this way the problems faced by the current applied protection strategies are identified and the issues which dictate a modification in protection logic of future protection schemes are well determined. The discrete-time dynamic simulation results validate the inadequacy of traditional time-graded protection schemes to offer a satisfactory level of protection selectivity. The observed protective device malfunctions verify the fact that a required modification will be needed in the future protection logic. There is a need to increase the availability of the DG-units during the fault, assure the selectivity if the protection scheme and speed up its performance. Moreover, enhanced fault ride-through requirements are

extracted for each different type of DG-unit. A unique fault ride-through specification is determined for each specific type of DG-unit. The derived fault ride-through requirements are compared to typically used undervoltage protection settings.

This thesis illustrates the transition from traditional protection strategies to future intelligent distribution grid protection schemes. It demonstrates how the universal adoption of numerical relays, the emergence of new standard communications protocols (IEC61850) and the unprecedented advances in sensor and communication technologies stimulate a whole new wave of innovation in the protection scheme landscape of DG-supplied distribution grids. These recent technological advances permit the migration from today's strictly local-information-based protection to innovative smart communications-assisted integrated or distributed protection schemes. Furthermore, details of the novel peer-to-peer communication mechanisms, included in IEC61850, which permit the implementation of high-speed protection schemes, are discussed. The merits of fully-centralized protection schemes, in contradiction to distributed protection strategies, are enumerated. Such intelligent protection strategies are fast, flexible and guarantee a high level of protection selectivity.

In the thesis, a novel concept of a smart protection strategy is designed and developed. The strategy is intended for any arbitrary DG-supplied distribution grid. The goal of the proposed smart protection scheme is to minimize the fault clearing time, ensure the protection selectivity and increase the availability of the DG-units during the fault. Two different arrangements of the underlying hardware and communication infrastructure architectures, which accommodate the smart protection strategy, are thoroughly explained. The flowcharts of both generalized protection algorithms are provided.

The novel fully-centralized communication-based protection algorithm is applied on a typical Dutch distribution grid. The real-time hardware implementation of the protection scheme that makes use of advanced sensor and microprocessor technology and a communication infrastructure is illustrated. The proper performance and selectivity of the proposed protection scheme is validated by means of discrete-time dynamic simulations through various scenario cases. The proposed intelligent algorithm assures the protection selectivity, by minimizing the fault clearing time and eliminating the problem of massive disconnection of DG-units in the network.

Samenvatting

Een Intelligent Algoritme met Toepassing in Smartgridbeveiliging

Elektriciteitsdistributienetten zullen in de toekomst een groot aandeel gedistribueerde opwekkers bevatten. Dit werkt een geleidelijke maar onvermijdelijke transitie van passieve naar actieve distributienetten in de hand. Het veelvuldig toegepaste passieve distributienetontwerp, waarbij de richting van vermogensstromen eenduidig is (en vooraf bekend), is tegen die veranderingen slecht bestand. Gedistribueerde opwekkers hebben een aanzienlijke invloed op vermogensstromen en spanningsprofielen, en compliceren daardoor de toepassing van de voor zulke distributienetten alom toegepaste beveiligingsconcepten. In dit proefschrift staat de beveiliging van een voor Nederland gebruikelijk distributienet met ondergrondse kabelverbindingen centraal, en wordt de invloed van gedistribueerde opwekkers aan de hand van de volgende stappen onderzocht:

- Verkennen van de noodzaken voor snellere en intelligentere beveiligingsconcepten in het distributienet van de toekomst;
- aantonen van de invloed van recente technologische ontwikkelingen op beveiligingsfilosofieën en hoe deze nieuwe, gecentraliseerde en gedistribueerde, door communicatiemiddelen ondersteunde, beveiligingen mogelijk maken;
- ontwikkelen van een beveiligingsconcept voor distributienetten met een grote hoeveelheid gedistribueerde opwekkers, onafhankelijk van de netstructuur, dat selectiviteit garandeert en de beschikbaarheid van gedistribueerde opwekkers tijdens fouten in het net verbetert; en
- toepassen van het ontwikkelde concept op een distributienetwerk zoals dat voorkomt in Nederland.

Dit proefschrift begint met een analyse hoe gedistribueerde opwekkers de bestaande beveiligingen in middenspanningsnetten beïnvloeden en onderbouwt een transitie naar intelligentere beveiligingsconcepten. Daartoe wordt het gedrag van de vaak toegepaste tijdsafhankelijke en tijdsafhankelijke maximaalstroomtijdbeveiliging beschouwd voor twee scenario's met gedistribueerde opwekkers in het middenspanningsnet. Dit voorbeeld maakt niet alleen problemen met de huidige netbeveiligingen inzichtelijk, maar geeft ook duidelijk richting aan de wijze waarop deze kunnen worden verbeterd. Traditionele, tijdstaffelde beveiligingsmethodes zijn onvoldoende toereikend bij aanwezigheid van gedistribueerde opwekkers. De onderliggende beveiligingslogica moet worden gewijzigd om een betrouwbare beveiliging te garanderen. Simulaties in het tijddomein maken

duidelijk dat conventionele netbeveiligingen niet langer voldoen en dat de onderliggende logica moet worden verbeterd en uitgebreid. De mogelijkheid van gedistribueerde opwekkers om tijdens kortsluitingen aan het net te blijven en dit net te ondersteunen moet niet door de beveiliging worden ingeperkt. Echter, dit mag niet ten koste gaan van de selectiviteit en de snelheid van de beveiliging. Het proefschrift beschrijft een nieuwe methode om deze *fault-ride through*-mogelijkheden toe te passen.

Het proefschrift richt zich op de overgang van traditionele beveiligingsconcepten naar concepten met meer intelligentie, en is toegespitst op distributienetwerken. De alomtegenwoordigheid van numerieke beveiligingsrelais, het standaardiseren van communicatieprotocollen (zoals bijvoorbeeld vastgelegd in IEC-norm 61850), en recente vooruitgang in sensor- en communicatietechnologie leiden tot grote vernieuwingen in het beveiligen van distributienetten. Zij maken de overgang mogelijk van beveiligingen die slechts op basis van lokaal beschikbare informatie werken naar innovatievere en intelligentere beveiligingsconcepten die van communicatie gebruikmaken, al dan niet centraal aangestuurd. In de context van IEC-norm 61850 worden *peer-to-peer*-communicatiemethodes onderzocht, die onder meer zeer snelle netbeveiliging mogelijk maken. Daarnaast worden de voordelen van volledig gecentraliseerde beveiliging ten opzichte van gedistribueerde beveiligingsfilosofieën behandeld, onder meer op het gebied van snelheid, flexibiliteit en selectiviteit.

In dit proefschrift wordt een blauwdruk ontwikkeld van een nieuw en intelligent beveiligingsconcept, dat algemeen toepasbaar is voor distributienetten met gedistribueerde opwekkers, en onafhankelijk is van de netstructuur. Het verhogen van de algemene beschikbaarheid van deze opwekkers tijdens fouten in het net is de voornaamste doelstelling. In het proefschrift worden twee verschillende uitvoeringen van zowel de onderliggende hardware als van de toegepaste communicatie-infrastructuur in detail uiteengezet; stroomdiagrammen van beide algoritmes worden gegeven.

Een uitvoerig voorbeeld toont hoe het nieuwe, volledig op communicatie gebaseerde beveiligingsalgoritme zijn toepassing vindt op een voor Nederland gebruikelijk distributienet. Daarbij wordt de praktische hardware-implementatie van het algoritme, welke gebruik maakt van moderne sensor- en microprocessortechnologie, aanschouwelijk gemaakt. Simulaties in het tijddomein toetsen het gedrag van het ontwikkelde beveiligingsconcept voor verschillende scenario's. Het ontwikkelde intelligente algoritme bewerkstelligt een hoge mate van selectiviteit door het minimaliseren van afschakeltijden en het vermijden van de anders grootschalige afschakeling van gedistribueerde opwekkers in het netwerk bij fouten.

Contents

Summary	i
Samenvatting.....	iii
1 Introduction	1
1.1 Background and motivation.....	1
1.1.1 Impact of DG on distribution grid operation	2
1.2 DG definition.....	3
1.3 Common distribution grid structures.....	4
1.4 Migration towards a smart grid	6
1.4.1 Goals and drivers for a smart grid	7
1.4.2 The four technology layers of a smart grid.....	9
1.4.3 Smart grid applications	11
1.5 Problem definition	11
1.6 Objectives and research questions.....	13
1.7 A research project in intelligent power systems.....	13
1.8 Outline of the thesis.....	15
2 An overview of the protection principles in distribution networks	17
2.1 General information about protection systems.....	17
2.1.1 Relay technology and performance	17
2.1.2 Digital and numerical relay models.....	18
2.2 Distribution grid protection devices	20
2.2.1 Overcurrent protection.....	20
2.2.2 Distance protection	21
2.2.3 Differential protection	22
2.2.4 Directional protection	23
3 The necessity of future smart protection schemes in Dutch MV grids.....	25
3.1 Introduction	25
3.2 The influence of DG on the protection of MV grids.....	26
3.2.1 False tripping	26
3.2.2 Protection blinding.....	27
3.2.3 Automatic reclosing.....	28
3.2.4 Unwanted islanding	28
3.3 Case studies	29
3.3.1 Analysis of protection blinding	29
3.3.2 False tripping analysis	32
3.4 Evaluating conventional overcurrent time-graded protection schemes.....	34
3.4.1 Modeling of an existing MV grid using Marlab/Simulink	34
3.4.2 Relay protection settings.....	35
3.5 Simulation results	40
3.5.1 Nuisance tripping of DG-units scenario	45

3.5.2	Sympathetic tripping scenario	46
3.5.3	Intensity of protection blinding scenario	49
3.5.4	Operation of distance protective devices	50
3.6	Transient stability issues	52
3.7	Extracting fault ride-through specification for DG-units	52
3.7.1	Derivation of FRT requirements for external grid faults	53
3.7.2	Derivation of FRT requirements for faults at the DG-unit terminals	54
3.7.3	Discussion of results	57
3.7.4	Feasibility of the FRT robustness of DG-units	57
3.8	Summary	57
3.9	Conclusions	58
4	Getting smart: technological advances rule the protection of the future	61
4.1	Introduction	61
4.2	Substation automation systems	62
4.3	Ethernet communication networks	62
4.4	The IEC61850 standard	63
4.4.1	Key features and main benefits	64
4.4.2	System architecture	65
4.4.3	Protection performance requirements	66
4.4.4	Modeling approach	68
4.4.5	Time synchronization issues	70
4.4.6	Mapping to real protocols	70
4.4.7	Security and dependability	72
4.5	Migration to totally integrated protection	72
4.5.1	The SASensor system	73
4.6	Summary	77
5	A novel concept of a smart protection strategy	79
5.1	Introduction	79
5.2	New concept of a fully-centralized protection philosophy	80
5.2.1	Utilized protection principles	80
5.2.2	Proposed protection strategy I	81
5.2.3	Proposed protection strategy II	84
5.3	Example case	86
5.4	Conclusions	90
6	Application of the intelligent protection algorithm for Lelystad grid	91
6.1	Introduction	91
6.2	Algorithm application for Lelystad distribution network	92
6.2.1	Protection settings of the implemented functions	95
6.3.2	Simulation results	98
6.3	Network reconfiguration scenario cases	104
6.3.1	Fault detection and isolation in zone 12	104
6.3.2	Fault detection and isolation in zone 13	106
6.3.3	Fault detection and isolation in zone 14	109
6.3.4	Fault detection and isolation in zone 7	111
6.4	Non-reconfiguration network scenario cases	111
6.4.1	Fault detection and isolation in zone 15	111
6.5	Acceptance and cost efficiency of the new technology	112

6.6	Summary.....	113
6.7	Conclusions	114
7	General conclusions and future possible work	115
7.1	General conclusions and thesis contribution	115
7.2	Recommendations for future work.....	117
A	Parameters of the Lelystad distribution network.....	119
B	Dynamic modeling of power systems with distributed generation	127
B.1	Introduction	127
B.2	Dynamic modeling of power systems	127
B.3	Dynamic models of the DG-units.....	129
B.3.1	Dynamic model of a squirrel cage induction generator wind turbine	129
B.3.2	Dynamic model of a split-shaft microturbine.....	131
B.3.3	Dynamic model of a diesel synchronous generator.....	133
	References.....	137
	List of Publications	145
	Acknowledgements	147
	Curriculum Vitae.....	149

Chapter 1

Introduction

1.1 Background and motivation

The conventional structure of electrical power systems is such that the electric power is generated in large generating stations at a relatively small number of central locations [1]. This structure is illustrated in Figure 1.1 [2]. In these stations the voltage is increased to High Voltage (HV) and transmitted over long distances through an inter-connected HV transmission network. The voltage is then stepped down to Medium Voltage (MV) and Low Voltage (LV) and distributed through radial distribution networks to the end users, simply referred to as “loads”. Loads can be connected at MV or LV.

These conventional large electric power systems have existed for more than 50 years, have been improved over the years and offered a number of advantages. However, over the last few years, a number of factors have led to an increased interest in Distributed Generation (DG) schemes [3]. According to the Kyoto protocol, the European Union is obliged to reduce greenhouse gas emissions substantially to prevent climate change. According to the CIRED survey [4], among the policy drivers which encourage distributed generation, the following ones are prioritized:

- Reduction in gaseous emissions (mainly CO₂),
- Energy efficiency or rational use of energy,
- Deregulation or competition energy,
- Diversification of energy resources.

The CIGRE report [5] lists similar reasons but with additional emphasis on commercial considerations, such as:

- Availability of modular generating plant,
- Easiness of finding sites for smaller generators,
- Short construction time and lower capital costs for smaller plants,
- Generation may be sited closer to load, which may reduce transmission costs.

Hence DG is gaining more and more attention worldwide as an alternative to large-scale centralized generating stations. Another fact is that the price of transmission technologies increases whereas the price of the distribution technologies decreases. Currently, many governments have programs to support the exploitation of the new renewable energy sources for electric power generation (such as wind, photovoltaic, fuel cells). Therefore, a large number of conventional as well renewable power plants such as Combined Heat and Power plants (CHP), microturbines, wind turbines and Photovoltaic (PV) systems are being connected to distribution networks.

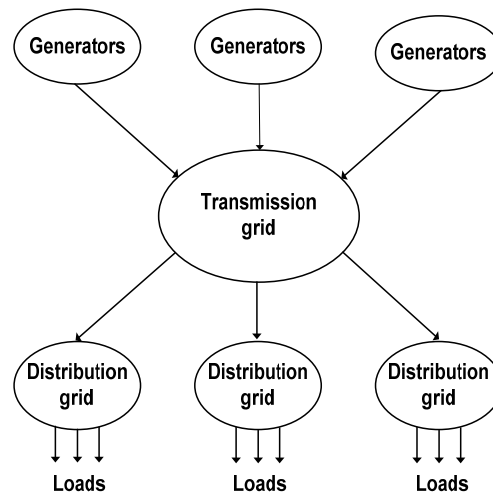


Figure 1.1. Conventional vertically-operated power system [2]

1.1.1 Impact of DG on distribution grid operation

The DG integration drastically changes the nature of the existing radial distribution networks from passive (containing only loads) to active (containing a combination of loads and small- to medium-scale generators). Thus, the distribution grid of the future may be characterized by the possibility of reversed direction of power flows. Figure 1.2 illustrates the nature of this vertical to horizontal oriented transition. These profound alterations have a considerable effect on the operation of the distribution grid, which is still treated in a more or less passive way. The effects of DG on an existing distribution network could be positive or negative depending on the position and the size of the generators installed. Nevertheless, the integration of DG may negatively impact important distribution and transmission grid features such as local power flow [6], protection and fault current level [7], stability [8], voltage control, grid losses, power quality, etc. These problems have been extensively researched in the literature. For instance, in [9] voltage rise and power quality issues due to the implementation of DG are discussed in detail.

Besides these aforementioned affects, DG connection can endanger the proper performance of the protection system. DG integration undoubtedly changes the fault level. The ability of the DG-unit to contribute to the fault current determines this impact on the

fault level. Specifically, the interface between DG-unit and the grid strongly determines the contribution of the fault current. Directly connected DG-unit does contribute to the fault current, whilst inverter-coupled DG-unit hardly contribute to the fault current rise [10]. Moreover, large contributions to the fault current may cause grid's equipment rating to be exceeded. In these situations fault current limitation is necessary. Since significant contributions of the DG-units to the fault currents affect the measured currents by the protective devices, applied protection systems in the distribution grid are affected as well. This can lead to incorrect operation of the protection system and cause fault detection and selectivity problems.

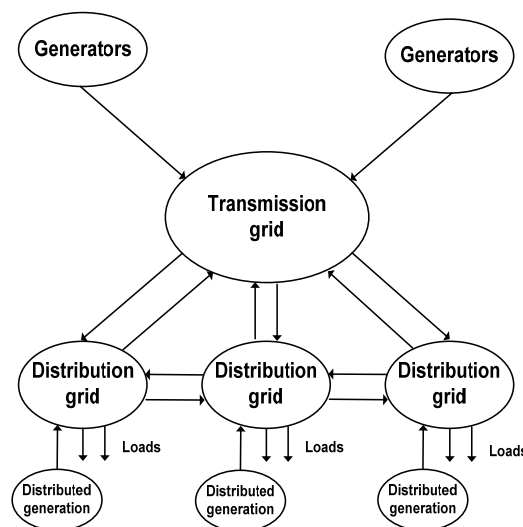


Figure 1.2. Horizontally-operated power system [2]

The larger the DG penetration level in a distribution grid, the more difficult the modeling and analysis of the short-circuit behavior of such a system. At present, in the Netherlands the penetration level of DG reaches up to 30% in certain regions. In the future, this number will for sure continue to grow and cause impacts on the distribution network protection. Taking into account the growing penetration levels of DG, distribution grid protection becomes an important issue in the future power systems.

1.2 DG definition

In the literature many terms and definitions are used for designating a small and geographically spread generation. In [11] DG is defined as an electric generation facility connected to a local electric power system through a Point of Common Coupling (PCC). An overview of definitions of DG can be found in [12] where it is stated that the definition given in [13] is a good approach without noting the specific characteristics of DG such as

DG technology, DG rating or mode of operation. In this thesis Distributed Generation is defined according to [13]:

Distributed generation is an electric power source connected directly to the distribution network or to the customer side of the meter.

The rating of the DG-unit is not specified in the given definition of DG. The categories of different ratings of distributed generation suggested in [14] and also used in this thesis are:

- Micro DG: $20 \text{ W} < 5 \text{ kW}$
- Small DG: $5 \text{ kW} < 5 \text{ MW}$
- Medium DG: $5 \text{ MW} < 50 \text{ MW}$
- Large DG: $50 \text{ MW} < 300 \text{ MW}$ (connected to the transmission grid)

Examples of different DG technologies of the suggested categories are given in Table 1.1.

Table 1.1. Overview of DG technologies and sizes [13]

Technology	Average unit size
Combined cycle gas turbine	30 - 400 MW
Internal combustion engines	5 kW – 10 MW
Wind turbine	200 W – 3 MW
Photovoltaic arrays	20 W – 100 kW
Fuel cells	200 kW – 2 MW
Battery storage	500 kW – 5 MW

References [6, 8] provide an extensive overview of the state-of-the-art DG technology including their characteristics and modeling. Additionally, reference [15] provides a detailed classification of the DG according to the principles of operation and the interface between the distribution grid and the DG-unit. It is stated that converter-connected DG hardly contribute to a fault current and can be neglected in fault current calculations and the evaluation of the protection system.

1.3 Common distribution grid structures

The distribution grid structures are classified in three categories:

- Radial grid structure,
- Loop grid structure,
- Meshed grid structure.

The different structures for the distribution grid are depicted in Figure 1.3. Currently MV distribution networks are always operated with a radial arrangement and are often subdivided into two different levels: trunk feeders and lateral branches. In the radial grid structure, each substation or customer is coupled over a single line or a cable to a central

point of supply. In this context, in case of the occurrence of a line or cable failure the total service interruption time corresponds to the complete repair time of the line or cable. This constitutes a significant drawback.

The low degree of reliability that is obtainable with radial network can be significantly improved by adding emergency ties that provide alternative routes for power supply in case of outages or scheduled interruptions. These emergency ties end up with an open switch so that radial structure is maintained during normal conditions. An important class of such networks is the open-loop networks, which are usually employed in urban power distribution systems. In the case of pure open-loop networks (containing no laterals), the service restoration is ensured through the emergency tie that connects the ends of the feeder. In the case of spurious open-loop networks, laterals exist. However, priority customers are supplied through the main feeder, which can be completely re-energized in the event of a fault. This kind of alternative grid structure is more adapted in rural distribution networks. Last years, the addition of emergency ties for some main laterals becomes an issue of high importance due to the ever-increasing utility care about long interruptions.

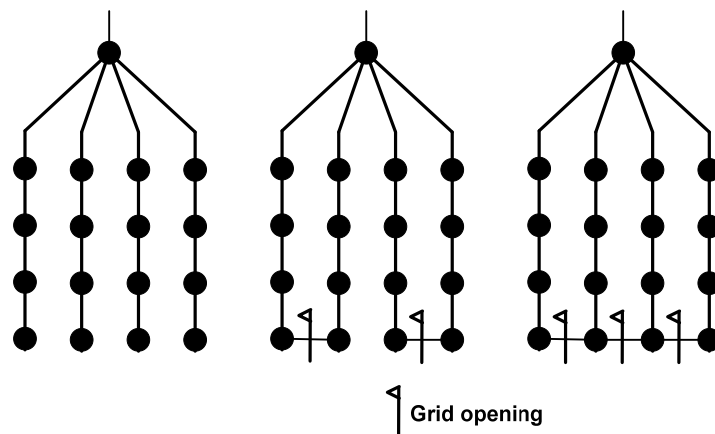


Figure 1.3. a) Radial grid structure b) Loop grid structure c) Meshed grid structure [1]

On the other hand, in a closed-loop structure all substations or customers are connected by two lines or cables. On the occurrence of a circuit, the faulted section is isolated and consequently the loop is separated in two parts. After the disturbance restoration, the faulted section is energized again and the two parts of the loop are reconnected. The service interruption time corresponds in this case to the required time needed for the fault restoration and the achievement of the essential switching actions.

In the meshed grid structure, all substations or customers are connected by more than two lines or cables. Meshed networks have well known advantages versus radial schemes: a reduction of power losses, a better voltage profile, a greater flexibility and ability to cope with the load growth and an improvement of power quality due to the fault level increase at each bus [16]. It is prominent to observe that these advantages can be maximized by optimizing the number and position of the emergency ties. Without careful planning strategies, the adoption of a meshed scheme can also worsen some technical aspects of the

network operation. Obviously compared to radial arrangement, a meshed network presents some drawbacks: a more complex planning and operation that consequently involves a higher cost and a rising of short-circuit current in each node that implies the substitution of the existing circuit breakers due to the overcoming of their interrupting capacity. Thus, it is more desirable to optimize the position of the used additional ties to mesh the existing radial distribution networks. Conclusively, it can be said that the current MV distribution networks are already meshed and they will become even more meshed in the future due to reasons of reliability.

1.4 Migration towards a smart grid

Last years, in the electric power industry there is an explosion of talks and activities about smart grids both in national news and professional conferences. The term “smart grid” has been used to describe a digitized and intelligent version of the present-day power grid. Although there is some debate on what specifically constitutes a smart grid, a consensus is forming regarding its general attributes. In the United States the following attributes of a smart grid are commonly cited [17]:

- It is self-healing (from power disturbance events),
- It enables active participation by consumers in demand response,
- It operates resiliently against both physical and cyber attacks,
- It provides quality power that meets 21st century needs,
- It accommodates all generation and storage options,
- It enables new products, services and markets,
- It optimizes asset utilization and operating efficiency.

In Europe, a smart grid is described, according to a recent European Commission report, as one that is [18]:

- flexible as it fulfills customers’ needs while responding to the changes and challenges ahead,
- accessible as it grants connection access to all network users, particularly renewable power sources and high-efficiency local generation with no or low carbon emissions,
- reliable as it assures and improves security and quality of supply, consistent with the demands of the digital age, with excellent resilience in the face of hazards and uncertainties,
- economical as it provides best value through innovation, efficient energy management and “level playing field” competition and deregulation.

The smart grid concept is also developing in China. According to the non-profit Joint US-China Cooperation on Clean Energy the term ‘smart grid’ refers to an electricity transmission and distribution system that incorporates elements of traditional and cutting-

edge power engineering, sophisticated sensing and monitoring technology, information technology and communications to provide better grid performance and to support a wide range of additional services to consumers. A smart grid is not defined by what technologies it incorporates but rather by what it can do. [19]

However, such high-level characterizations of a smart grid, while helpful at the strategic level, leave plenty of room for confusion and very different interpretations due to a lack of specifics [20]. It is little wonder that people sometimes confuse the smart grid with smart meters and Advanced Metering Infrastructure (AMI) or with interoperability in communications. In this section, the drivers for the smart grid and its scope are sketched out, its distinguishing features are envisioned and it is discussed what makes the smart grid smart. Additionally, the technical challenges that a smart grid must deal with as well as the capabilities it must have, in order to meet those challenges successfully are presented.

1.4.1 Goals and drivers for a smart grid

Power grids in the industrialized countries are aging and being stressed by operational scenarios and challenges never envisioned when the majority of them were developed many decades ago. The main challenges are summarized below [21]:

- Deregulation unleashed unprecedented energy trading across regional power grids, presenting power flow scenarios and uncertainties the system was not designed to handle.
- The increasing penetration of renewable energy in the system further increases the uncertainty in supply and at the same time adds stress to the existing infrastructure due to the remoteness of the geographic locations where the power is generated.
- Our digital society depends on and demands power supply of high quality and high availability.
- The threat of terroristic attacks on either the physical or cyber assets of the power grid introduces further uncertainty.
- There is an acute need to achieve sustainable growth and minimize environmental impact via energy conservation, i.e. by switching to green and renewable energy sources. This objective can only be met by increasing energy efficiency, reducing peak demand and maximizing the use of renewable energy.

In the industry and among many national governments there is a growing consensus that the answer to these challenges is the smart grid technology. This trend is evidenced by the specific provision and appropriation of multi-billion-dollar amounts on the part of the US government for research and development, demonstration and deployment of smart grid technologies and the associated standards [22]. The European Union and China have also announced huge amounts of funding for smart grid technology research, demonstration and deployment.

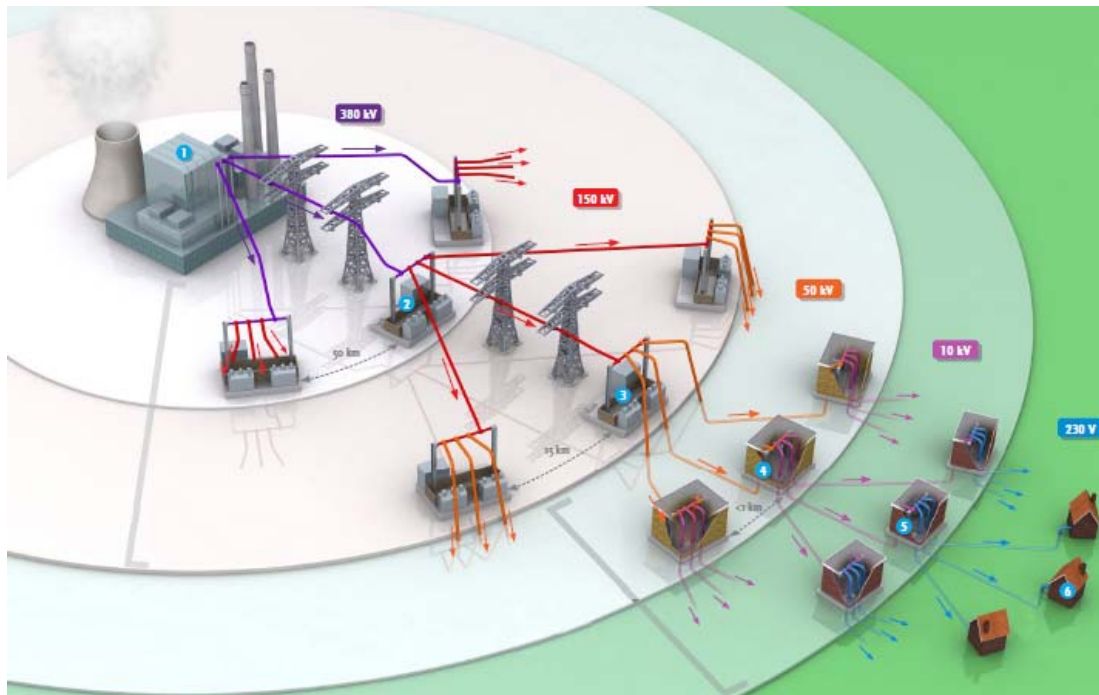


Figure 1.4. Present grid. (Illustratie:© 2011 www.kennisinbeeld.nl)

The objective of transforming the current power grid into a smart grid is to provide reliable high-quality electric power to digital societies in an environmentally friendly and sustainable way. This objective will be achieved through the application of a combination of existing and emerging technologies for energy efficiency, renewable energy integration, demand response, wide-area monitoring and control, HVDC, flexible ac transmission systems (FACTS), and so on [23].

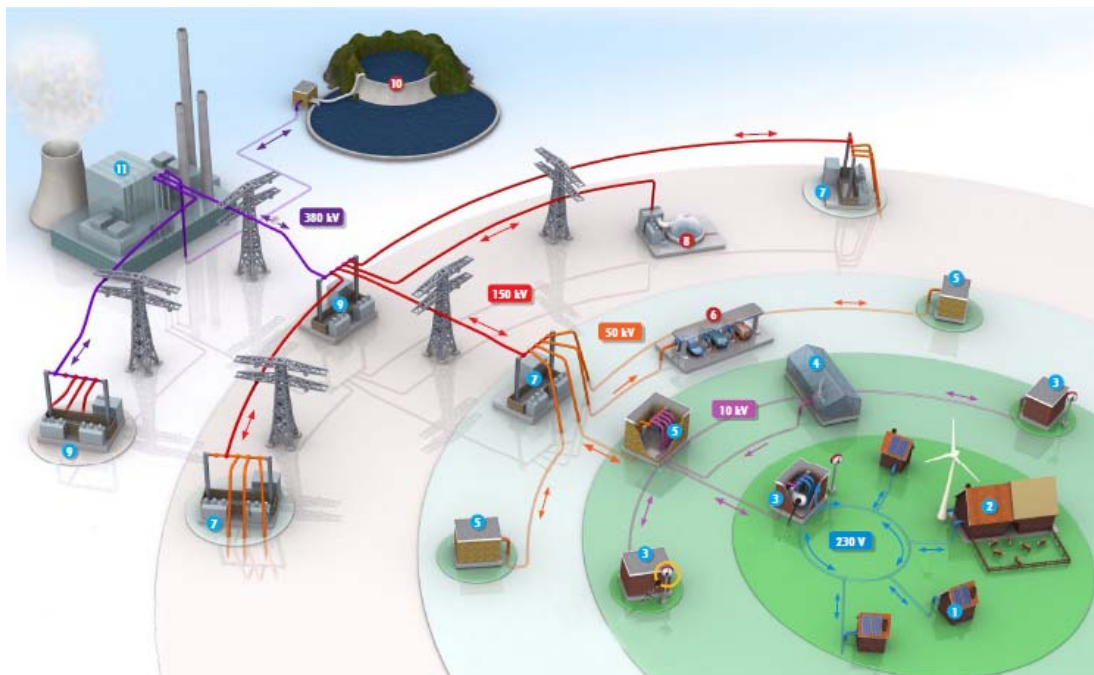


Figure 1.5. Future smart grid. (Illustratie:© 2011 www.kennisinbeeld.nl)

The scope of the smart grid extends over all the interconnected electric power systems, from centralized bulk generation to DG, from high-voltage transmission systems to low-voltage distribution systems, from utility control centers to end-user home-area networks, from bulk power markets to demand response service providers, and from traditional energy resources to distributed and renewable generation and storage. The transition from the present grid to a smart grid and the key differences between the two are illustrated in Figures 1.4 and 1.5. It can be observed that there is a fundamental shift in the design and operational paradigm of the grid: from central to distributed resources, from predictable power flow directions to unpredictable directions, from a passive grid to an active grid. In this context, the grid will be more dynamic in its configuration and its operational condition, which will present many opportunities for optimization but also many new technical challenges.

1.4.2 The four technology layers of a smart grid

The four essential building blocks of the smart grid can be depicted using a layered diagram, as shown in Figure 1.6.

- The physical layer (power conversion, transport, storage, consumption),
- The sensor/actuator layer which perceives the environment and effects desired changes in the physical system,
- The communication layer which collects the sensors information and propagates the measured and control signals,
- The decision intelligence layer that digests the information and generates control signals intended to change the state of the system.

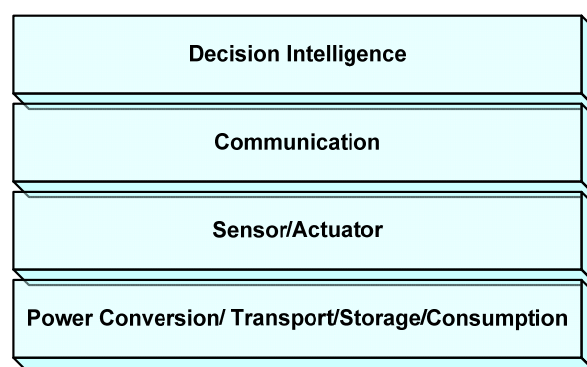


Figure 1.6. Smart grid technology layers [21]

The four basic building blocks, mapped to the required needs of the electric power system, are shown in Table 1.2. The physical layer is where the energy is converted, transmitted, stored and consumed. Solid-state technology, power electronics-based building blocks, superconducting materials, new battery technologies and so on all provide fertile ground for innovations.

Table 1.2. The four building blocks mapped to the electric power system [21]

Building blocks	Power system mapping
Sensor system	Current transformer (CT), voltage transformer (VT), phasor measurement unit (PMU), smart meter, temperature, pressure, acoustic and so on
Communication infrastructure	Power line carrier (PLC), wireless radio, advanced metering infrastructure (AMI), home area network (HAM), fiber optic networks
Control algorithms (applications)	Wide area monitoring and control, microgrid management, distribution load balancing and reconfiguration, demand response, optimal power flow (OPF), voltage and var optimization (VVO), fault detection, identification and recovery (FDIR), automatic generation control (AGC), inter-area oscillation damping, system integrity protection scheme (SIPS), and so on
Actuator/physical system	HVDC, FACTS, energy storage systems, reclosers, automatic switches, breakers, switchable shunts, on-load tap chnagers, hybrid transformers, and so on.

The communication and Information Technology (IT) layer performs the task of propagating the required information from the sensors to the controllers that process the information and transmit the control directives back to the actuators. The IT layer serves to provide responsible, secure and reliable information dissemination to any point in the grid where the information is needed by the decision intelligence layer. In most cases data are transferred from field devices back to the utility control center, which acts as the main repository for all the utility's data. However, device-to-device (controller-to-controller or IED (Intelligent Electronic Device)-to-IED) communication is also common as some real-time functionality can only be achieved through inter-device communication. Interoperability and security are essential to assure ubiquitous communication between systems of different media and topologies, and to support plug-and-play for devices that can be auto-configured when they are connected to the grid without human intervention. Additionally, the accelerating deployment of AMI is a big step in building a two-way communication platform for enabling advanced distribution applications.

The smartness of the smart grid lies in the decision intelligence layer, which is made of all the computer programs that run in relays, IEDs, substation automation systems and control centers. These programs process the information collected from the sensors or disseminated from the communication and IT systems. They provide control directives or support business process decisions that manifest themselves through the physical or actuator layer. Some application examples of control algorithms are given in Table 1.2. Such advanced control algorithms provide the 'smart' in smart grids. Therefore, "application, application and application" constitute the three value generators for the smart grid [23].

Nevertheless, the focus of the industry efforts so far has been mostly on the interoperability of the communication and information model, as suggested by the National Institute of Standards and Technology (NIST) Smart Grid Interoperability standard roadmap

and the International Electrotechnical Commission (IEC) documents on smart grid standardization [24].

1.4.3 Smart grid applications

As the system supply and consumption become more decentralized and distributed, the system condition will become more dynamic and less predictable. Therefore, the development of demand, supply, and power flow control strategies will become essential in protecting, managing and optimizing the new grid. In the following section, some application examples of the future smart grid are summarized [21]:

- Microgrid control and scheduling (demand response and efficiency) [25]
- Intrusion detection and countermeasures (cybersecurity)
- Equipment monitoring and diagnostic systems (asset management)
- Wide-area monitoring, protection and control [26]
- On-line system event identification and alarming (safety and reliability)
- Power oscillation monitoring and damping (stability)
- Voltage and var optimization (energy efficiency and demand reduction)
- Voltage collapse vulnerability detection (security)
- Autonomous outage detection and restoration (self-healing)
- Intelligent load balancing and feeder reconfiguration (energy efficiency)
- Self-setting and adaptive relays (protection)
- End-user energy management systems (consumer participation, efficiency)

1.5 Problem definition

The current protection philosophy relies on the use of current-based time-graded relays. This is a very powerful protection philosophy for passive distribution grids. However, with the increasing number of DG-units in the distribution system, the protection philosophy needs to be reconsidered and adjusted. The need for this adjustment depends on the penetration level and the technology of the DG-units. The decentralized production units can affect the protection of the distribution network in many ways. This impact can lead among others to the failure of fault current detection or the unjustified switching-off of a healthy part of a feeder. Thus, the needs and the arguments of migration towards intelligent protection strategies should be addressed.

In this dissertation, a typical existing 10 kV Dutch Medium Voltage distribution grid consisting only of cables has been studied. Discrete dynamic models of the test network and all the applied protection schemes have been developed and simulated in Matlab/Simulink environment. The distribution grid has been modeled in detail including all dynamic models of the incorporated DG-units. The simulations performed in this thesis considered only

three-phase and two-phase faults. Since DG-units are operated with an isolated neutral point, the plants do not contribute to high single-phase-to-ground faults. Single-phase-to-ground faults have been studied only from the stability point of view since they constitute the most common fault type.

In this dissertation, the following specific problems have been investigated:

Demonstrating the reasons why future protection schemes should be fast and smart. Conventional protection systems apply traditional time grading principles to obtain selectivity. Therefore, it is important to evaluate the effectiveness of traditional protection schemes for the case of distribution grids supplied with a high penetration level of DG-units. The problems faced by the current applied schemes should be identified and the issues which dictate a modification in future protection logic should be determined as well. In this way, the technical requirements which specify the future protection coordination principles are clarified.

Explaining how the recent technological advances permit the transition from traditional to intelligent protection schemes. Future distribution grid protection schemes should be fast, flexible and guarantee a high level of protection selectivity. Actual implementation of such intelligent protection strategies can be feasible by means of applying the recent technological advances in sensor technology, communication infrastructure, and digital relaying. Additionally, the emergence of innovative standard communication protocols plays a significant role in revolutionizing traditional protection strategies and in making communication-aided integrated or distributed protection schemes possible.

Developing a novel concept of a smart protection strategy intended for any arbitrary network. The goal of the proposed protection philosophy is to increase the during-fault DG availability as high as possible, ensure high-level of protection selectivity and to provide as short as possible fault clearing time. Aspects regarding the real implementation of the scheme and the usage of multi-functional protection principles are examined. The immeasurably significant benefits of changing the distribution grid structure from radial to loop operation just before the fault isolation are qualitatively explained.

Applying the novel concept of a smart protection algorithm on an existing representative Dutch distribution grid. The evaluation of the new intelligent algorithm by means of simulations is necessary to validate its ability to prevent protection selectivity problems, to ensure a high-speed protection performance, to assure an enhanced DG-availability during disturbances and to prevent distribution grid transient instabilities. The demonstration of different hardware architectures and communication infrastructure arrangements, which accommodate the new protection strategy, plays a significant role.

1.6 Objectives and research questions

The following research objectives have been achieved in this dissertation:

- evaluating the performance of traditional time-graded protection schemes in Dutch distribution networks supplied with a high penetration level of DG-units,
- justifying the reasons why future distribution grid protection schemes should be intelligent and fast,
- demonstrating how recent technological advances (communication infrastructures, standard communication protocols, sensor technologies) stimulate the revolution of distribution grid protection strategies and how they permit the real implementation of fully centralized or distributed communication-assisted protection schemes,
- developing a novel intelligent algorithm that guarantees protection selectivity and increases the availability of the local DG-units during and after a disturbance.
- evaluate the novel intelligent algorithm by means of applying it on an existing Dutch DG-supplied distribution grid.

The research questions related to these objectives are:

1. *Are conventional time-graded protection schemes suitable for distribution networks supplied with a high penetration level of DG-units?*
2. *Is a modification in protection logic of future power systems necessary?*
3. *Which issues dictate the requirement for future fast and smart protection schemes?*
4. *How should future smart protection systems look like, how should they be set and what components are needed for this transition?*
5. *What is the influence of the new protection strategy on the stability of the distribution grid?*

1.7 A research project in intelligent power systems

The research presented in this thesis has been performed within the framework of the ‘Intelligent Power Systems’ program, part of the IOP-EMVT research program (Innovation Oriented research Program – Electro-Magnetic Power Technology), which is financially supported by AgentschapNL, an agency of the Dutch Ministry of Economic Affairs.

This project focuses on the short-circuit behavior of various types of DG and the consequences these units might have on distribution grid operation. The project is divided in three parts, as depicted in Figure 1.7:

1. System behavior of the distribution grids including DG
2. Short-circuit behavior of various types of DG
3. Protection philosophy of distribution grids including DG

The goal of the first part is to gain insight on how distribution grids with a large number of DG have to be managed during and after a disturbance. Up until now DG is disconnected immediately after a disturbance or voltage dip. With an increasing number of DG in the future this is not acceptable and research has to be done to determine what suitable ride-through requirements are and what the effect is of keeping DG connected to the grid. Besides that, proposals have to be made what the desirable grid support is of various types of DG after a grid disturbance. The first part of this research project resulted in the publication of the Ph.D. dissertation entitled “Distribution grid operation including distributed generation”, authored by Dr. E. Coster [15].

The second part focuses on the behavior of the various types of DG during a short-circuit in the distribution grid. Therefore, detailed models of these units have to be developed and implemented in simulation software. With the aid of these models an accurate prediction of the behavior of the distribution grid can be given. To obtain the desirable grid support the ability of the DG-unit to participate in the grid support is investigated and modifications to the control system will be proposed.

The third part of the project concentrates on the protection philosophy of distribution grids including DG. With the developed models of the DG-units different protection philosophies can be developed in order to increase the availability of these units after a disturbance. The research presented in this thesis belongs to this part of the project. This thesis constitutes the second published dissertation within the project.

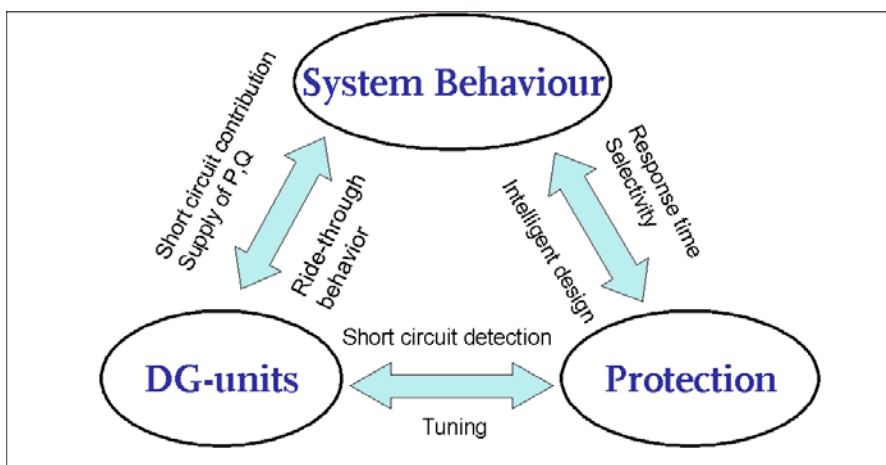


Figure 1.7. Consistency of the predefined subproblems.

1.8 Outline of the thesis

This section presents an outline of the thesis.

Chapter 1 – A definition of distributed generation is provided and the influence of DG on distribution grid operation is discussed. The influence of the DG integration on the performance of the protection schemes is specially highlighted. Furthermore, the drivers for the smart grid are sketched out, the technical challenges it must deal with and its distinguishing features and capabilities are presented.

Chapter 2 – The characteristics of a good relay performance are introduced and the classification of the protective devices, based on the employed technology, is provided. The basic definitions concerning digital relaying and the structure of the protection systems are given. The categories of the numerical relay models are explained and the generalized phasor-based numerical relay structure is discussed. The functional principle and general setting rules of the different types of relays applied in distribution systems are presented.

Chapter 3 – The arguments why future distribution grid protection schemes should be fast and smart are justified. Conventional time-graded protection schemes are evaluated for an existing DG-supplied representative Dutch distribution grid. The simulation results demonstrate their inadequacy in terms of protection selectivity. These highlighted protective device malfunctions dictate the required modifications which will be needed in the future protection logic so that protective device selectivity is assured and relay speed performance as well as DG during-fault availability is increased. Furthermore, the chapter examines issues related to the extraction of enhanced fault-ride-through specification requirements for each different type of DG-unit. The determination of a unique FRT specification, which falls within the transient stability criteria of each specific type of DG-unit, is explained and compared with typically used undervoltage protection settings.

Chapter 4 – This chapter shows how the universal adoption of numerical relays, the emergence of new standard communications protocols (IEC61850) and the unprecedented advances in sensor and communication technologies as well as infrastructure stimulate a whole new wave of innovation in the protection scheme landscape of DG-supplied distribution grids. It additionally illustrates how the migration from today's strictly local-information-based relay protection towards the development of innovative smart communication-assisted protection schemes becomes possible. Furthermore, details of the novel peer-to-peer communication mechanisms, included in IEC61850, which permit the implementation of high-speed protection schemes, are discussed. Finally, the merits of fully-centralized protection schemes, in contradiction to distributed protection strategy, are enumerated.

Chapter 5 – A novel protection concept intended for distribution networks supplied with a high penetration level of DG-units is proposed. Two different arrangements of the underlying hardware and communication infrastructure architectures, which can accommodate this smart protection strategy, are shown. The flowcharts of both protection algorithms are depicted and their advantages and disadvantages are highlighted.

Chapter 6 – The novel fully-centralized communication-based protection concept is applied on Lelystad distribution network. The real-time organization of both the hardware architecture and communication infrastructure of the new protection algorithm is illustrated. The proper performance and selectivity of the proposed protection scheme is validated by means of discrete-time dynamic simulations through various scenario cases and highlight the numerous benefits of the intelligent protection algorithm. The simulation results verify the fact that the proposed protection strategy assures protection selectivity, by ensuring a high-speed protection performance, thus eliminating the problem of nuisance tripping of DG-units.

Chapter 7 – General conclusions and recommendations for further research are given.

Chapter 2

An overview of the protection principles in distribution networks

2.1 General information about protection systems

In distribution networks, a number of ancillary systems are present to assist in meeting the requirements of a reliable, secure and economic power system operation. The important ones are the protection systems which are installed to clear faults during network operation and to limit a possible damage of the distribution network equipment. An automatic operation of the protection systems is necessary to isolate faults on networks as soon as possible in order to minimize the damage. The economic costs and benefits of a protection system must be considered in order to present a suitable balance between the requirements of the protection scheme and the available financial resources [27]. In this chapter, the classification of the numerical relay models is provided and the generalized phasor-based numerical relay structure is explained. Furthermore, the characteristics of a good relay performance are introduced and the classification of the protective devices, based on their employed technology, is given. Moreover, the functional principles and the general setting rules of the different types of relays applied in distribution systems are presented.

2.1.1 Relay technology and performance

The relay application for the protection of power systems dates back nearly 100 years ago. Since then, the technology employed to construct relays has improved significantly in terms of relay size, weight, cost and functionality. Based on the applied technology for their construction, relays can be chronologically classified, as following [28]:

Electromechanical relays: which were the first relays to be largely employed in the electric industry. Due to the nature of their principle of operation, which is based on the creation of a mechanical force to operate the relay contacts, they are relatively heavier and bulkier than relays constructed with other technologies.

Solid-state or static relays: which were based on analog electronic circuitry that appeared in the early 60s. Static relays showed significant advantages over electromechanical relays, however they also presented serious disadvantages.

Digital relays: which incorporate Analog-to-Digital-Converter (ADC) to sample the incoming analog signals and use microprocessors to define the logic of the relays. High accuracy and integration of multifunctional algorithms constitute fundamental benefits of this technology.

Numerical relays: which utilize dedicated digital signal processor cards to perform special digital signal processing (DSP) applications.

A good performance of a relay in a power system is related to the following characteristics [29]:

Reliability: The ability of a relay to operate correctly. It has two elements:

- Dependability, which is the certainty of a correct operation upon the occurrence of a fault, and:
- Security, which is the ability to refrain from unnecessary operation.

Selectivity: The ability of a relay to maintain continuity of supply by disconnecting the minimum section of the network necessary to isolate the fault.

Speed: The ability of a relay to achieve a minimum operating time to clear a fault in order to avoid damage to equipment.

Sensitivity: The ability of a relay to identify an abnormal operating condition that exceeds a certain threshold value.

2.1.2 Digital and numerical relay models

Digital and numerical relay models are generally divided into two categories: the phasor-based models which take into account only the fundamental frequency components of the incoming signals, and the transient-based models which take into consideration the high frequency as well as decaying DC components of the signals in addition to the fundamental frequency components. The generalized phasor-based numerical relay concept consists of a minimum set of hardware modules and software functions [30]. The schematic diagram of a generalized numerical relay structure is depicted in Figure 2.1.

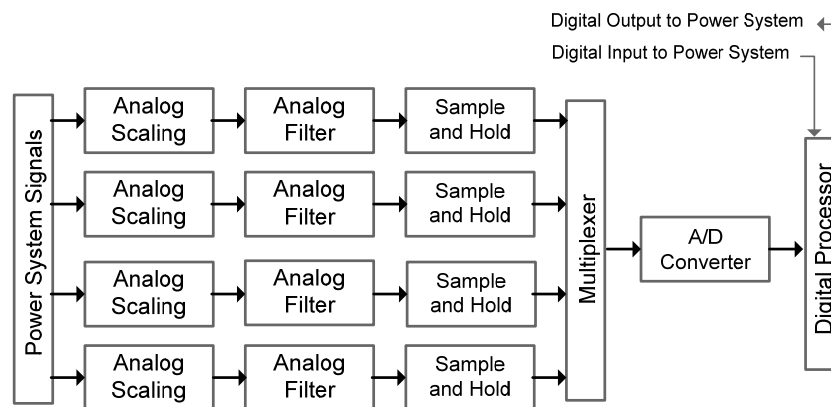


Figure 2.1. Generalized numerical relay structure [30]

The following hardware modules and functions constitute the generalized numerical relay:

Isolation and analog signal scaling: current and voltage waveforms acquired from instrument transformers are scaled down to convenient voltage level.

Analog anti-aliasing filtering: low-pass filters (i.e. Butterworth, Chebyshev, elliptic) are used to avoid the phenomena of aliasing in which the high frequency components of the input signals appear to be parts of the fundamental frequency components.

Analog-to-digital conversion: the input waveforms are sampled at discrete time intervals. In order to achieve this, each analog signal is passed through a sample-and-hold module and conveyed, one at a time, to an ADC by a multiplexer.

Phasor estimation algorithm: a software algorithm implemented in the microprocessor estimates the amplitude and phase of the waveforms provided to the relay. The phasor estimation makes use of the sampled values over a specified data window. After the phasors' calculation, a new sample is incorporated to the data window, the oldest sample is discarded and the process continues seamlessly. These algorithms are divided in the following categories:

a) Non-recursive short window algorithms [31] (Miki and Mikano, Mann and Morrison, Rockefeller and Udren, Golbert and Shovlin, etc.).

b) Non-recursive long window algorithms (Discrete Fourier Transform, Walsh Functions, Least Square Error, etc.), which the most popular phasor estimation techniques employed in contemporary numerical relays. Modern digital relays typically use 80 samples per cycle (4 kHz).

c) Recursive algorithms (Kalman Filtering, Recursive Least Square Error, etc.)

Relay algorithm and trip logic: the equations and parameters that represent the protection algorithm as well as the associated trip logic are implemented in the software of the microprocessor used in the relay. The microprocessor acquires the status of the switches, performs protective relay calculations and finally provides control outputs to the circuit breakers. The processor may also support self-testing, communication ports, target display, time clocks and other tasks.

2.2 Distribution grid protection devices

2.2.1 Overcurrent protection

Overcurrent relays are common protection devices that are used as a part of a primary and/or back-up relay protection in distribution networks. Overcurrent relays issue a trip signal to the circuit breaker when the monitored current exceeds a predetermined minimum operating current value. They are classified into definite-time and inverse-time based on their tripping time [29]. Definite-time overcurrent relays operate when the current exceeds a preset value over a certain predetermined time period. On a contrary, inverse-time overcurrent relays operate within a time interval which is inversely proportional to the fault current. This relay type can thus ensure short tripping time for very high currents. They are classified in three categories according to their characteristic curve: inverse, very inverse and extremely inverse relays. The operation time of the inverse-time relay is defined according to IEC 60255 by the following expression [29]:

$$t = \frac{k \cdot \beta}{\left(\frac{I}{I_{pickup}} \right)^\alpha - 1} \quad (2.1)$$

where the parameters α and β determine the slope of the characteristic, k is the time multiplier, I is the fault current level and I_{pickup} is the pick-up current. The parameters α and β of the standardized IEC 60255 curves are displayed in Table 2.1. For the definite-time overcurrent relays, the generic rule for the selection of the minimum operating current is to set it higher than twice (200%) of the maximum load current and lower than half (50%) of the minimum end-of-line phase-to-phase fault current. For inverse-time overcurrent relays, the pick-up current is usually set to $1.5 \cdot I_{nom}$ of the protected element to allow some overload. The protection system demonstrates an acceptable level of selectivity only when the protection device closest to a fault operates. A coordinated operation between two successive relays is obtained by applying a Coordinating Time Interval (CTI) which is also known as time grading. Relay coordination process requires that the farther the relay is from the fault, the longer is its time setting. In other words, the time setting of overcurrent relays is in an increasing order from the fault location. CTI is defined as the time between the operations of two serial relays. For both definite/inverse-time relays CTI is usually in the range of 0.2 to 0.5 s. Figure 2.2 shows the time coordination for definite and inverse time-overcurrent relays that are part of a line protection.

Table 2.1. IEC 60255 constants for standard overcurrent relays [29]

Relay type	α	β
Inverse	0.02	0.14
Very inverse	1.00	13.50
Extremely inverse	2.00	80.00

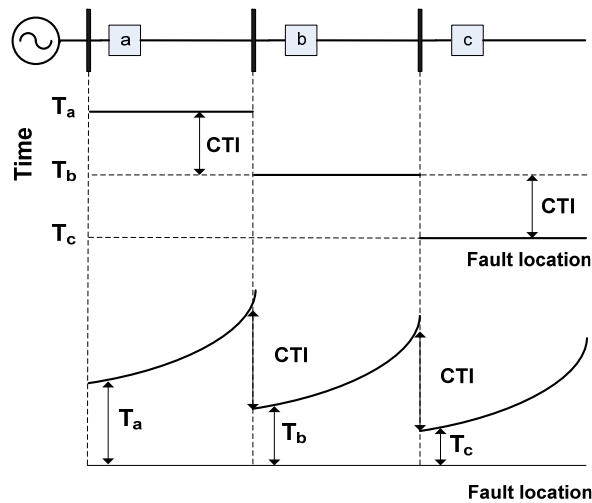


Figure 2.2. Relay coordination for line protection: definite-time and inverse-time relays

2.2.2 Distance protection

Distance protection has been widely used for protecting subtransmission grids which usually have a ring or meshed grid structure. Distance relays use voltages and currents acquired at the relay location to calculate the apparent impedance of the protected line. The calculated impedance is compared to the predetermined impedance that is called reach of the relay. When the measured apparent impedance is less than the impedance-reach, the relay issues a trip command to the appropriate circuit breaker. Most distance protection devices feature one of the following operating characteristics: impedance, admittance or mho, susceptance, conductance, etc [32].

The selectivity of distance relays is provided by using different impedance-reaches in conjunction with different time delays associated with those settings. Thus, time-stepped distance schemes ensure adequate discrimination for faults that may occur in different line sections. The combination of an impedance-reach and its associated time delay is known as a protection zone. It is a common practice to provide distance relays with three protection zones. The time grading is usually 0.3-0.4 sec. Distance protection devices contain phase-to-phase as well as phase-to-ground elements that respond to phase-to-phase or phase-to-ground faults in their operating areas. Details about the measured impedance during symmetrical and asymmetrical faults can be found in [30]. The operating characteristics of a three-zoned impedance relay are shown in Figure 2.3. The impedance reach of zone-1 (z_{m1}) is usually set between 80% and 85% of the line impedance leaving the remaining 20% to 15% as a safety margin. This safety margin ensures that errors and inaccuracies introduced by instrument transformers could prevent the relay from operating for faults in other than its own protection zone (over-reach). Time setting for zone-1 is T_1 . The second zone (z_{m2}) covers the last 20% of the line section and 50% of the next line section. To obtain

selectivity, faults within the second zone are cleared in T2. The zone-3 (z_{m3}) reaches usually up to the next two substations with a time setting of T3.

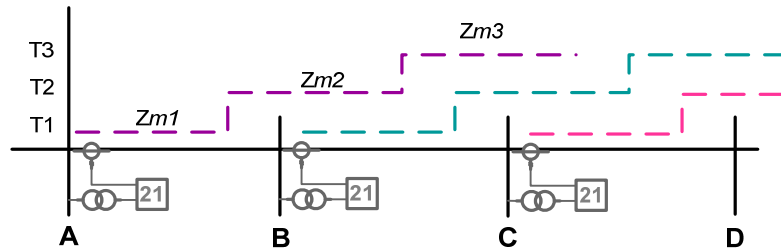


Figure 2.3. Impedance zones of a feeder protected by distance protection relays

2.2.3 Differential protection

The differential protection is one of the most reliable and popular techniques in power system protection. It offers a very short fault clearing time, which makes it very selective. The differential relay compares the currents that enter with the currents that leave a zone and operates when the vector difference of these current quantities exceeds a predetermined value. Thus, if the net sum of the currents that enter and leave a protection zone has a low value, there is no fault in the protection zone. However, if the net sum does not have a low value, a fault exists in the zone and a trip signal is generated. The protected zone can be a line, a transformer, a busbar with more than two feeders, etc.

Differential relays are categorized into non-restraint and restraint differential relay protection [33]. The non-restraint relay considers only the differential current to trigger the operation of the protection device, as depicted in Figure 2.4(a). The percentage restraint differential protection employs the restraint current together with the operating current to define the relay operation on a coordinate plane, as shown in Figure 2.4(b). Thus, restraint differential protection overcomes the problems related to the identification of light internal faults while keeping the advantages of the basic non-bias differential scheme. The line which divides the coordinate plane in two parts is the characteristic of the differential relay. The upper part is the operating region while the lower part is the restraining region. Typical characteristic of differential relays presents a small slope for low currents to allow sensitivity for light internal faults (single slope characteristic). For higher currents the slope of the characteristic may be much higher (dual slope characteristic), which requires that the operating current is higher in order to cause tripping of the differential relay. In general the operating and restraint currents in the differential relay, in the case the protected zone is a line, are equal to:

$$I_{op} = |I_{D1} + I_{D2}| \quad (2.2)$$

$$I_{rt} = k \cdot |I_{D1} - I_{D2}| \quad (2.3)$$

where I_{D1} and I_{D2} are the secondary currents on the pilot wires of the current transformers and k is a compensation factor, generally taken between the values of 0.2 to 0.4. Mismatches of the ratios of the current transformers used at the different sides of a differential protection zone can be easily corrected in a numerical relay by a scaling parameter in the microprocessor software.

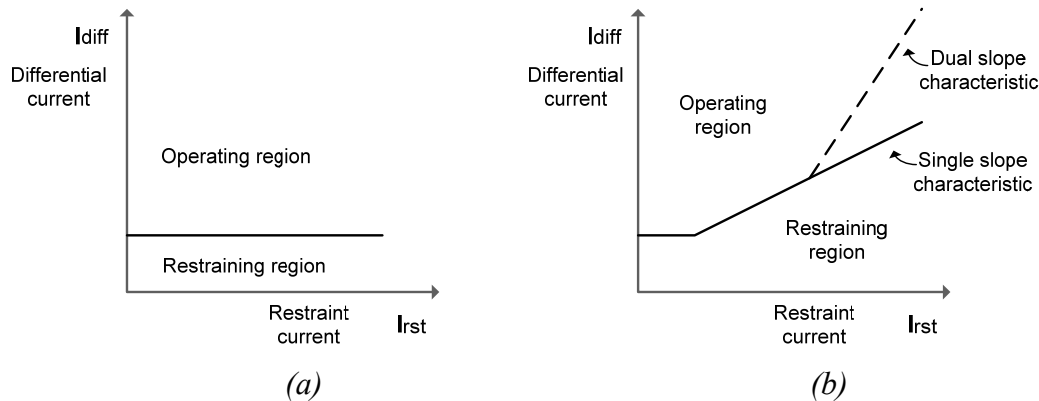


Figure 2.4. (a) Characteristic of a non-restraint differential relay (b) Characteristic of a percentage restraint differential relay

2.2.4 Directional protection

The application of overcurrent relays in radial distribution grids ensures reliable and selective protection from disturbances since there is only one source of supply. However, selective protection operation of overcurrent relays in multi-source distribution grids with a ring or meshed grid structure is almost impossible. Thus, the protection devices in a multi-source closed-loop system have to be direction sensitive. The overcurrent relay needs current measurement to decide if a fault occurred or not. The directional relay is the relay that has an additional element for the determination of power flow direction in the associated distribution feeder. Due to the fact that the current measurement does not give power flow direction an additional variable must be used. The additional variable is usually a voltage measurement. Therefore, the power flow direction is commonly determined by a reference voltage signal. Directional element uses the relationship of the current and the voltage to determine the power flow direction. Figure 2.5 depicts the block scheme of a directional overcurrent relay. The directional block can be set to trip in forward or reverse direction of the power flow. A trip signal is generated when both the overcurrent block and the directional block coincide with the selected settings [15].

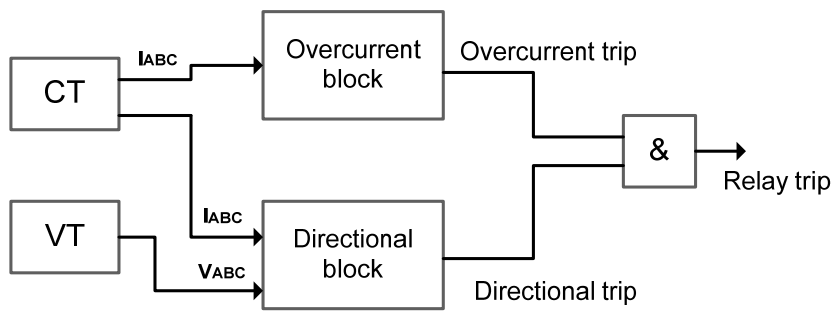


Figure 2.5. Block scheme of directional overcurrent relay [15]

Chapter 3

The necessity of future smart protection schemes in Dutch medium voltage grids

3.1 Introduction

This chapter focuses on how distributed generation may influence a fault detection and isolation in medium voltage distribution networks. Therefore, an explanation of all possible protection problems is provided. An existing Dutch distribution network supplied with distributed generation is investigated in terms of fault detection and coordination protection problems. The evaluation of the current applied time-graded overcurrent protection schemes is performed and prominent weaknesses of the protection schemes are indicated through various scenario cases. In this context, the problems faced by today's applied protection schemes are identified and the issues which dictate the necessity of future modifications in protection logic are determined. The discrete-time dynamic simulations showed the occurrence of protection malfunctioning in terms of the selectivity and the massive disconnection of DG-units during disturbances in the observed network. The observed technical problems clarified the requirements which specify the future protection coordination principles. The required future protection philosophy will need to speed up the protection performance, assure the selectivity and enhance the DG during-fault availability.

In the second part of the chapter, issues related to the extraction of enhanced fault ride-through specification requirements for each specific type of DG-unit are examined. A unique fault ride-through specification is derived for each different type of DG-unit based on its transient stability criteria, and is compared with typically applied undervoltage protection settings. It is concluded that the during-fault DG availability can be significantly increased in the future, if the DG undervoltage protection settings are adjusted according to the derived curves.

3.2 The influence of DG on the protection of MV grids

The distribution network is traditionally designed based on the assumption of unidirectional flow of power and currents. In other words, the power is assumed to be fed from higher voltage levels and distributed further to lower voltages and finally, to the customers. The same idea applies for the fault currents, which are assumed to flow downwards. This assumption enables relatively simple protection schemes to achieve a fast and selective protection operation. However, DG integration in the distribution networks radically changes this basis. Since DG-units contribute to all faults occurring in the network, fault current amplitudes can be significantly modified [34], [35]. Both power flow and fault currents may now have an upwards direction and therefore DG may disturb the network protection. At this moment, the protection is considered to be the biggest technical barrier of a widespread use of distributed generation among network utilities.

Common protection problems in MV grids supplied with DG are described in [36], [37], [38], [15]. Problems that can occur are:

- inadvertent relay tripping under faults on other neighboring DG outgoing feeders (false tripping),
- missed relay operation under faults beyond the connection point of the DG-unit (protection blinding),
- fuse-recloser coordination,
- unsynchronized automatic reclosing,
- prohibition of automatic reclosing.

The appearance of these kinds of problems depends on the characteristics of DG. During short-circuit faults, DG generates fault current that depends strongly on the generator type [15]. Additionally, the type of the distribution grid and consequently the applied protection system determine these problems. Thus, the problems of protection blinding and false tripping can occur in distribution grids, which utilize underground cables and overhead lines, while fuse-recloser coordination and automatic reclosing problems only occur in distribution grids with overhead lines.

3.2.1 False tripping

Unnecessary disconnection of a healthy feeder occurs due to the contribution of DG to the short circuit current in an adjacent feeder connected to the same substation, as illustrated in Figure 3.1. In this case, the DG-unit's fault current contribution has an upstream direction on the feeder towards the fault point. The contribution of the DG can exceed the pickup current of the overcurrent relay and trip the healthy feeder before the actual fault is cleared [39]. This mechanism is known as false or sympathetic tripping and belongs to the category of protection selectivity problems. This phenomenon is possible when the fault current

direction is not recognized by the relay, which is the typical situation in many present installations.

In [37] it is discussed that in some cases false tripping can be avoided by finding appropriate relay settings. Increasing the pickup current setting may be impossible since it could result in a less sensitive feeder protection wherein not all faults would be cleared anymore. However, increasing the fault clearing time of the relay on the feeder including DG in comparison with the adjacent feeders may serve to avoid the possible problems.

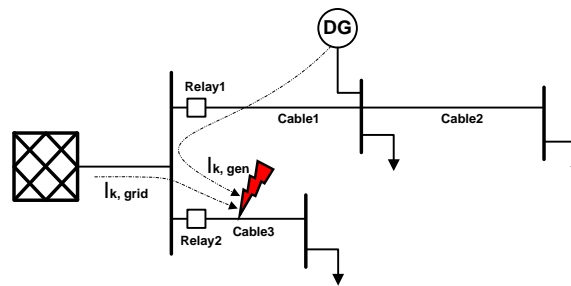


Figure 3.1. An example of a false tripping [39]

3.2.2 Protection blinding

Let us consider a MV feeder to which a DG-unit is planned to be connected, as depicted in Figure 3.2. Initially, prior to the DG integration, the feeder overcurrent relay is adjusted to detect the worst-case fault (two-phase fault) at the tail part of the feeder. When a DG-unit is connected to the feeder between the feeding substation and the fault point, overall fault currents increase in the network, due to the DG-unit fault current contribution to all short-circuit faults. However, the fault current measured by the feeder relay is actually decreased for the same fault, due to fault current division between the feeding sources. An analytical description of this problem is given in [15] where analytical equations of the key parameters which determine the effect of DG on the fault current are presented by means of a generic test feeder. The analytical description shows that the grid contribution is determined by the total feeder impedance, the local short-circuit power at the substation, the generator size and location.

This mechanism belongs to the fault detection protection problems. The blinding effect may result in delayed protection operation in case of inverse-time overcurrent relays and even in totally operation blocking in case of definite-time relays [39]. Typically, the protection is not blocked totally, but it is immediately activated after the DG disconnection. The problem can be resolved by decreasing the current setting of the observed overcurrent relay. However, such an approach is in conflict with the prevention against unwanted operation of overcurrent relays under faults on adjacent outgoing feeders connected to the same substation.

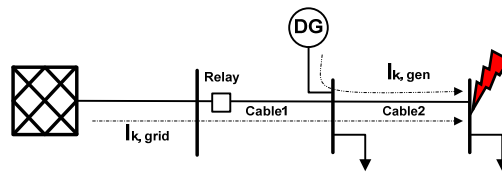


Figure 3.2. Principle of protection blinding [39]

3.2.3 Automatic reclosing

In overhead medium voltage networks, approximately 80% of the temporary faults are usually cleared with autoreclosing. The arc extinguishes during the dead time of the reclosing sequence. DG seems rather incompatible with reclosing practices. It can happen that DG prevents arc deionization and the temporary fault becomes persistent. In some cases during the dead time of the reclosing sequence the generators in the network tend to drift away from the frequency in relation to the network. Hence, a reconnection without any synchronization may cause serious damage to generator equipment. To avoid out-of-phase reclosing, quick and reliable Loss-of-Mains (islanding) [LOM] protection is required [40]. DG-units should be rapidly disconnected during the dead time of the reclosing sequence.

3.2.4 Unwanted islanding

Critical situations can occur when a part of a network is islanded and a DG-unit is connected. In most cases islanding is undesirable for the following reasons [41], [42]:

- Reconnection of an island is problematic, especially when automatic reclosing is applied.
- Power quality cannot be guaranteed in the island. There may occur voltage or frequency instability.
- Safety problems to maintenance personnel arise when islands are back-energized.

In order the distribution system to be safely and reliably protected, LOM protection is usually considered necessary. The requirements for LOM protection are specified in several interconnection regulations. Even though national and international recommendations vary in general, there are some common requirements described:

- In the case of voltage or frequency abnormality, DG should be disconnected from the network.
- In the case of autoreclosing application, the DG must be tripped from the network before the reclosing, so that there is enough time for the fault arc to extinguish.

Several techniques are available to detect the LOM condition. Typical passive techniques include under/overvoltage, under-/overfrequency, rate of change of frequency (ROCOF) and voltage vector shift. Active methods contain reactive error export and system impedance monitoring.

3.3 Case studies

The goal of this section is to determine whether typical network protection problems might occur in Dutch MV grids and if they do for which values of distribution network parameters. Since typical Dutch distribution networks predominantly consist of underground cables and only permanent faults occur, investigations are focused on the first two problems of protection blinding and false tripping.

3.3.1 Analysis of protection blinding

Initially, the problem of protection blinding has been examined. The influence of the number of DG-units, their relative position in the feeder and the total feeder length in the grid current contribution during different fault type disturbances was studied in more details. For this purpose, a simple test network with the structure shown in Figure 3.2 has been created. The test grid consists of an external grid and 3 MV nodes which are connected by 2 line connections. The 3-bus test network was defined and modelled in Matlab/Simulink environment. A Diesel synchronous generator with power 3.125 MVA was connected to the feeder. The studied cases were performed for both a regular underground cable and an overhead line connection. The cable connection was modeled as regular cable aluminium conductors with 240 mm² cross-section. The electrical parameters of both the cable and line types are given in Tables 3.1 and 3.2 [43]. The impedance of a cable system differs from the impedance of overhead lines. It can be seen from the tables that the impedance of the overhead line is larger than the impedance of the cable.

Table 3.1. Cable electrical parameters

Line type	Sequence	R [Ω /km]	H [Ω /km]	F [Ω /km]	Inom [A]
Cable	Positive/Negative	0.125	0.248e-3	0.5e-6	457
	Zero	0.835	0.471e-3	0.3e-6	

Table 3.2. Overhead line electrical parameters [43]

Line type	Sequence	R [Ω /km]	H [Ω /km]	F [Ω /km]	Inom [A]
Overhead line	Positive/Negative	0.37	1.274e-3	9e-9	430
	Zero	0.64	4.84e-3	8e-9	

For convenience a definite overcurrent relay was assumed at the beginning of the feeder. Concerning the cable case scenario, first the settings of the overcurrent relay at the beginning of the feeder were calculated for the different cable feeder lengths. These currents were calculated without the contribution of the generator. Subsequently, in the test grid the total feeder length, the location and the rated power of the generator were modified to investigate the blinding effect [44], [39]. The flowchart illustrated in Figure 3.3(a) contains three loops to modify the cable lengths (which determines the relative position of DG on the

feeder), the rated power of the generator and the total feeder length. The length of the two cables was adjusted by 20% of the total feeder length. L_Cable1 in the flowchart corresponds to the cable length between the feeding substation and the DG-unit. After the modification of the cable lengths, the second loop is entered which increases the total feeder length up to 50 km with a step of 5 km per iteration. The third loop increases the generator size. Repetitive calculations have been therefore performed. The maximum DG rated power is 9.375 MVA, which corresponds to 120% DG penetration level in the test grid (3 DG-units connected to the test grid).

Figure 3.4 displays the simulation results covering the three DG penetration levels and corresponds to different fault types. The blinding effect occurs in case the relay pickup current is higher than the grid current contribution, thus, when the grid current surface goes below the pickup current surface. As it can be observed from the figures there occurs no blinding even for 3 DG-units, for extremely long feeder lengths and two-phase fault type [39]. As the DG share increases, the blinding phenomenon becomes more dominant. Another significant observation is that the relative position of DG in the feeder plays an important role. Simulated results show that the most severe DG location (from the point of view of blinding problem) is approximately at the middle of the feeder for intermediate DG penetration levels.

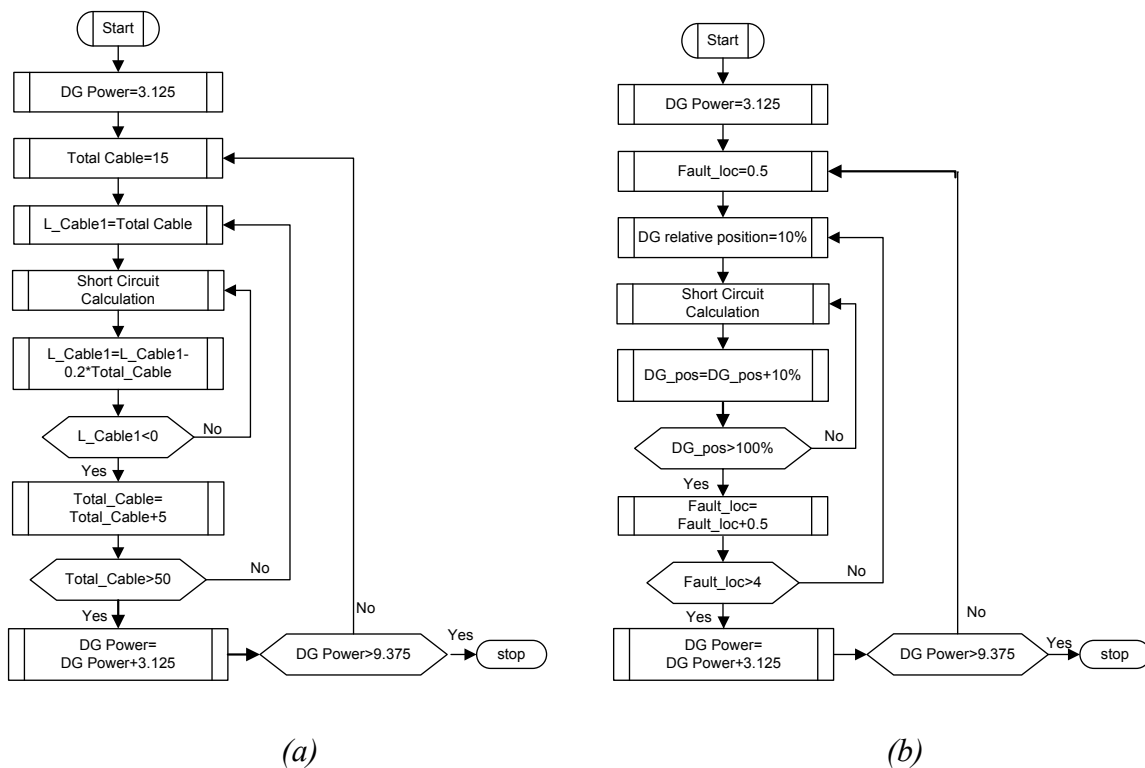


Figure 3.3. Flowchart illustrating the procedure of changing parameters a) protection blinding b) false tripping [44], [39]

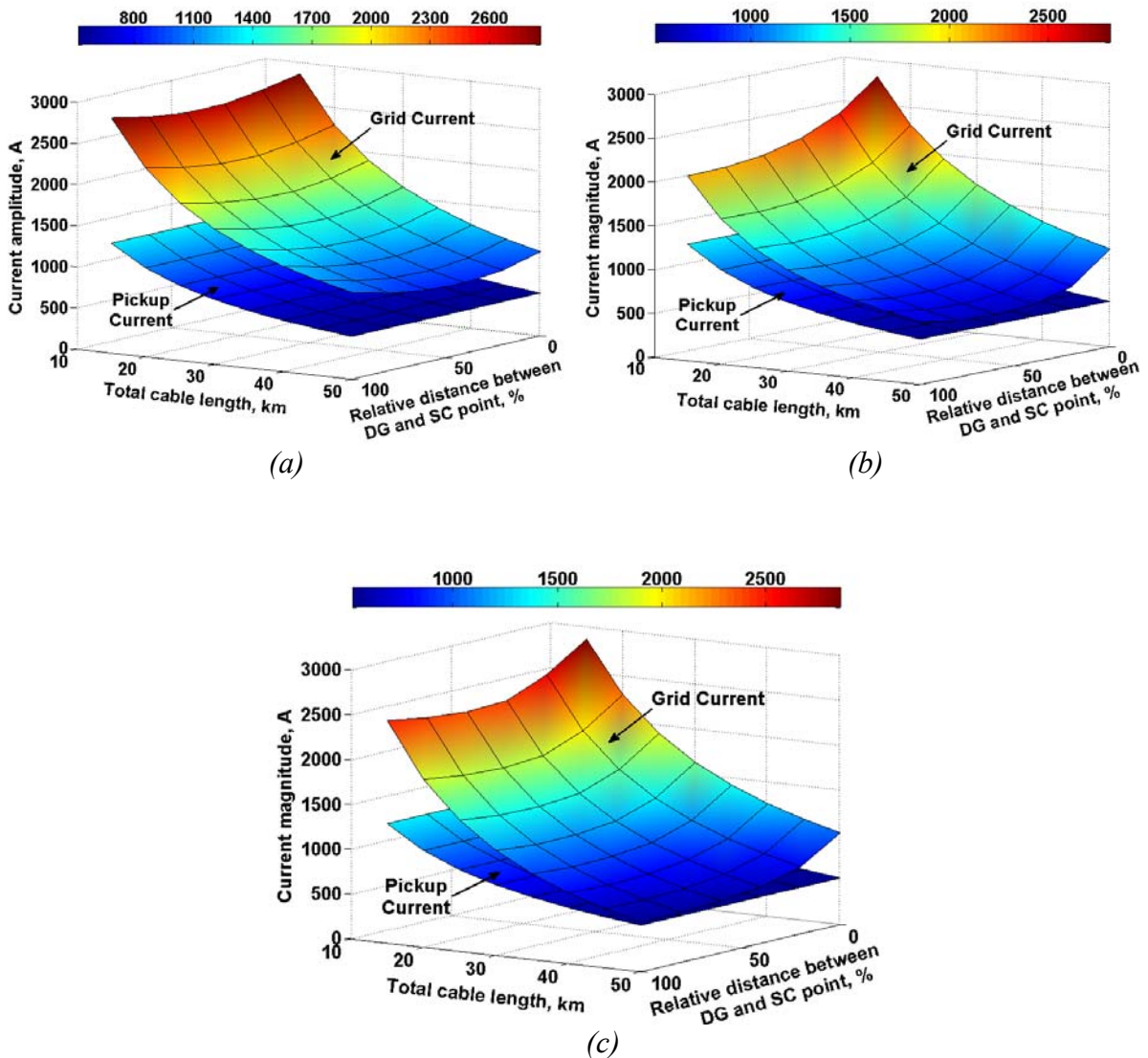


Figure 3.4. I_{grid} as function of the cable feeder length and DG position a) 1DG-unit, 3-phase fault b) 2DG-units, 2-phase fault c) 3DG-units, 3-phase fault [44], [39]

However, the equivalent scenario corresponding to the overhead line case reveals that problems arise for this case. Figure 3.5 presents the fault current seen by the relay for three different penetration levels and two different types of faults for the case of 15km total feeder length. The results reveal that blinding of protection occurs even for this short feeder length. Simulated results for longer feeder lengths are not depicted since the pickup current is below the nominal capacity of the line for these cases and for nominal load the feeder is switched off unnecessarily. For these cases, the pickup current needs to be modified to allow an overload of the feeder.

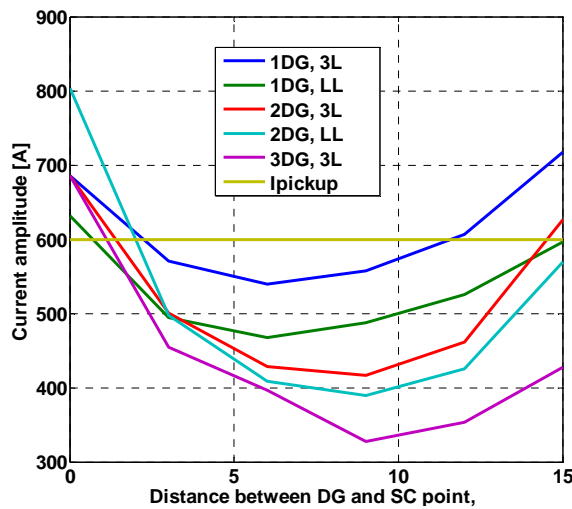


Figure 3.5. I_{grid} as function of DG position on the overhead line feeder

3.3.2 False tripping analysis

In order to study the problem of false tripping in more details, a similar procedure is repeated. DG interconnect protection has been omitted like in the previous case study.

The same test grid is extended with a second feeder in order to determine the impact of the grid parameters on the operation of the DG feeder relay (Relay1) in Figure 3.1. The fault location of the added feeder is iteratively modified within the range of 0.5 to 4 km with a step of 0.5 km, as illustrated in Figure 3.3(b). For each iteration, the relative position of the DG-unit in the feeder is adjusted by 10% of the full feeder length (15 km). The short-circuit contribution of the DG feeder is recorded for three different DG penetration levels in the network. Two scenario cases are performed corresponding to both cable and overhead line connections.

Figures 3.6 and 3.7 present the results obtained for the cases of the double and triple DG penetration level corresponding to the scenario case of the underground cable test network. As we can see, a false tripping occurs in both cases and the relative position of the DG in the feeder plays an important role. The results of the simulations show that the most severe DG location (from the point of view of false tripping) is at the beginning of the feeder. Additionally, it can be concluded that the situation is most probable when the fault location is near the substation. Similar results are obtained for the case of the feeder consisting of overhead lines, shown in Figure 3.8, with the significant difference that now the problem is much more expressed in comparison to the cable scenario for the 2DG penetration level.

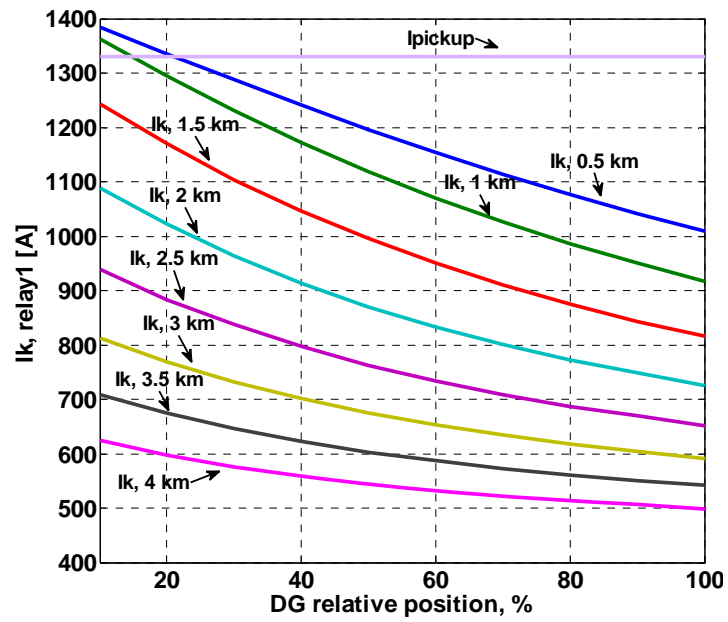


Figure 3.6. $I_{k''}$ of Relay1 as a function of the fault location and DG position (2DG-units).
(An underground cable scenario case).

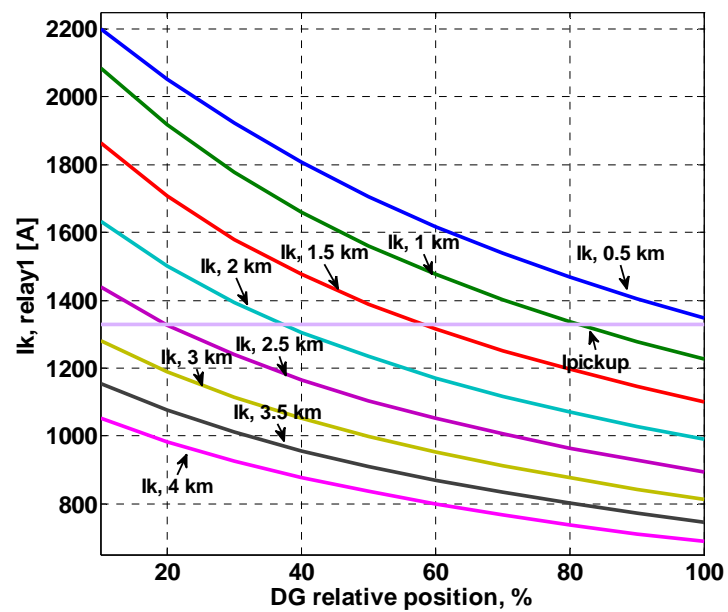


Figure 3.7. $I_{k''}$ of Relay1 as a function of the fault location and DG position (3DG-units).
(An underground cable scenario case).

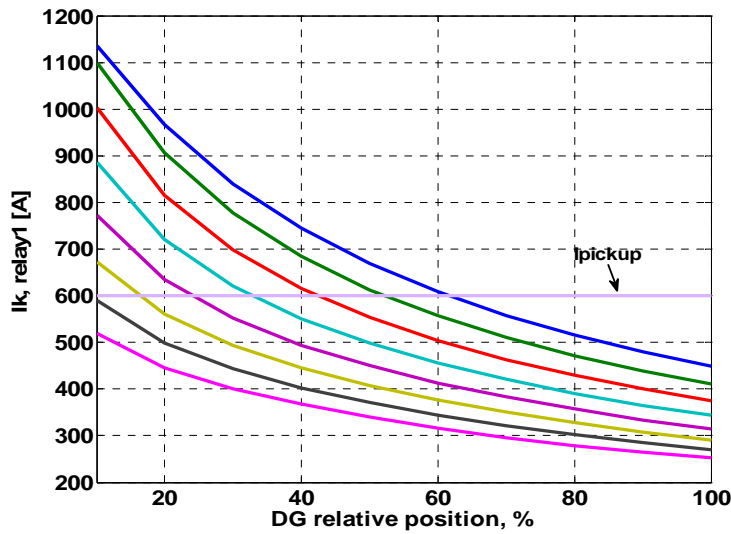


Figure 3.8. I_k of Relay1 as a function of the fault location and DG position (2DG-units). (An overhead line scenario case).

3.4 Evaluating conventional overcurrent time-graded protection schemes

3.4.1 Modeling of an existing MV grid using Matlab/Simulink

In this part of the chapter, conventional definite and inverse time overcurrent protection schemes have been evaluated for a typical large-scale distribution network in the Netherlands supplied with a high penetration level of DG-units, namely the 10 kV Lelystad distribution network. This network falls into the special category of the Dutch representative distribution networks whose feeders consist of underground cables featuring short lengths. These special characteristics of Dutch MV grids distinguish them from the rest European distribution networks which predominantly utilize overhead lines. The one-line schematic diagram of the Dutch cable MV network analyzed in this dissertation is shown in Figure 3.9. Six feeders with a total load of 10.8 MW are represented in detail, while the other feeders are modeled in the form of an aggregated load with 18 MW peak power consumption. The total installed capacity of the DG units is 10.7 MW. Based on this, the penetration level of DG (PL) can be determined. The PL is the ratio between the total active power of all DG-units installed in the given area P_{DG} and the peak active power of the load in the same area P_{load} [2]:

$$PL = \frac{P_{DG}}{P_{load}} \cdot 100\% = 37\% \quad (3.1)$$

Modeling and simulations have been performed by using Matlab/Simulink and SimPowerSystems toolbox. The DG-units in the test network are represented by:

- three Squirrel Cage Induction Generator (SCIG) wind turbines (SCIG1, SCIG2, SCIG3 in Figure 3.10) with apparent power ratings of 0.66 MVA each;
- a 0.25 MVA split shaft microturbine (Mturbine);
- two Combined Heat Power (CHP) plants each consisting of ten 0.25 MVA microturbines (CHP1, CHP2);
- a 3.125 MVA Diesel generator (Diesel).

All parameters of the Lelystad distribution network are given in Appendix A, whilst detailed information concerning the dynamic models of all DG-units included in the grid model can be found in Appendix B. A SCIG wind turbine model has been utilized, which is available in Matlab/SimPowerSystems. A detailed description of the wind turbine dynamic model is given in [45]. The diesel generator model [46] is characterized by the electrical and mechanical equations of a synchronous machine. Excitation and governor circuits of the generator are modeled as well. The model parameters of the split shaft microturbine and its detailed description can be found in [47]. Since the electromechanical behavior is of main interest for this study, the recuperator and the heat exchanger are not included in the model. The CHP generator model is an aggregated model consisting of 10 microturbines. All generators are connected to the network through Dyn transformers with grounded earth point on the low voltage side (not shown in Figure 3.9). The distribution network is coupled to the transmission grid using two 47 MVA 150/11 kV transformers. The loads are represented by constant impedances. The external system to which the distribution network is connected is assumed to behave as an ideal voltage source.

It is also worth pointing out that Lelystad distribution network exhibits a ring arrangement, even though it is radially operated. This ring architecture can be observed by the existence of 8 emergency ties (included in the network as demonstrated in Figure 3.9) which serve to provide alternative power supply routes in case of outages or scheduled interruptions. In the arrangement of a radial operation, these emergency ties (either between neighboring feeders or between parts of the feeder itself) consist of an open switch which maintains the radial structure of the grid during normal operations.

3.4.2 Relay protection settings

In the actual medium voltage grid, all feeders are equipped with definite time overcurrent relays. However, the section of the parallel connected cables in feeder ZPD 2.07 is protected with a combination of distance and overcurrent relays. Additionally, the busbars to which Tr3 is coupled, are protected with differential relays. The current settings of the relays are based on short-circuit calculations and the time grading is done in a way that selectivity is satisfied. Appropriate protection settings are found by calculating worst-case fault situations.

In this part of the chapter, the influence of different DG penetration levels on various protection schemes is discussed. Two protection schemes are evaluated:

- Protection by definite time overcurrent relays,
- Protection by inverse time overcurrent relays.

Simulations are repeated for two different DG penetration levels:

- PL1=37%, corresponding to the nominal DG penetration level,
- PL2=74%, (double penetration level) by keeping the same share of DG and halving the loading of the network ($L2=L1/2$).

The circuit breaker and relay locations along the feeders in the network are indicated by the small orange rectangles included in the schematic diagram of the grid, as displayed in Figure 3.9. The considered definite and inverse time overcurrent protection schemes have been evaluated for classical time grading of 300ms for the successive feeder relays in order to guarantee selectivity. The pickup value of the definite overcurrent relays is based on 50% of the end-of-section phase-to-phase fault current. The short-circuit currents were calculated without the contribution of the plants. Furthermore, I_{pickup} was checked to be larger than 200% of the feeder maximum load current. For the settings of the inverse time overcurrent relays, the parameters of the pickup current I_{pickup} and the time multiplier k are determined. The pickup current value is obtained by applying:

$$I_{pickup} = \frac{1,5 \cdot I_{nom}}{CTR} \quad (3.2)$$

In (3.2) I_{nom} is the nominal current of the protected feeder and CTR is the Current Transformer (CT) transformation ratio. The time multiplier setting is determined by:

$$k = \frac{t}{\beta} \left[\left[\frac{I_k^n}{I_{pickup}} \right]^{-1} \right]^\alpha + t_{grading} \quad (3.3)$$

The lowest time multiplier setting is assigned to the relay which is farthest from the source. The time multiplier settings are calculated for a normal inverse characteristic ($\alpha=0.02$ and $\beta=0.14$) and $t_{grading}=0.3$ s. The values of the time multiplier settings k are calculated by equation (3.3) based on the selected pick-up and fault currents, the selected relay characteristic and the associated fault clearing time of each relay along the feeder. In Table 3.3 an overview of the relay settings of both protection schemes is given. The CTs and VTs have been modeled by taking into account their corresponding ratios, which are additionally displayed in Table 3.3.

Furthermore, the interconnect protection of the DG-unit itself at the Point of Common Coupling (PCC) was taken into account. The major functions of an interconnect protection are [48]:

- Disconnection of DG when it is no longer operating in parallel with the distribution network,
- Protection of the grid system from damage caused by the connection of DG,
- Protection of the generator from damage from the grid system.

The inclusion of the DG interconnect protection is of the highest interest since it gives us the opportunity to observe the coordination between the network protection and the DG

connection protection as well as to investigate their possible interference. In the modeling, the DG connection point was equipped with typical protection devices for under/overvoltage. No separate relays for islanding detection are used. The DG interconnect protection locations are indicated by the small red circles included in the schematic diagram of the grid, depicted in Figure 3.11. The DG interconnect protection settings are presented in Table 3.4. Figure 3.10 depicts the position of the DG interconnect protection at the PCC.

Table 3.3. Overview of overcurrent protection settings

Relay	CT ratio	Definite time		Inverse time	
		$I_{>>}$ [A] [Primary side]	$t_{>>}$ [s]	k	I_p [Primary side]
G1	750/5	2000	0.325	0.1038	720
G2	750/5	2000	0.325	0.1038	720
G3	750/5	2000	0.325	0.1038	720
G7	300/5	2000	0.025	0.0106	360
B1	200/5	2000	0.325	0.1349	240
B2	200/5	1800	0.025	0.0104	240
R1	300/5	2000	0.025	0.012	360
C1	100/5	2000	0.025	0.0145	120
D1	400/5	2000	0.325	0.124	480
D2	250/5	1500	0.025	0.0113	300
E1	400/5	2000	0.925	0.2249	480
E2	400/5	1500	0.625	0.152	480
E3	200/5	1500	0.325	0.1125	240
E4	100/5	1000	0.025	0.0113	120

Table 3.4. DG-units protection settings

Protection type	Setting	Operation time [s]
Undervoltage $V<$	0.9 p.u.	1
Undervoltage $V<<$	0.8 p.u.	0.2
Overvoltage $V>$	1.1 p.u.	30
Overvoltage $V>>$	1.15 p.u.	0.2

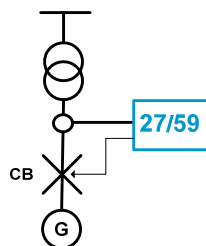


Figure 3.10. Location of the DG interconnect protection

Relays G4, G5 and G6 are modeled with an impedance distance characteristic. Since the impedance distance characteristic is inherently non-directional, it is supervised by a directional element to avoid trippings for faults behind the relays. The directional elements

are set to trip in a forward direction of the power flow. For the directional impedance distance relays G4, G5 and G6, we assumed that their first zone operation covers the 80% of the length of their protected cables and that their second zone of operation covers the 120%. The total impedance of the protected cable that each impedance distance relay monitors equals to:

$$Z_i = 7.37 \cdot (0.0469 + j \cdot 0.0899) = 0.3456 + j \cdot 0.6629 \quad (3.4)$$

The calculated impedance ratios utilized by the directional impedance distance relays, are determined as follows:

$$\text{Impedance ratio} = \frac{\text{Voltage ratio of the VT}}{\text{Current ratio of the CT}} \quad (3.5)$$

Therefore for each impedance relay holds according to the provided data:

$$\text{Impedance ratio} = \frac{10.000/100}{750/5} = 0.67 \quad (3.6)$$

Accordingly, the settings for the distance relays are set as:

$$Z_1 = ((0.3456 + j \cdot 0.6629) / 0.67) \cdot 0.8 = 0.4127 + j \cdot 0.7916 \quad (3.7)$$

$$Z_2 = ((0.3456 + j \cdot 0.6629) / 0.67) \cdot 1.5 = 0.77385 + j \cdot 1.4842 \quad (3.8)$$

$$|Z_1| = 0.8927 \quad (3.9)$$

$$|Z_2| = 1.3391$$

The values of the impedances in equations (3.4) through (3.9) are given in Ohms. The settings for the distance relays were set as:

- $Z_{AB/BC/CA}$ (first zone) = 0.8927, $t_{\text{delay}} = 0.025$ s
- $Z_{AB/BC/CA}$ (second zone) = 1.3391, $t_{\text{delay}} = 0.325$ s

Figure 3.11 depicts the phase-to-phase impedance elements of the first and second zone of relays G4, G5 and G6.

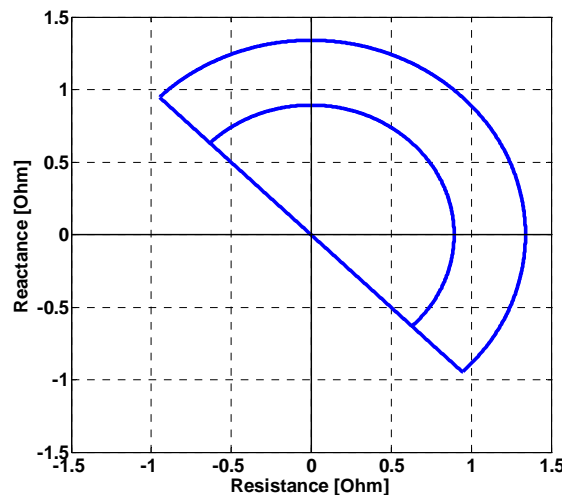


Figure 3.11. First and second zone phase-to-phase impedance elements in Ohm-phase domain

3.5 Simulation results

In order to analyze thoroughly the effects of the DG on the requirements for the protection of distribution networks, detailed simulation studies are required. Therefore, simulations are carried out to investigate the influence of the contribution of the DG-units to the short-circuit current on the fault clearing time. The definite and inverse time protection schemes and settings are applied on the investigated network and simulations are performed to evaluate the impact of the DG on the operation of network protection. Therefore, the simulation results are obtained after having applied the network protection settings displayed in Tables 3.3 and 3.4. One of the key issues was to study the coordination between network protection and the protection of the DG-units.

The system is subjected to various three-phase and two-phase faults at different locations, as shown in Figure 3.9. The justification for this choice is that the incorporation of DG-units into the grid influences the operating conditions of the protective relays only under inter-phase faults and not for ground faults. The reason for this is the fact that the DG-unit transformers have an isolated neutral point at the MV-side. As a result of that, they do not influence the zero-sequence fault current level and its flow in the distribution network. Another significant point is that the single-phase-to-ground short-circuits are self-extinguishing faults in underground cable systems since Dutch MV-grids are operated on an isolated grounding principle [7]. These are the reasons why only three-phase and inter-phase short-circuits were taken into account.

Tables 3.5, 3.6, 3.7 and 3.8, depict the simulation results for four different scenario cases:

- Scenario case 1: definite time protection scheme for PL1
- Scenario case 2: inverse time protection scheme for PL1
- Scenario case 3: definite time protection scheme for PL2
- Scenario case 4: inverse time protection scheme for PL2

Regarding the fault locations in the section of the parallel connected cables:

- Fault 1a is a two-phase fault located at a 75% distance from relay G4
- Fault 1b is a three-phase fault located at a 40% distance from relay G4
- Fault 2a is a two-phase fault located at a 90% distance from relay G5
- Fault 2b is a three-phase fault located at a 95% distance from relay G5

Fault initiation is at 100 ms for all case scenarios. Fault clearing time indicates the total sum of the relay tripping time and the circuit breaker contact opening time since the instant of fault inception. The circuit breaker contact opening time is assumed to be 75ms for all the investigated case scenarios. The fault locations and types, the triggered relays and their corresponding fault clearing times, and finally the disconnection time of the DG-units (all in sec) are presented for all case scenarios.

In general, the simulation results verified that the conventional network protection schemes are not adequate when there is a high share of DG-units connected to the network.

The evaluation of the current applied protection schemes shows that while the proper relays are triggered, almost all DG-units are disconnected by the undervoltage protection before the fault is cleared by the grid protection. For the definite and inverse time studied protection schemes as well as for both DG penetration levels, we observe that for fault locations #1a, #1b, #2a, #2b, #4, #9 and #11 all DG-units of the grid get disconnected before the fault is cleared by the grid protection. A similar situation holds for fault locations #10, #12 and #13 for which loss of all the generators of the complete faulty feeder is noticed. The DG-units remain connected to the network only in the cases when the fault clearing time is shorter than the DG interconnect protection disconnection time. This can be observed in the cases of fault locations #3, #5, #6, #7, #8 and #14.

*Table 3.5. Scenario case I: definite-time protection scheme, PL1
Fault clearing time and DG availability [39]*

Fault location / type	Relay t_{FCT} [s]	SCIG1 t_{disc} [s]	SCIG2 t_{disc} [s]	SCIG3 t_{disc} [s]	CHP1 t_{disc} [s]	CHP2 t_{disc} [s]	Diesel t_{disc} [s]	Mturbine t_{disc} [s]
1a / LL	G4 0.219 G1 0.529	0.387 V<<	0.387 V<<	0.387 V<<	0.388 V<<	0.386 V<<	0.389 V<<	0.382 V<<
1b / 3L	G1 0.528 G4 0.217	0.386 V<<	0.386 V<<	0.386 V<<	0.386 V<<	0.385 V<<	0.388 V<<	0.382 V<<
2a / LL	G2 0.528 G5 0.518	0.381 V<<	0.381 V<<	0.382 V<<	0.382 V<<	0.381 V<<	0.387 V<<	0.379 V<<
2b / 3L	G2 0.526 G5 0.445	0.378 V<<	0.378 V<<	0.379 V<<	0.378 V<<	0.378 V<<	0.383 V<<	0.377 V<<
3 / 3L	G7 0.203	-	-	-	-	-	-	-
4 / LL	B1 0.505	0.380 V<<	0.380 V<<	0.380 V<<	0.390 V<<	0.389 V<<	0.392 V<<	0.388 V<<
5 / LL	B2 0.209	0.381 V<<	0.381 V<<	0.381 V<<	-	-	-	-
6 / 3L	R1 0.202	-	-	-	-	-	-	-
7 / 3L	C1 0.202	-	-	-	-	-	-	-
8 / LL	D2 0.204	-	-	-	-	-	0.380 V<<	-
9 / 3L	D1 0.503	0.388 V<<	0.389 V<<	0.389 V<<	0.377 V<<	0.388 V<<	0.378 V<<	0.385 V<<
10 / LL	D1 0.505	-	-	-	0.386 V<<	-	0.386 V<<	-
11 / 3L	E1 1.103	0.389 V<<	0.390 V<<	0.390 V<<	0.394 V<<	0.377 V<<	0.456 V<<	0.377 V<<
12 / LL	E2 0.807	-	-	-	-	0.388 V<<	-	0.380 V<<
13 / LL	E3 0.510	-	-	-	-	0.392 V<<	-	0.380 V<<
14 / LL	E4 0.216	-	-	-	-	-	-	-

As aforementioned, simulation of short-circuits for all different scenario cases show that all disturbances are cleared. Protection blinding is not observed since all faults are

cleared each time by the appropriate relays. Thus, generally speaking it can be concluded that the protection of the Lelystad distribution network is not affected by the connection of DG-units in terms of protection blinding. This is justified by the fact that the investigated network is characterized by relatively short cable lengths and high short-circuit power of the external (transmission) grid.

*Table 3.6. Scenario case II: inverse-time protection scheme, PL1
Fault clearing time and DG availability*

Fault location / type	Relay t_{FCT} [s]	SCIG1 t_{disc} [s]	SCIG2 t_{disc} [s]	SCIG3 t_{disc} [s]	CHP1 t_{disc} [s]	CHP2 t_{disc} [s]	Diesel t_{disc} [s]	Mturbine t_{disc} [s]
1a / LL	G4 0.219 G1 0.419 D2 0.410	0.387 V<<	0.387 V<<	0.387 V<<	0.388 V<<	0.386 V<<	0.389 V<<	0.382 V<<
1b / 3L	G1 0.418 G4 0.217	0.386 V<<	0.386 V<<	0.386 V<<	0.386 V<<	0.385 V<<	0.388 V<<	0.382 V<<
2a / LL	G2 0.418 G5 0.518 D2 0.321	0.381 V<<	0.381 V<<	0.382 V<<	0.382 V<<	0.381 V<<	0.387 V<<	0.379 V<<
2b / 3L	G2 0.416 G5 0.445 D2 0.340	0.378 V<<	0.378 V<<	0.379 V<<	0.378 V<<	0.378 V<<	0.383 V<<	0.377 V<<
3 / 3L	G7 0.201	-	-	-	-	-	-	-
4 / LL	B1 0.432	0.380 V<<	0.380 V<<	0.380 V<<	0.390 V<<	0.389 V<<	0.392 V<<	0.388 V<<
5 / LL	B2 0.207	0.381 V<<	0.381 V<<	0.381 V<<	-	-	-	-
6 / 3L	R1 0.200	-	-	-	-	-	-	-
7 / 3L	C1 0.197	-	-	-	-	-	-	-
8 / LL	D2 0.205	-	-	-	-	-	0.380 V<<	-
9 / 3L	D1 0.496 D2 0.312	0.389 V<<	0.389 V<<	0.389 V<<	0.377 V<<	0.388 V<<	0.378 V<<	0.387 V<<
10 / LL	D1 0.573 D2 0.318	-	-	-	0.386 V<<	-	0.386 V<<	-
11 / 3L	E1 0.721	0.389 V<<	0.390 V<<	0.390 V<<	0.394 V<<	0.377 V<<	0.456 V<<	0.377 V<<
12 / LL	E2 0.699	-	-	-	-	0.388 V<<	-	0.380 V<<
13 / LL	E3 0.503	-	-	-	-	0.392 V<<	-	0.380 V<<
14 / LL	E4 0.206	-	-	-	-	-	-	-

Another significant observation is that false tripping takes place in the case of inverse time protection schemes for both cases of DG penetration level. This happens for fault locations which are very close to the main substation and for fault locations close to a strong sustainable short-circuit current contributing synchronous generator. For example, it occurs for disturbances located at #2a, #2b, #9 and #10.

Furthermore, we can see that the current protection schemes, featuring in most of the cases a simple time-graded overcurrent protection philosophy along each outgoing feeder of the main substation, allow the acceptance of loss of a complete feeder or large parts of the feeders. Additionally, the assessment of the clearing time for different fault locations helps to compare the performance of the different overcurrent time-graded protection schemes. Comparison of the definite and inverse protection schemes leads to the conclusion that inverse overcurrent protection yields shorter fault clearing time in comparison to the definite overcurrent protection. Nevertheless, it does not prevent the massive DG disconnection for faults located everywhere on the network and it additionally allows the isolation of large parts of the feeder.

*Table 3.7. Scenario case III: definite-time protection scheme, PL2
Fault clearing time and DG availability*

Fault location / type	Relay t_{FCT} [s]	SCIG1 t_{disc} [s]	SCIG2 t_{disc} [s]	SCIG3 t_{disc} [s]	CHP1 t_{disc} [s]	CHP2 t_{disc} [s]	Diesel t_{disc} [s]	Mturbine t_{disc} [s]
1a / LL	G4 0.219	0.387	0.387	0.387	0.388	0.386	0.389	0.382
	G1 0.529	V<<	V<<	V<<	V<<	V<<	V<<	V<<
1b / 3L	G1 0.528	0.386	0.386	0.386	0.386	0.385	0.388	0.382
	G4 0.217	V<<	V<<	V<<	V<<	V<<	V<<	V<<
2a / LL	G2 0.528	0.381	0.381	0.382	0.382	0.381	0.387	0.379
	G5 0.518	V<<	V<<	V<<	V<<	V<<	V<<	V<<
2b / 3L	G2 0.526	0.378	0.378	0.379	0.378	0.378	0.383	0.377
	G5 0.445	V<<	V<<	V<<	V<<	V<<	V<<	V<<
3 / 3L	G7 0.203	-	-	-	-	-	-	-
4 / LL	B1 0.505	0.380	0.380	0.380	0.390	0.389	0.391	0.388
		V<<	V<<	V<<	V<<	V<<	V<<	V<<
5 / LL	B2 0.209	0.381	0.381	0.381	-	-	-	-
		V<<	V<<	V<<				
6 / 3L	R1 0.203	-	-	-	-	-	-	-
7 / 3L	C1 0.203	-	-	-	-	-	-	-
8 / LL	D2 0.204	-	-	-	-	-	0.379 V<<	-
9 / 3L	D1 0.503	0.388	0.388	0.388	0.376	0.384	0.377	0.384
		V<<	V<<	V<<	V<<	V<<	V<<	V<<
10 / LL	D1 0.505	-	-	-	0.379 V<<	-	0.380 V<<	-
11 / 3L	E1 1.103	0.388	0.389	0.389	0.385	0.376	0.392	0.376
		V<<	V<<	V<<	V<<	V<<	V<<	V<<
12 / LL	E2 0.807	-	-	-	-	0.380 V<<	-	0.378 V<<
13 / LL	E3 0.513	-	-	-	-	0.387 V<<	-	0.378 V<<
14 / LL	E4 0.216	-	-	-	-	-	-	-

This is shown in Figure 3.12 which depicts the fault currents seen by relays E1 and E2 following different types of faults at locations #11 and #12 for both definite and inverse

time protection schemes corresponding to penetration level 1 as well as 2. For all cases inverse time relays activate faster and it can be additionally observed that there is small fault current magnitude difference between the scenario cases I/II and the scenario cases III/IV. The major conclusion that can be drawn is that the penetration level does not play an important role whilst the predominant element regarding the fault current contribution is determined by the short-circuit power of the external grid. Moreover, Figure 3.13 illustrates the terminal voltage of the DG-units following a three-phase fault at location #11 for both definite and inverse time protection schemes corresponding to penetration level 1. It can be observed that for the generators which are connected to the faulty zone the voltage gets zero, whilst for the remaining DG-units the voltage retains its nominal voltage after fault clearance for both cases. The difference in the voltage dip duration, between scenario case I and II, can be clearly noticed.

*Table 3.8. Scenario case IV: inverse-time protection scheme, PL2
Fault clearing time and DG availability*

Fault location / type	Relay t_{FCT} [s]	SCIG1 t_{disc} [s]	SCIG2 t_{disc} [s]	SCIG3 t_{disc} [s]	CHP1 t_{disc} [s]	CHP2 t_{disc} [s]	Diesel t_{disc} [s]	Mturbine t_{disc} [s]
1a / LL	G4 0.219 G1 0.419 D2 0.410	0.387 V<<	0.387 V<<	0.387 V<<	0.388 V<<	0.386 V<<	0.389 V<<	0.382 V<<
1b / 3L	G1 0.418 G4 0.217	0.386 V<<	0.386 V<<	0.386 V<<	0.386 V<<	0.385 V<<	0.388 V<<	0.382 V<<
2a / LL	G2 0.418 G5 0.518 D2 0.321	0.381 V<<	0.381 V<<	0.382 V<<	0.382 V<<	0.381 V<<	0.387 V<<	0.379 V<<
2b / 3L	G2 0.416 G5 0.445 D2 0.340	0.378 V<<	0.378 V<<	0.379 V<<	0.378 V<<	0.378 V<<	0.383 V<<	0.377 V<<
3 / 3L	G7 0.201	-	-	-	-	-	-	-
4 / LL	B1 0.431	0.380 V<<	0.380 V<<	0.380 V<<	0.390 V<<	0.389 V<<	0.391 V<<	0.389 V<<
5 / LL	B2 0.207	0.382 V<<	0.382 V<<	0.382 V<<	-	-	-	-
6 / 3L	R1 0.200	-	-	-	-	-	-	-
7 / 3L	C1 0.197	-	-	-	-	-	-	-
8 / LL	D2 0.206	-	-	-	-	-	0.380 V<<	-
9 / 3L	D1 0.493 D2 0.369	0.392 V<<	0.392 V<<	0.392 V<<	0.377 V<<	0.391 V<<	0.378 V<<	0.388 V<<
10 / LL	D1 0.569 D2 0.332	-	-	-	0.387 V<<	-	0.383 V<<	-
11 / 3L	E1 0.721	0.392 V<<	0.393 V<<	0.393 V<<	0.394 V<<	0.377 V<<	0.403 V<<	0.377 V<<
12 / LL	E2 0.695	-	-	-	-	0.389 V<<	-	0.380 V<<
13 / LL	E3 0.500	-	-	-	-	0.400 V<<	-	0.380 V<<
14 / LL	E4 0.205	-	-	-	-	-	-	-

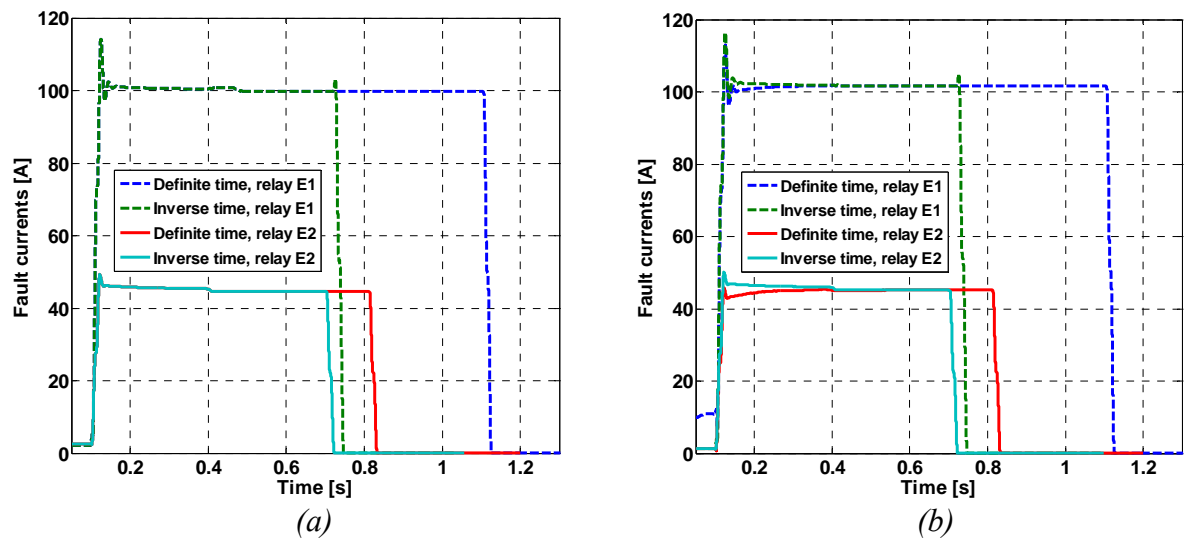


Figure 3.12. I_k'' of relay E1 following a three-phase fault at location #11 (dotted plots). I_k'' of relay E2 following a two-phase fault at location #12, (continuous plots). (a) The plots correspond to scenario cases I and II (b) the equivalent plots for scenario cases III and IV

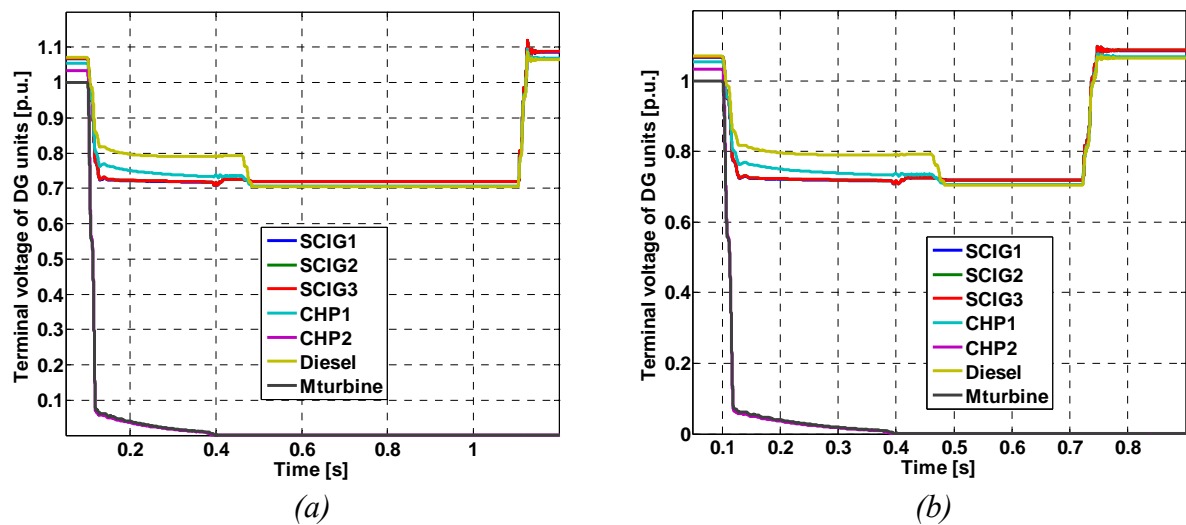


Figure 3.13. Terminal voltage (in [p.u.]) of DG-units following a three-phase fault at location #11 a) for scenario case I b) for scenario case II

3.5.1 Nuisance tripping of DG-units scenario

As aforementioned, for all scenario cases the vast majority of disturbances lead to mass disconnection of DG-units in the network. Figure 3.14 depicts the variation of terminal voltage, terminal current, active and reactive power of the DG-units for a three-phase fault at location #9 corresponding to scenario case 1 (application of definite time protection scheme and PL1). It is clearly seen that at the moment of DG disconnection active/reactive

powers and terminal currents become zero. It can be also seen that the synchronous generator contributes a sustainable short-circuit current to the disturbance in contradiction with the rest induction-based DG-units.

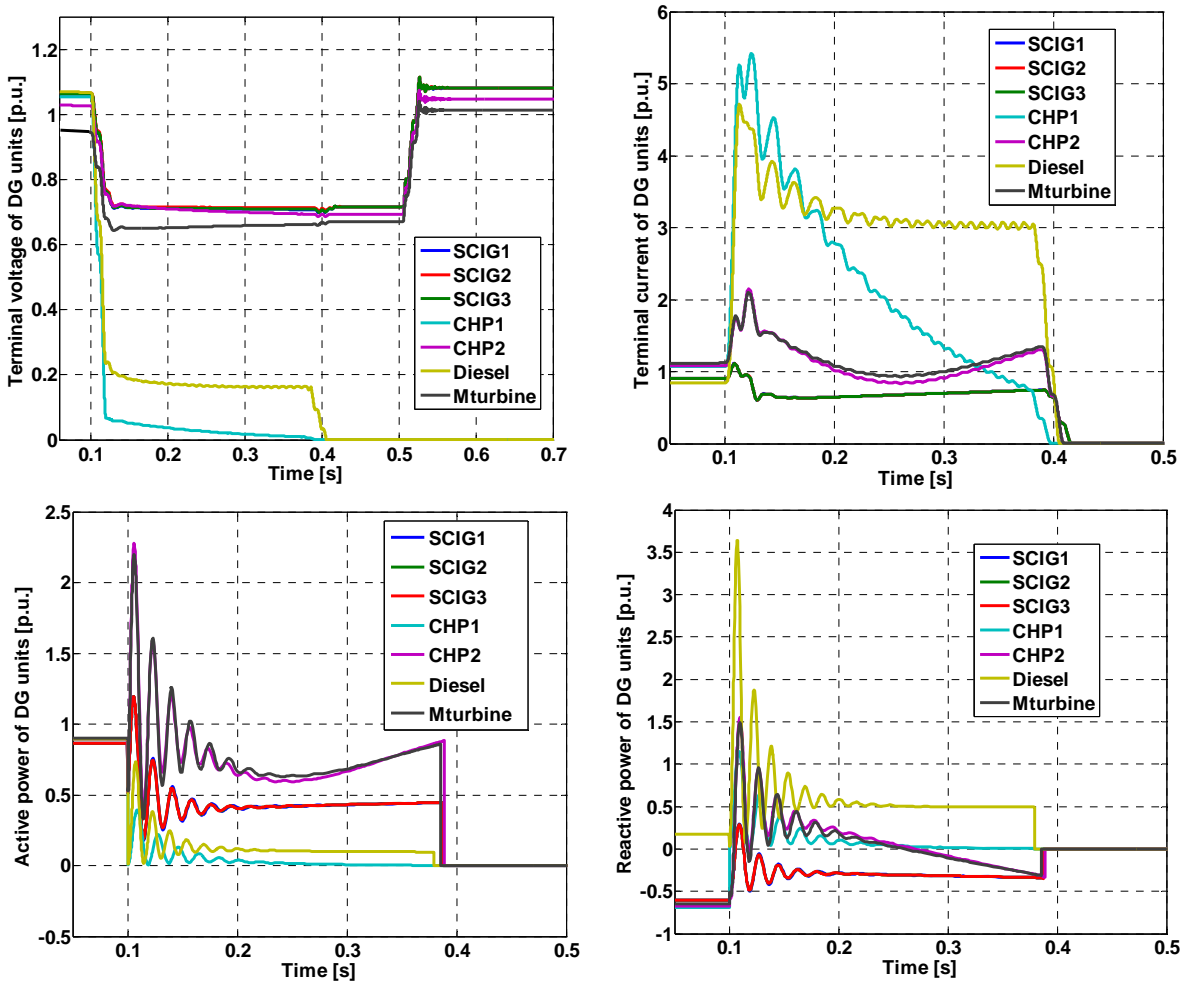


Figure 3.14. Terminal voltage, terminal current, active and reactive power in [p.u.] of DG-units following a three-phase fault at location #9 for scenario case I. [39]

Additionally, it can be observed that the terminal voltage of the DG-units connected to the faulty section of the feeder becomes zero while for the rest of the disconnected generators the terminal voltage at the PCC retains its nominal value reflecting the clearance of the fault. The major outcome of this section is that in the future a fast protection scheme is required to prevent the DG disconnection in the sound zones.

3.5.2 Sympathetic tripping scenario

The most problematic cases (from the point of view of false tripping) are three-phase faults occurring below the first downstream protective device of the feeders which do not include DG-units such as feeders 2.18, 2.03, ZPD 2.07. The possibility of sympathetic

tripping of relays in the network for these worst case scenarios during upstream fault currents was thus thoroughly examined and plots derived from these simulation results are provided in this section. For a three-phase fault located at point #7, fault current peaks of relays B1, E1 and D1 are observed, as depicted in Figure 3.15. However, the current contributions decay rapidly and therefore, cannot cause unwanted feeder tripping even with the initial settings. Since the contributions of all feeders remain under their pick-up currents, false tripping does not occur for this fault location. Figure 3.15 illustrates the upstream fault currents of relays D1, E1 and B1 covering all the different scenario cases. It can be observed by these plots that the fault clearing time is identical for both protection schemes and penetration levels. Additionally, it is noticed that for penetration level 2 the upstream fault current contribution is higher versus the short-circuit current contribution for penetration level 1, as expected. Conclusively, it can be said that the maximum upstream fault current contribution is negligible in comparison to the initial settings. It is evident that since the worst-case faults at the beginning of the studied feeders do not cause problems, there are no expected problems regarding the upstream currents during disturbances for longer distances on the faulted feeders.

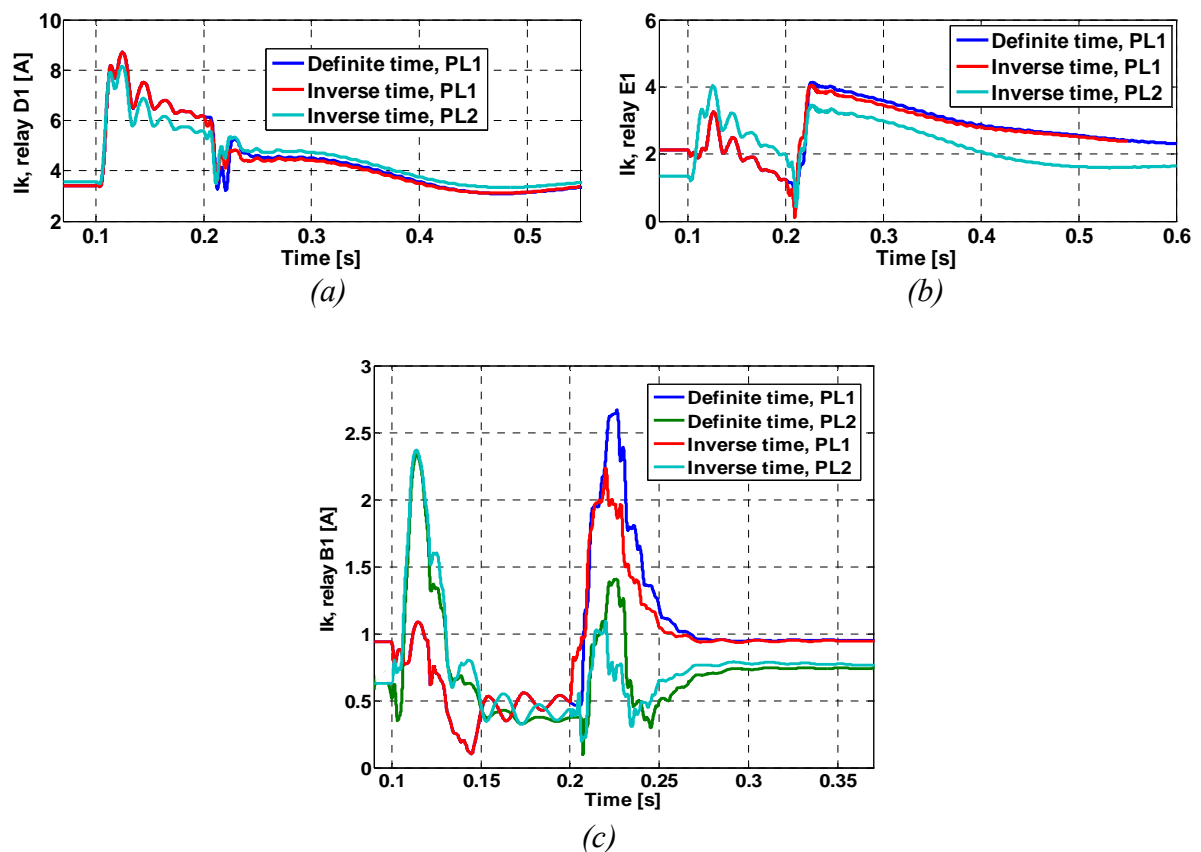


Figure 3.15. (a) I_k of relay D1 following a three-phase fault at location #7, for scenario cases I, II and IV (b) I_k of relay E1 following a three-phase fault at location #7 for scenario cases I, II and IV (c) I_k of relay B1 following a three-phase fault at location #7 for scenario cases I, II, III and IV

Figure 3.16 depicts the variation of terminal voltage, terminal current, active and reactive power of the DG-units for the three-phase fault at location #7 corresponding to scenario case 1 (i.e. application of definite time protection scheme and PL1). It is clearly seen that all DG-units remain connected to the network and all their terminal parameters retain their nominal values. It is additionally observed that the terminal voltage dip magnitude of all DG-units drops below 0.8 [p.u.], however the fault clearing time is less than 200 ms, so generators do not get disconnected.

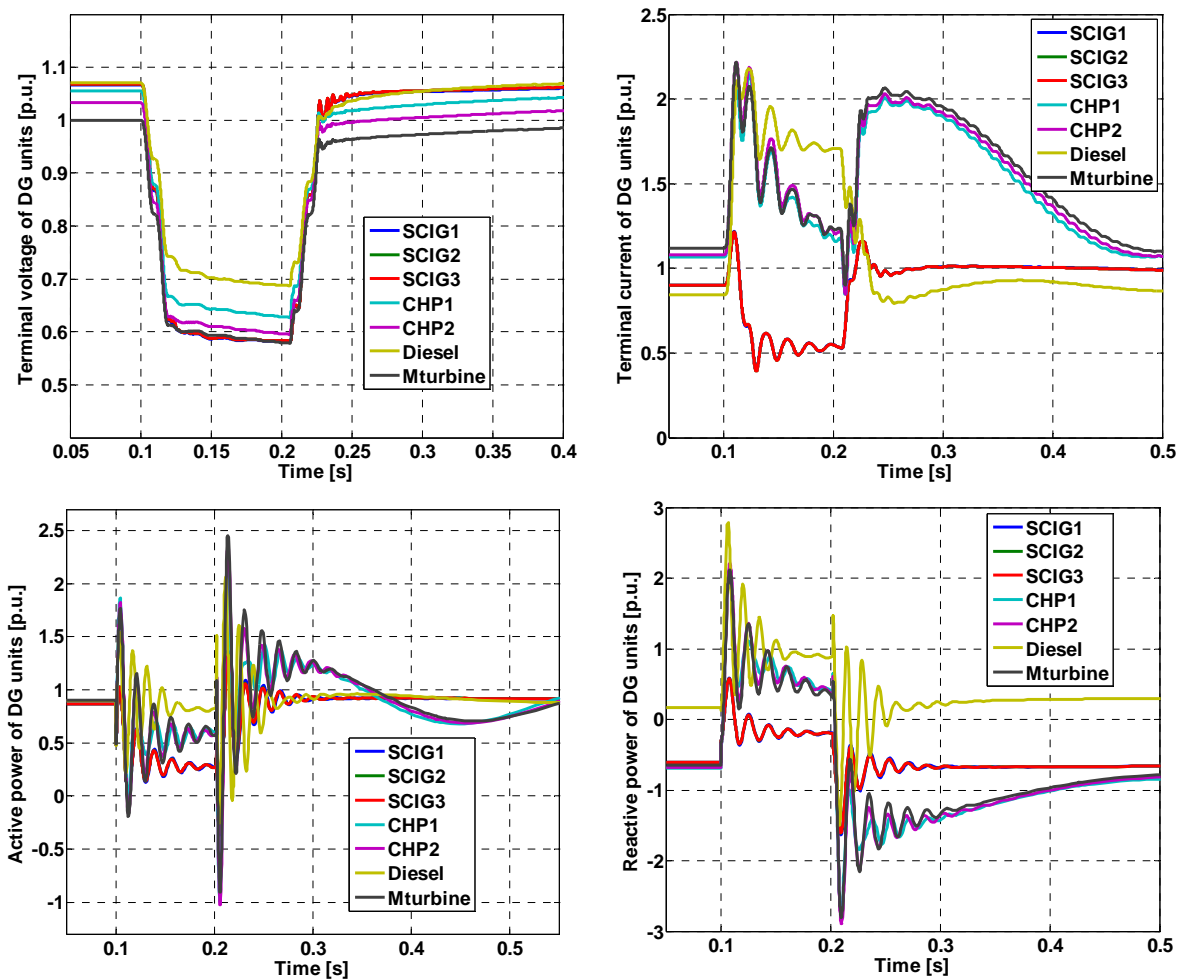


Figure 3.16. Terminal voltage, terminal current, active and reactive power in [p.u.] of DG-units following a three-phase fault at location #7 for scenario case I.

As aforementioned, during the short-circuit calculations for each fault location the contribution of all feeders, which are connected to the main substation, is assessed. However, we can see that for some locations false tripping occurs. For these cases, the feeder contributions exceed the pick-up currents of the corresponding protective devices.

Figure 3.17(a) presents the fault currents seen by the triggered relays following a three-phase fault at location #9 (represented by the dotted lines on the plot) for scenario cases I and II. It can be seen that the fault is cleared by the relay D1 for both definite and inverse

time protection schemes and having almost identical fault clearing time, however relay D2 is also unnecessarily triggered because of the high fault current contribution of the Diesel driven synchronous generator. The continuous plots in the same figure depict the fault currents seen by the triggered relays of the grid following a two-phase fault at location #10, once again corresponding to scenario cases I and II. In this case, the inverse time characteristics of relay D1 give a longer tripping time versus to the equivalent definite time characteristics. The justification for this is that location #10 is more distant to the relay D1 and the Diesel generator has been already unnecessarily disconnected. Similar plots indicating the false tripping of relay D2 are displayed (Figure 3.17(b)) for fault locations #2a and #2b covering the protection systems of both definite and inverse time characteristics.

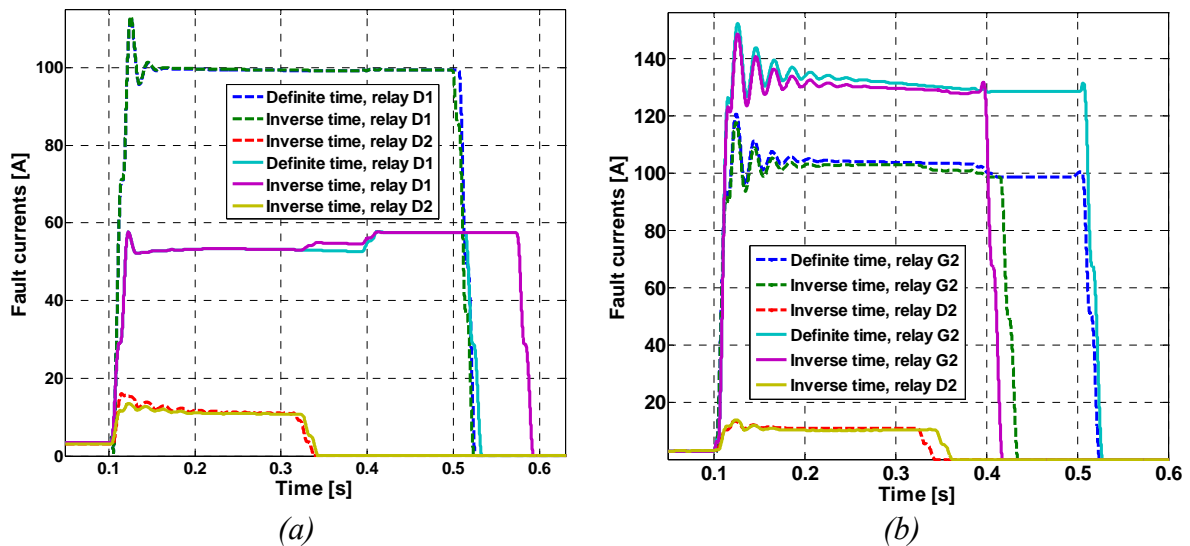


Figure 3.17. (a) I_k'' of triggered relays following a three-phase fault at location #9, for scenario cases I and II (dotted plots). I_k'' of triggered relays following a two-phase fault at location #10, for scenario cases I and II (continuous plots) (b) I_k'' of triggered relays following a two-phase fault at location #2a, for scenario cases I and II (dotted plots). I_k'' of triggered relays following a three-phase fault at location #2b, for scenario cases I and II (continuous plots)

3.5.3 Intensity of protection blinding scenario

The worst case fault scenarios in terms of protection blinding, are phase-to-phase short-circuit faults occurring at the end of the feeders including DG-units. Therefore, in this section these kinds of disturbances are analyzed. Figure 3.18 depicts the fault currents seen by relays B2 and D1 following a two-phase fault at locations #5 and #10 equivalently and covering all possible scenario cases both with and without DG-units connected to the investigated network. As it can be seen from the plots, the blinding phenomenon can be hardly observed and it is not likely to result in protection blinding problems in the test grid.

Therefore, correct protection operation (in terms of protection blinding) is not endangered as fault currents remain still much higher than protection settings. This can be additionally justified by the fact that Lelystad Distribution Network is a relatively powerful grid characterized by short feeder lengths. The contribution of the DG-units to the short-circuit currents are marginal and so is the effect on the fault clearing time.

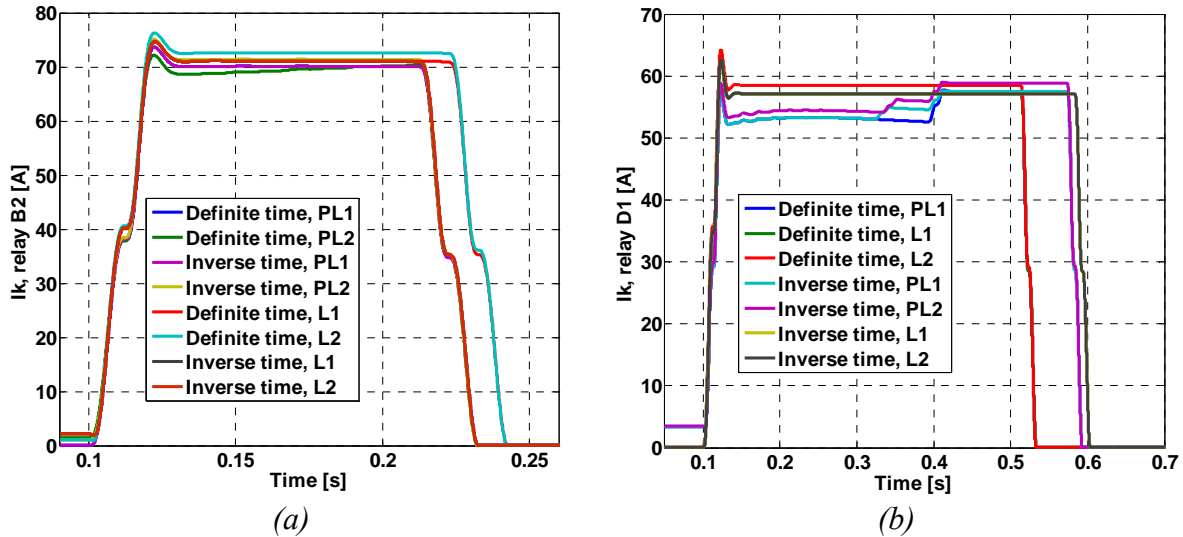


Figure 3.18. (a) I_k of relay B2 following a two-phase fault at location #5, for all scenario cases with and without DG-units (b) I_k of relay D1 following a two-phase fault at location #10 for all scenario cases with and without DG-units

3.5.4 Operation of distance protective devices

Figure 3.19 depicts in an R-X diagram the Z_{AB} trajectory traces that the impedance vectors of relays G4, G5 and G6 follow during different type of fault disturbances located at various points along the section of the parallel connected cables.

In Figures 3.19 (a) and (b) relay G4 sees the fault in its first zone of operation. It can be also observed that there is an increased point concentration even in the second zone of the distance relay. However, since the duration of their presence is less than the time delay of the second zone of the relay, it does not get activated. For contemporary digital distance relays this duration is equal to $(N-1)/T_S$ where N is the number of consecutive points of impedance inside the protection zone and T_S is the sampling frequency of the digital relay. We additionally notice that for relays G5 and G6 the vectors of impedances that they monitor enter neither the first nor the second region of operation and consequently do not trip.

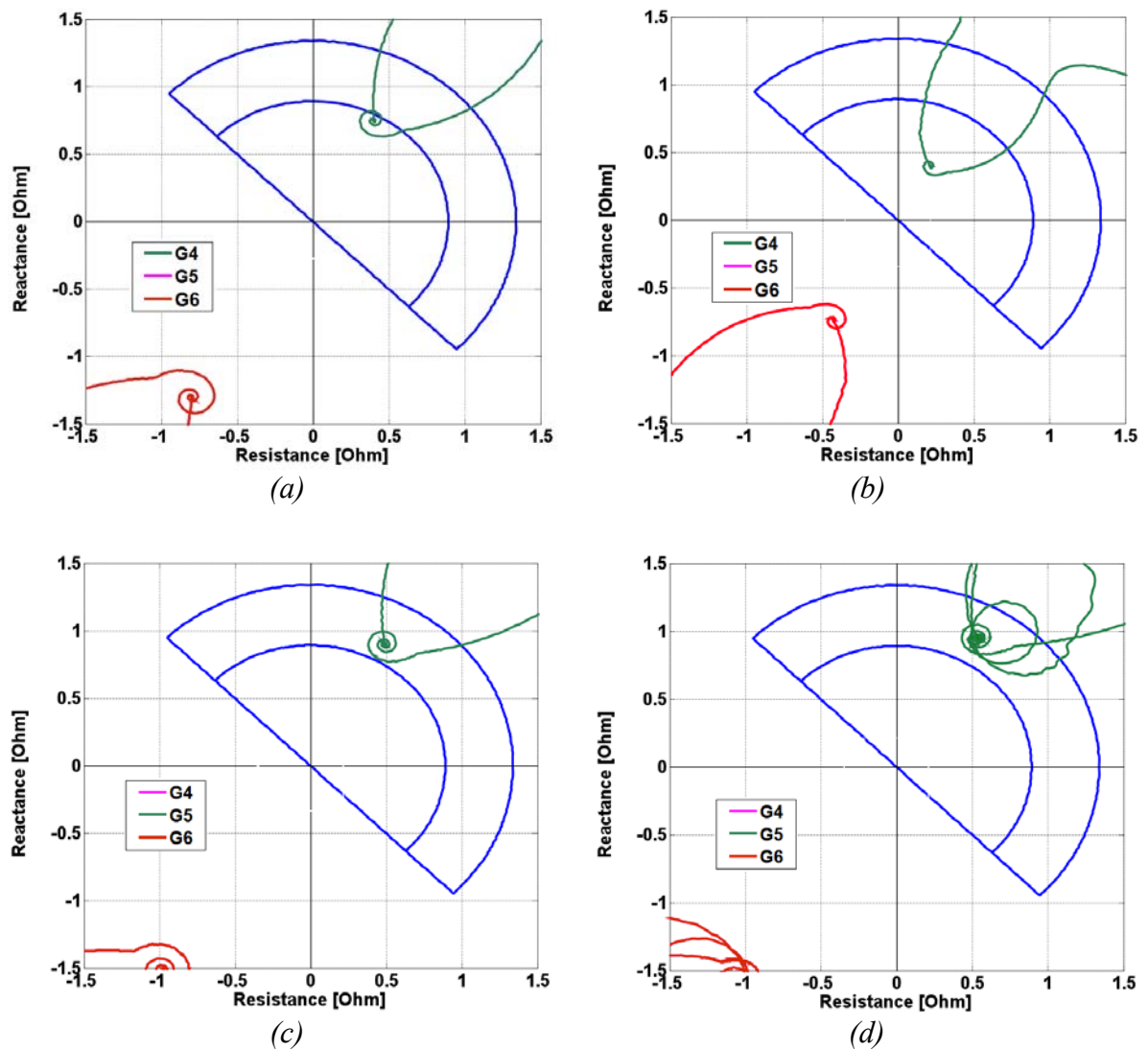


Figure 3.19. Z_{AB} trajectory traces of relays G4, G5 and G6 following (a) a two-phase fault at location #1a (b) a three-phase fault at location #1b (c) a two-phase fault at location #2a (d) a three-phase fault at location #2b. All for scenario case I

Concerning Figures 3.19 (c) and (d) it is noticed that there is an increased point density in the interior of the second zone of relay G5. Therefore, relay G5 sees the fault in its second zone of operation and gets activated with the time delay that corresponds to the second zone. Relays G4 and G6 do not trip since the corresponding impedance vectors do not exceed the borders of their tripping regions. Another significant observation is that for fault disturbances which happen close to the main substation the relays detect the fault in a closer distance to them. For example, for fault disturbances 80-90% distance from the location of the relays, the first zone of operation of the relay gets activated. This is caused by the impact of the DG impedances on the fault impedance calculation, the phenomenon of which is called distance overreaching.

3.6 Transient stability issues

The effect of the protection system on the transient stability of DG-units is investigated in [15]. It is demonstrated that for typical Dutch distribution grids the fault clearing time exceeds for the vast majority of disturbance locations the Critical Clearing Time (CCT) of the DG plants, and causes unstable operation of them. This is an additional reason which justifies the migration towards intelligent protection schemes. This implies that the massive disconnection of DG-units can be potentially prevented by speeding up the fault clearing time of the protective system. Therefore, the fault clearing time of the protection system becomes time-critical and new possibilities for speeding it up should be explored.

References [49], [2], [50], [51] deal with transient stability analysis at the distribution network level, where transient stability problems were typically not an issue due to the passive character of distribution networks of the past. The transient stability analysis of Lelystad distribution network is examined in [49]. Results obtained from several case studies are presented and evaluated. The CCTs of the DG-units are determined for faults at different network locations. In [49] it is shown that problems with transient stability of DG might occur at the distribution network level, and therefore this issue has to be taken into account when new DG-units are to be connected to the network. Simulations show that for some types of DG-units transient stability problems are more pronounced (split-shaft microturbines), for some other types the effect is less expressed (CHP units, diesel units based on synchronous generators) and for some it is not an issue at all (wind turbines). The microturbine appears to be the most critical element due to its low inertia. It is thus demonstrated that in principle transient stability problems might occur in distribution networks with DG, such analysis has to be performed, and, if necessary, the protection settings have to be adjusted accordingly to avoid these problems.

3.7 Extracting fault ride-through specification for DG-units

As aforementioned, international standards and national grid codes specify requirements for the connection of DG-units to distribution level grids. The common practice is to immediately disconnect the units in case of a disturbance. According to IEEE Std 1547, the DG clearing time should be based on the during-fault voltage range. The standard states that for voltage levels less than 0.5 p.u. the recommended clearing time is 160 ms, while for voltage levels between 0.5 and 0.88 p.u. it is 2 s. In the Netherlands, the typical settings of the undervoltage relays of the DG-units are 0.8 p.u. for the voltage magnitude and 0.2 s for the time delay [52]. However, as the aggregate installed capacity of DG increases, the immediate disconnection of the DG-units will be no longer acceptable and new requirements for the integration of the DG-units will be needed. Thus, it can become important to keep them connected to the grid during and after the disturbance. In

this section the Fault Ride-Trough (FRT) capabilities of the network embedded DG-units were examined with the aid of their CCTs determination [50], [51].

3.7.1 Derivation of FRT requirements for external grid faults

Initially, the CCTs of the distributed generators embedded into the investigated distribution network were determined in case of different external grid faults. The ideal voltage source of the grid model (which represents the external grid) was substituted by a three phase programmable voltage source accompanied by its equivalent source impedance. An iterative procedure was followed for the extraction of the CCT points. The voltage dip magnitude was adjusted to a certain value and the duration of the voltage dip was modified repetitively until the determination of the stability boundary (CCT) [50]. The magnitude of the voltage dip indicates the distance to the fault in the external grid. When this iteration was completed, the process started all over for a different value of voltage magnitude. The results are illustrated in the Tables 3.9, 3.10 and 3.11 (V_{grid} is the external grid voltage) correspondingly for the microturbine, CHP1 and CHP2 units.

Table 3.9. CCT of the microturbine for different external faults [50]

V_{grid} [p.u.]	0	0.1	0.2	0.3	0.4	0.5	0.534	0.6
t_{cct} [ms]	508	535	607	718	928	1478	1979	stable

Table 3.10. CCT of the CHP1 for different external faults [50]

V_{grid} [p.u.]	0	0.1	0.2	0.3	0.4	0.47	0.492	0.6
t_{cct} [ms]	554	579	674	827	1128	1641	1979	stable

Table 3.11. CCT of the CHP2 for different external faults [50]

V_{grid} [p.u.]	0	0.1	0.2	0.3	0.4	0.5	0.522	0.6
t_{cct} [ms]	531	562	636	756	986	1622	1969	stable

Simulations regarding the SCIG wind turbine and diesel generator models revealed that these generators are always stable even for the worst external voltage dip depth and duration (0 p.u. and 2 sec). It can be concluded that the CCTs in case of external short-circuits increase with the distance to the fault, and for a remaining voltage level of the external grid of 0.6 p.u. and more there is no problem with the transient stability.

3.7.2 Derivation of FRT requirements for faults at the DG-unit terminals

In this part, the CCTs of the microturbine and the CHP unit were determined for faults at their terminals. The ride-through capabilities of the DG units were determined based on the method explained in [53]. Each equivalent model was connected through a 0.5 km cable to the programmable voltage source. The test networks were implemented in Matlab / Simulink. For each amplitude value of the applied voltage dip, the duration value of the voltage dip was modified and the CCTs were determined. As expected, the results of both cases are approximately identical and are illustrated in Table 3.12.

Table 3.12. CCT of the microturbine/CHP for faults at its terminal [50]

V_{grid} , [p.u.]	0	0.1	0.2	0.3	0.4	0.5	0.534	0.6
t_{cct} [ms]	655	691	759	718	882	1130	1979	stable

The extracted points were utilized for the formulation of the blue curve in Figure 3.20. The green CCT-voltage dip curve, (depicted in the same figure) corresponds to the points extracted in section 3.7.1. The comparison of the two curves emphasises the fact that an external fault is worse from CCT point of view than a fault at the terminals of the microturbine. The typical Dutch undervoltage protection settings as well as the undervoltage protection settings utilized by the German grid operator E.on Netz [54] (for generating units with a high symmetrical short circuit current) are also illustrated in the same figure (red and light blue curve correspondingly). A comparison between the typically used undervoltage protection settings and the derived CCT-voltage dip curves reveals that while in most cases the DGs are immediately disconnected, from stability point of view they could actually remain connected to the grid and support it after the clearance of the disturbance.

Additionally, Fig. 3.21 depicts the CCT-voltage dip curve of the CHP unit (blue curve). It is compared by different utilized undervoltage protection requirements at the DG interconnection point, such as Cenelec (red curve), IEEE Std. 1547-based (light blue curve) and German grid operator's Eon Netz requirements. The figure justifies the observation that the adjustment of the DG undervoltage protection settings according to the derived CCT-voltage dip curves can significantly increase the availability of the generation units [50]. It can be also observed that national grid codes (Dutch, German) are even stricter than international standards (IEEE Std. 1547).

The green, blue and red CCT-voltage dip curves in Fig. 3.22 result from points which are summarised in Tables 3.9, 3.10 and 3.11 respectively. A comparison between the blue and green curve emphasises that CHP1 is less critical in terms of external faults than CHP2 from CCT point of view. The derived curves are compared with the typical Dutch undervoltage protection settings. The frequency of DG-unit disconnections can be significantly reduced when these curves are applied.

However, special attention has to be paid during this adjustment since the CCT-curve, which is determined based on the simulation of the three-phase fault on the terminals of the generator, does not necessarily represent the worst case situation. External faults sometimes might be more critical. Therefore, to prevent instability for such situations (for the points between green and blue curves on Figure 3.20) certain safety margin has to be introduced to the settings of undervoltage protection of DG [51].

Exactly the same procedure was repeated to determine the CCT curve of the rest DG-units. Simulations concerning the wind turbine and diesel generator models reveal that these generators are always stable even for the worst voltage dip depth and duration. Single-phase-to-ground faults were also simulated and they did not lead to instability for all DG types.

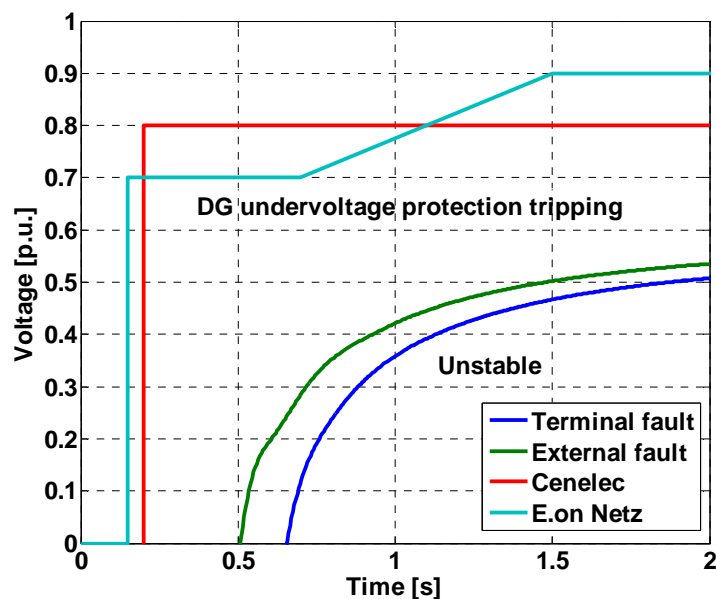


Figure 3.20. CCT of the microturbine as a function of the voltage dip (remaining voltage) for different external faults and for faults at its terminal. Comparison of both the typical Dutch undervoltage protection settings and the equivalent settings of the grid operator E.on Netz with the derived CCT-voltage dip curves. [51]

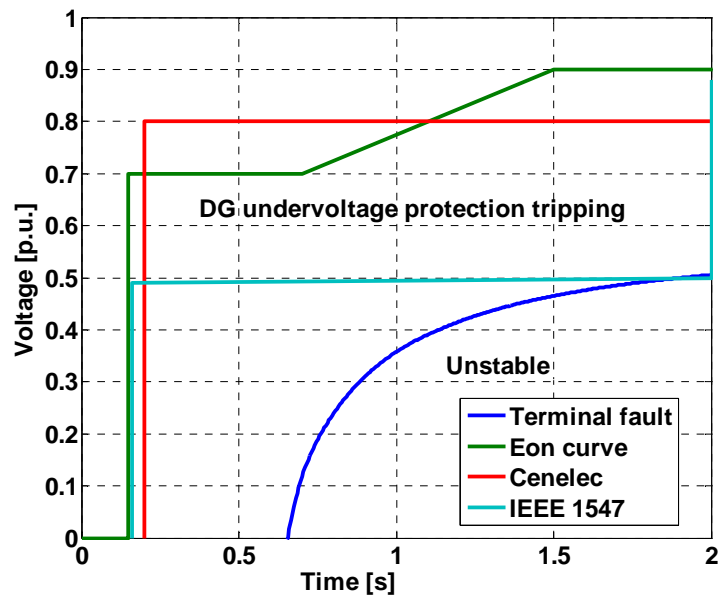


Figure 3.21. CCT of the CHP unit as a function of the voltage dip (remaining voltage) for faults at its terminal. Comparison of the typical Dutch undervoltage protection settings, the equivalent settings of the grid operator E.on Netz and the IEEE Std. 1547 recommended settings with the derived CCT-voltage dip curve. [50]

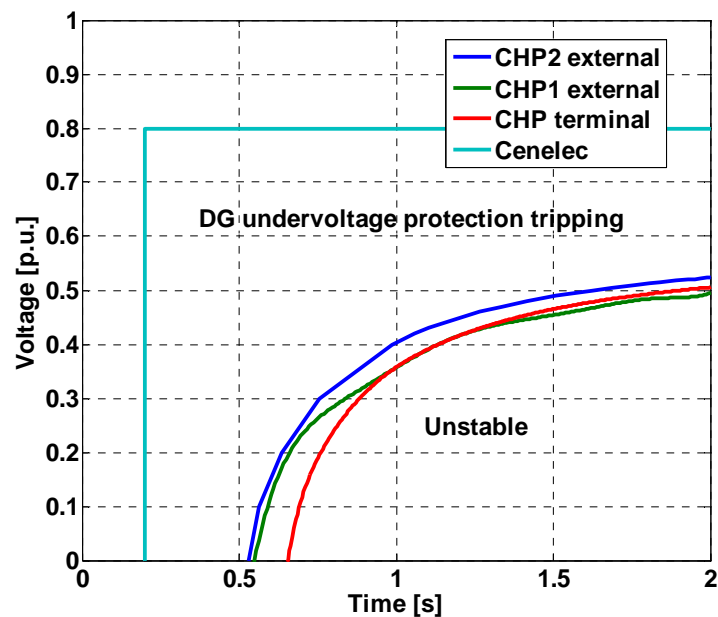


Figure 3.22. CCT of the CHP1, CHP2 and CHP model as a function of the voltage dip (remains voltage) for different external faults and for faults at its terminal. Comparison of the typical Dutch undervoltage protection settings with the derived CCT-voltage dip curves. [50]

3.7.3 Discussion of results

This section shows that, while the IEEE Std. 1547 makes no distinction between different types of DG-units (it does not state directly any limits of the recommended clearing time with respect to transient stability of DG-units), each specific type of DG-unit influences the transient stability independently and consequently its DG undervoltage protection settings at the interconnection point [50]. Thus, keeping some types of DG-units (for example, wind turbines) connected during a disturbance for a longer time (fault ride-through capability) might result in increased support to the grid, preventing unnecessary tripping of a large number of DG-units and prevent possible power deficit in the system after fault elimination. Therefore, it is proposed that DG undervoltage protection settings should be different for different types of DG-units, and that undervoltage settings can be determined based on transient stability analysis (also certain safety margin has to be introduced and coordination with network protection has to be performed). This is an important issue for highly densed networks with high penetration level of DG, like the typical power systems of the Netherlands, where the penetration level of DG is reaching 25-30%.

3.7.4 Feasibility of the FRT robustness of DG-units

As aforementioned, modern wind plants are largely immune to transient stability. The inherent characteristics of wind turbines make transient stability a much smaller concern for wind plants than for CHP or microturbine generators for which transient stability is a major limitation. Therefore, for this type of plants FRT requirements can be evaluated, once their transient stability has been established. Nevertheless, the electrical violence of a nearby fault is highly stressful to the critical elements of the plant. In general, it can be very challenging to design plants that accommodate almost any FRT requirement. Plant auxiliaries must maintain continuity through the voltage depressions and the manufacturers have to improve them to meet these new FRT requirements. Furthermore, the system stresses imposed on the plant during the postfault recovery must also be tolerated. It is necessary that the plant with all its auxiliary systems can reliably ride through those faults. Contemporary manufacturers are able to harden, with prior knowledge of an FRT specification, the generating equipment and plant auxiliary systems to withstand even the most severe FRT requirements [55].

3.8 Summary

In the first part of the chapter, conventional definite and inverse time overcurrent protection schemes have been evaluated for a typical Dutch DG-supplied underground cable

distribution network. Directional impedance distance relays have been additionally modeled for the section of the parallel connected cables. The two protection schemes have been examined for two different DG PLs. Classical time grading has been applied and relay settings have been determined based on well-known rules. DG interconnect protection has been considered by modeling under-/overvoltage relays at the PCC. The performed simulations reveal that for both studied protection schemes as well as DG PLs almost all DG-units get disconnected by the undervoltage protection before the fault is cleared by the grid protection. Therefore, for all scenario cases the vast majority of disturbances lead to massive DG disconnection. It was also noticed that protection blinding is hardly observed for Dutch MV grids which are characterized by high external short-circuit power of the external grid. Another significant observation was that false tripping occurred in the case of inverse time protection schemes and for fault locations close to the main substation and close to sustainable fault current contributing DG sources. Inverse time overcurrent protection schemes yielded shorter fault clearing times in comparison to the definite ones, however they did not prevent the massive DG disconnection. Furthermore, the influence of DG fault current contribution on the performance of the directional impedance distance relays was observed. The detected protection problems verify the fact that conventional protection philosophies are not adequate in the case of a high PL of DG integration.

As aforementioned, present settings of DG undervoltage protection lead to massive tripping of DG-units over large areas in case of short-circuits. Therefore, in the second part of the chapter, the extraction of a unique FRT specification for each specific type of DG-unit was achieved. It was thus proposed that different FRT capabilities can be derived for each different DG type (in contradiction to the standard based recommended settings) and that the DG availability can be significantly increased by means of compliance of the extracted FRT requirements with the DG undervoltage protection settings. This is important as it permits much more optimal utilization of DG-units FRT capabilities, while at the same time guarantees their transient stability. It should be always considered that FRT capabilities, which contribute to the reliability of the power system, do neither exceed the critical clearing time nor fall beyond the limits of the transient stability criteria.

3.9 Conclusions

The simulation results carried out in this chapter verify the inadequacy of today's protection schemes in DG-supplied distribution grids. The existing protection schemes consist of definite or inverse time overcurrent characteristics according to conventional grading principles. Such conventional protection concepts lead to high fault clearing times, unselective trippings and massive DG disconnections which are unacceptable in a deregulated multi-owner energy market. The simulation results indicate that the maximum permissible fault clearing times should be shortened in order to accommodate an increase of

DG availability and to guarantee the post-fault grid stability. Additionally, the observed technical problems verify the fact that information from one location does not suffice to trigger disconnection at this location, because it does not reflect what is going on elsewhere in the network. A relay directed by local information provides only effective protection for electrical components in the immediate surroundings. However, in the future new protection coordination principles should be developed which permit the concurrent processing of information originating from multiple locations. Thus, new protection coordination strategies, which overcome protection selectivity problems, avoid unacceptable high fault clearing times and maximize the amount of DG-units which remains connected to the distribution grid, will be required.

This implies that new software algorithms need to be proposed that will be capable of efficiently increasing the protection speed performance and the DG during-fault availability, while simultaneously assuring the protective device selectivity. Directional protection and concurrent processing of multi-origin information will be necessary to guarantee the protection selectivity. The goal is the development of a smart protection strategy that makes use of sensors, communication links, intelligent units, and so on. The protection system should be easily scalable and adaptable to the possibility of arbitrary DG connection to any zone of the network.

Chapter 4

Getting smart: technological advances rule the protection of the future

4.1 Introduction

In recent years, the evolution of modern microprocessor relays is remarkable. Contemporary microprocessor relays integrate multiple functions, such as metering, protection, automation, control, digital fault recording and reporting, that efficiently accommodate various power system services. For this reason, they are referred to as IEDs. Furthermore, regarding the ability of modern relays to communicate, we observe that nowadays virtually every relay is capable of communicating digitally with the rest of the power system. Since nowadays IEDs supersede old electromechanical relays and dominate in today's power infrastructure, protection specialists are given the opportunity to develop innovative communication-based distributed or integrated protection schemes. This makes it possible to extend today's strictly local-information-based relay protection to communication-based relay protection.

This chapter gives a broad overview of the developments and innovation presently taking place in the protection field. These rapid developments in the field of power system protection are predominantly stimulated by the universal adoption of numerical relays, the emergence of new standard communication protocols (IEC61850) and the unprecedented advances in sensor as well as communication technologies and infrastructures (SASensor, switched Ethernet). All these issues, which herald a whole new wave of innovation in the electrical protection landscape, are thoroughly described in this chapter.

4.2 Substation Automation Systems

Substation Automation Systems (SAS) have great impact on power system's operating costs, increased power quality, and reduced outage response. Early Supervisory Control and Data Acquisition (SCADA) systems acquired information from generation stations and substations through Remote Terminal Units (RTUs) to provide operators with system-wide knowledge to plan and operate the power system. These RTUs and SCADA systems used additional transducers and contacts that were separated from the protection systems to obtain system information. For these systems the information update was slow, on the order of several seconds to minutes. Later on, with the advent of the first substation IED networks more automation and control functions were available. These networked IEDs offered to the system operators all information they required and eliminated additional transducers, contacts and RTUs. Thus, a typical conventional substation structure included:

- parallel hardwired connection between IEDs and primary equipment,
- serial communication between IEDs and the station unit with utilization of legacy communication protocols,
- serial communication between the gateway of the station unit and network control centers.

Legacy communication protocols were typically developed with the dual objective of providing the necessary functions required by electric power systems while minimizing the number of bytes that were used by the protocol because of severe bandwidth limitations that were typical of the serial link technology available 10-15 years ago when many of these protocols were initially developed. These register/address-based protocols included independent standards such as IEC60870 and DNP3 managed by a committee, and funded by a collection of vendors and users that organize enhancements and testing. There were also many proprietary protocols included such as Modbus that were invented by a specific manufacturer and are vendor independent but for which enhancements and testing are performed by the vendor of the protocol [56]. Protocols of both varieties can coexist on an IED network to collectively serve many different functions. However, complex combinations of protocols make design and configuration of an overall SAS which integrates information from devices of different manufacturers a daunting task. Therefore, the need of a standardized communication protocol to enhance IED interoperability is required.

4.3 Ethernet communications networks

Ethernet technology has evolved from the initial CSMA/CD (Carrier Sense Multiple Access with Collision Detection) mechanism to today's native switched-based Ethernet, which is almost collision free [57]. Modern switched Ethernet uses separate, new

communications IEDs to reduce or eliminate data collisions. An Ethernet switch has multiple Ethernet ports. Each Ethernet port connects to an IED and forms a small network segment. This configuration eliminates the shared medium among multiple devices. The primary function of an Ethernet switch is to establish a direct connection between a sender and a receiver, based on the media access control address. This switching mechanism in today's Ethernet speeds up data transmission and makes megabit networks quite standard and gigabit networks possible. With the use of twisted paired fiber optical cables that separate the transmitted and received traffic contemporary switched Ethernet Local Area Networks (LANs) create a truly full-duplex and collision-free communication environment. Furthermore, this advanced networking protocol can be designed with deterministic transmission times, suitable for real-time and mission-critical tasks.

An Ethernet switch introduces a short but unavoidable switch processing latency delay, since it processes every message received or transmitted by each port. Additional switch queue latency is introduced when backlogs occur and messages wait in the switch transmitting memory queue to be sent out. When a message needs to go through several switches in a network to reach its destination, the communication system transfer time is the sum of all switch delays in the message path in the worst network configuration scenarios. In an Ethernet network, the latency of an Ethernet frame is comprised of the propagation delay through the medium (5 μ s/km in case of fiber-optic cables) and the delays in the queue buffers at each network egress port.

Present substation communication infrastructure is experiencing a dramatic change in order to accommodate new functions. Substation IED communications are migrating to Ethernet. Previously mentioned legacy protocols were adapted to run over modern networking protocols and are nowadays able to provide the same basic electric power system capabilities while bringing the advantages of modern network technologies to the substation. However, the protocols being used still minimize the bytes on the wire and do not take advantage of the vast increase in bandwidth that modern networking technologies deliver by providing a higher level of functionality that can significantly reduce the implementation and operational costs of substation automation. The emergence of new standard communication protocols specifically developed to overcome the inherent fundamental flaws of previous protocol approaches is promising.

4.4 The IEC61850 standard

The recent developments in the SA communications standards, i.e. the Utility Communication Architecture (UCA) 2.0 and the International Electrotechnical Commission (IEC) 61850 are clear indications of the importance of communication in achieving the goals of SA. UCA 2.0 and IEC61850 target the standardization of the language of communication between the devices of a SA system [58]. Standardization is regarded as the

key for the achievement of the interoperability within such systems. Moreover, the need for further advancement of an open and standard substation operational environment has led to increased research activity in the communication techniques and principles employed to make substation systems more robust, reliable, high-speed and secure.

UCA was commissioned by the Electric Power Research Institute (EPRI) in 1994 to identify the requirements, overall structure and specific communication technologies to implement the standardization scheme. The adopted approach defined the technical requirements for a system to control and monitor substations of any size. The Technical Committee (TC) 57 of the IEC began work on IEC61850 in 1996 with a similar target [59]. In 1997, the two groups joined to define a common international standard that would combine the work of both groups. The result of the harmonization process is the IEC61850 standard, which is a superset of UCA 2.0, while offering some additional features.

4.4.1 Key features and main benefits

One of the main objectives of IEC61850 is to provide a set of standard model structures for data and services and rules defining how to exchange these data. IEDs from different manufacturers that comply with these model definitions can then understand, communicate and interact to each other. The standard achieves this interoperability by “abstracting” the data and service models in IEC61850-7-x. The concept “abstract” means that these models are defined independently from the underlying communication protocols.

Furthermore, in addition to many client-server substation integration, automation and control functions, IEC61850 includes two real-time, peer-to-peer communications messaging protocols that are particularly useful for protection applications: Generic Substation Event (GSE) and Sampled Values (SV) messages. There exist two types of GSE messages, namely Generic Object Oriented Substation Event (GOOSE) and Generic Substation State Event (GSSE) [60]. The GOOSE message may convey different data types like analog, binary and integer values, while the GSSE message is limited to support binary-only event data. GOOSE, GSSE and SV messages behave in a multicast mode that permits simultaneous delivery of the same event message to multiple recipient IEDs. Many new exciting design possibilities are enabled by using multicast messages instead of point-to-point messages. Traditional protection techniques can be modified by means of SV and GOOSE messaging distributed across switched Ethernet networks. Therefore, these peer-to-peer communication mechanisms permit the development of revolutionary communication-aided distributed protection schemes. Definitely, since the speed, safety and reliability of the new protection schemes depend on the performance of these messages, a profound understanding of the fundamental mechanisms involved in these messages is required.

There are many benefits that can be realized using the IEC61850 standard in a substation integration project. The main advantages include:

- interoperability among IEDs from different vendors,

- simplified system design and commissioning using specified configuration tools and self-describing features,
- reduced installation cost by replacing wired information exchanges among IEDs with GOOSE messages,
- lower system design, commissioning, operation and maintenance costs,
- easy expansion to accommodate future system growth.

IEC61850 is designed to operate over modern networking technologies and delivers an unprecedented amount of functionality that is simply not possible with a legacy protocol approach. Thus, it enables fundamental improvements in the substation automation process. The unique characteristics of IEC61850 have a direct and positive impact on the cost to design, build, install, commission, and operate power systems. The following sections explain in details how all these benefits are offered with the advent of the new communication protocol.

4.4.2 System architecture

IEC61850 introduces the definition of SV services via the implementation of a process bus. According to the process bus idea, depicted in Figure 5.1, a substation distributed protection and control system is separated into three distinct levels:

- Substation Level
- Bay/Unit Level
- Process Level

The process layer of the substation is related to collecting information, such as voltage and current information, from the Instrument Transformers (ITs) which are connected to the primary power system components. It is additionally associated with remotely acquiring status information from circuit breakers and switches. IEC61850 specifies the collection of this data through two different protocol definitions, namely, Part 9.1 which defines a Unidirectional Multidrop Point-to-Point fixed link carrying a fixed dataset and Part 9.2 which defines a “configurable” dataset that can be transmitted on a multicast basis from one publisher to multiple subscribers [61]. In this concept, signals from voltage and current transducers (both conventional and non-conventional) as well as breaker status information are input into a Merging Unit (MU). The MUs sample the signals at an agreed, synchronized rate. In this way, any IED can input data from multiple MUs and automatically align and process the data. Currently, there is an implementation agreement that defines a base sampling rate of 80 samples per power system cycle for basic protection and monitoring and a “high” rate of 256 samples per power system cycle for high frequency applications such as power quality and high resolution oscillography [60].

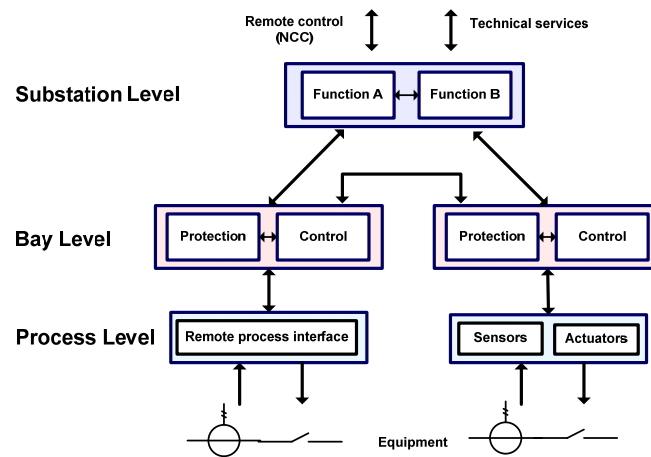


Figure 5.1. Levels and logical interfaces per IEC61850-1 [58]

Part 9.1 describes a pre-configured or “universal” dataset. This dataset includes 3-phase voltage, bus voltage, neutral voltage, 3-phase currents for protection, 3-phase currents for measurement and two 16-bit status words. Part 9.2 is a more generalized realization of SV data transfer. In 9.2, the dataset or “payload” is user-defined using the substation configuration language. Data values of various sizes and types can be united together in the dataset [58].

Conclusively, sampled current, voltage and breaker status information values are gathered, converted to digital representation, and formatted for subsequent transmission through the process bus LAN. Thus, process level information is communicated over the LAN to the protection and control devices which are located at the Bay/Unit Level. Protective functions are being performed at the Bay Level, while the overall substation-wide coordination, substation Human Machine Interface (HMI) and the SCADA system interface are performed at the Station level. The arrows in Figure 5.1 indicate all possible logical interfaces between the different levels. Therefore, it can be observed that various functions can be implemented either distributed (thus based on communications among IEDs over the substation LAN) or locally in a specific primary protection and control device. To satisfy these requirements, IEC61850 defines several ways for data exchange among IEDs that can be used for different forms of distributed applications.

4.4.3 Protection performance requirements

The different distributed functions impose different performance requirements that have to be considered in the design process of substation protection, control, monitoring and recording applications. The standard categorizes the message types for the typical substation functions and specifies their associated performance class requirements in terms of time duration of message transmission. Table 5.1 lists the message types [58].

Table 5.1. IEC61850 message types and performances [58]

Type	Applications	Performance class	Requirements (transmission time)
1A	Fast messages (trip)	P1	10 ms
		P2/P3	3 ms
1B	Fast messages (other)	P1	100 ms
		P2/P3	20 ms
2	Medium speed		100 ms
3	Low speed		500 ms
4	Raw data	P1	10 ms
		P2/P3	3 ms
5	File transfer		> 1000 ms
6	Time synchronization		(Accuracy)

The transmission time is the maximum allowable time duration to communicate a value from the logic processing of one device to the logic processing within a second device as part of an application. This transmission time is illustrated in Figure 5.2. Time t_a is the time duration of the communication processor algorithm within the Physical Device 1 (PD1), which creates and publishes the message. Time t_b represents the transmission time of the message across the network between the IEDs. Time t_c is the time duration of the communications processor algorithm within PD2, which receives and processes the message. The time duration to publish information in PD1, deliver it via a communications message, and act on it in PD2 is the information transfer time duration, represented by $T_{transfer} = t_{transmission} + t_{f2}$. Transfer time is easily measured as the time difference between the time-stamped sequential event records in IEDs with synchronized clocks. Therefore, $t_{transmission}$ though not measurable, it is easily calculated as $t_{transfer} - t_{f2}$ (the IED processing cycle duration).

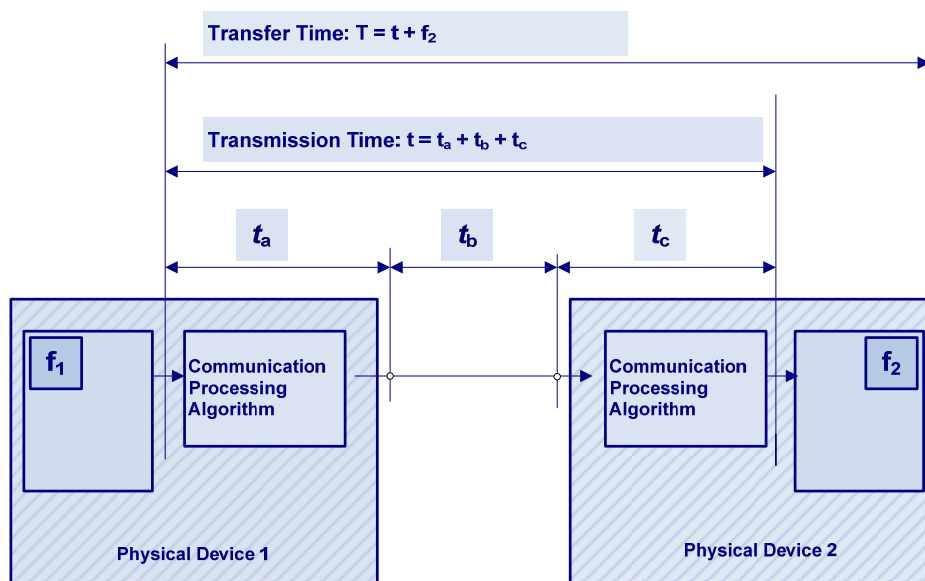


Figure 5.2. Definition of transmission time [58]

In this section, the message types which are predominantly related to protection applications are discussed. IEC61850 encompasses two independent groups of performance classes:

- for protection and control
- for metering and power quality applications

It defines three performance classes for control and protection applications, namely P1, P2 and P3. P1 applies typically to the distribution level of the substation, while P2/P3 applies to transmission level applications with high requirements. As it can be observed, the total transmission time of Type 1 messages can be anywhere between 3 to 100 ms depending on the application. Specifically, trip GOOSE messages are Type 1A fast messages featuring, for Performance Class P2/3 Type, a total back-to-back transmission time in the order of 3 ms which is suitable for critical protection applications.

Additionally, sampled raw data messages from the instrument transformers (conventional or optical CTs and VTs) and status information are classified under Type 4. The data consist in this case of a continuous stream of synchronized and digitized values. These messages are typical for Process bus applications. SV messages belong to this category.

4.4.4 Modeling approach

The core concept of this standard is the creation of a clear distinction between the physical and the logical world. Four basic building blocks are defined:

- physical devices,
- logical nodes,
- logical connections,
- functions.

The IEC61850 device model begins with a physical device. Within each physical device, there may be one or more logical devices. Each logical device contains one or more logical nodes. IEC61850-7-4 identifies the smallest possible function pieces that need to exchange information and refers to these functions as Logical Nodes (LNs). Each logical node consists of data sets, data attributes and associated communication services that are logically related to some power system function. Each element of data has a unique name. The Common Data Classes (CDC) specified in IEC61850-7-3 model these data sets and data attributes with common formats and structures. Each CDC describes the type and structure of the data within the logical node. Each CDC has a defined name and a set of CDC attributes with a defined name, type and specific purpose. Each individual attribute of a CDC belongs to a set of functional constraints that groups the attributes into categories. For instance, there are CDCs for status information, measured information, controllable status information, status settings, analogue settings, controllable analogue set point information.

Logical nodes exchange data with their peers and are grouped together into functions by using various logical connections. Mapping of logical nodes and functions into physical devices is totally free and can be ideally optimized to match individual user applications. Functions can be distributed across multiple devices (thus forming communications-based distributed functions) or mapped into a single physical device. Figure 5.3 illustrates how functions are realized using logical nodes and logical connections. In this example, a total of two functions (F1 and F2) distributed across three physical devices (PD1, PD2, PD3) is illustrated. Function F1 contains seven logical nodes (LN0 to LN6), while Function F2 contains four logical nodes (LN3, LN6 to LN8) with logical nodes being freely allocated across different physical devices. The logical connections between the logical nodes are marked as LC and the physical connections between the physical devices are PC. Logical connections are mapped to physical connections over the LAN with available transport mechanisms such as SV and GOOSE.

IEC61850 defines approximately 100 distinct logical nodes. There are logical nodes for automatic control, the names of which all begin with “A”. Likewise, there are logical nodes for metering and measurement (M), supervisory control (C), generic functions (G), interfacing (I), system logical nodes (L), protection (P), protection related (R), sensors (S), instrument transformers (T), switchgear (X), power transformers (Y), and other equipment (Z). Typical examples of logical nodes related to protection applications include PTOC (time overcurrent), PDIS (distance protection), XCBR (circuit breaker interface), TCTR (current transformer) [62]. For instance, the circuit breaker XCBR logical node contains a variety of data including Loc for determining if operation is remote or local, OpCnt for an operations count, Pos for the position, BlkOpn block breaker open commands, BlkCls block breaker close commands and CBOpCap for the circuit breaker operating capability.

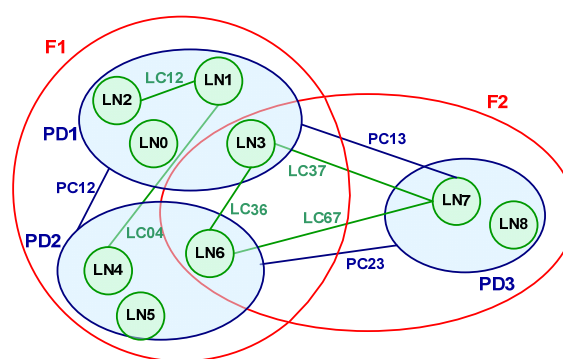


Figure 5.3. Relationship between functions, logical nodes and physical nodes [58]

Additionally, to configure IEC61850-based systems the standard specifies a substation configuration language that is based on extensive markup language. The various configuration files include:

- System specification description file that outlines a substation automation project, optionally including system one-line diagram.

- IED capability description file that describes the available functions (LDs) and services available from an IED.
- Substation configuration description file that describes the relationship among the IEDs in the substation automation project and their information exchange structures
- Configured IED description file that is the final file to download into an IED to enable its configured functions.

4.4.5 Time synchronization issues

Sampling time reliability is critical for SV-based process bus operation. Without synchronized time sampling it's impossible to combine SV outputs generated by multiple physical devices. The IEC61850 series of standards recommends the Simple Network Time Protocol (SNTP), as the primary synchronization method and recognizes the fact that the SNTP time accuracy (0.1 to 1ms) is insufficient for SV applications which require less than 1 μ s accuracy. In order to achieve the 1ms accuracy, the standard requires that the time synchronization accuracy is ten times faster than the required time-stamp accuracy. Thus, IED clocks must be synchronized 0.1 ms accuracy so that IED data time-stamps can be accurate to 1 ms.

In present-day installations microsecond level time synchronization is accomplished by distributing IRIG encoded time signals, according to the Global Positioning System (GPS) - based time synchronization method. On the physical layer, time signal distribution is accomplished using independent fiber-optic-based distribution networks. Thus, the time synchronization network is deployed as a separate network. Thus, two mission-critical and independent networks operate at the same:

- time synchronization network and
- process bus Ethernet-based LAN.

However, in case of two independent networks, redundancy becomes cost-prohibitive. Time synchronization problems can be significantly simplified by using one network for both time distribution and communication functions. The Ethernet-based substation LAN can therefore be the obvious candidate. A single network implementation can be accomplished by using IEEE 1588 "Precision Time Synchronization protocol (PTSP)" [63]. This standard uses hardware level time stamping to provide precise clock synchronization. IEEE 1588 will be included in the next revision of IEC61850 [62], thus fostering its wide deployment in the power system substation environment.

4.4.6 Mapping to real protocols

The abstract data and object models of IEC61850 define a standardized method of describing power system devices that enable all IEDs to present data using identical

structures that are directly associated with power system functions. These data and service object models can be mapped to any set of communication protocols. As long as two IEDs use the specified object models and the same mapping protocols, they are able to understand each other and exchange information. The Abstract Communication Service Interface (ACSI) models specified in IEC61850-7-2 define a set of communications services with defined behaviors and responses that enable all IEDs to behave in an identical manner. These ACSI models operate over a real set of protocols that are practical to implement and that can operate within the computing environments commonly found in the power industry. Specifically, the standard is built over the protocol layers of the International Standards Organization (ISO) Open System Interconnect (OSI) communication system model. The abstract models are constructed above the 7th layer (application) of the OSI model as shown in Figure 5.4 [59]. This ensures the compliance of the substation communication model to the evolution of communication technology. IEC61850-8 maps the abstract objects and services to the Manufacturing Message Specification (MMS) protocols. MMS is the only public protocol that supports complex named objects and a rich set of flexible services that can easily assist the mapping to IEC61850 service models in a straightforward manner.

In addition to the mapping to the application layer, Part 8.1 defines profiles for the other layers of the communication stack that are dependent on the service provided as shown in Figure 5.4. As it can be seen, different data models are mapped to the communication services in order to meet the service and performance requirements of the different types of substation data traffic. SV and GOOSE messages are expected to meet high real-time requirements of fast and reliable message transmission, since they are the most important messages on the process bus of a distributed protection system. Therefore, they are directly mapped into the Ethernet data frame, thereby eliminating processing of any middle protocol layers. Moreover, the Ethernet technologies TCP/IP and UDP transport MMS and SNTP respectively.

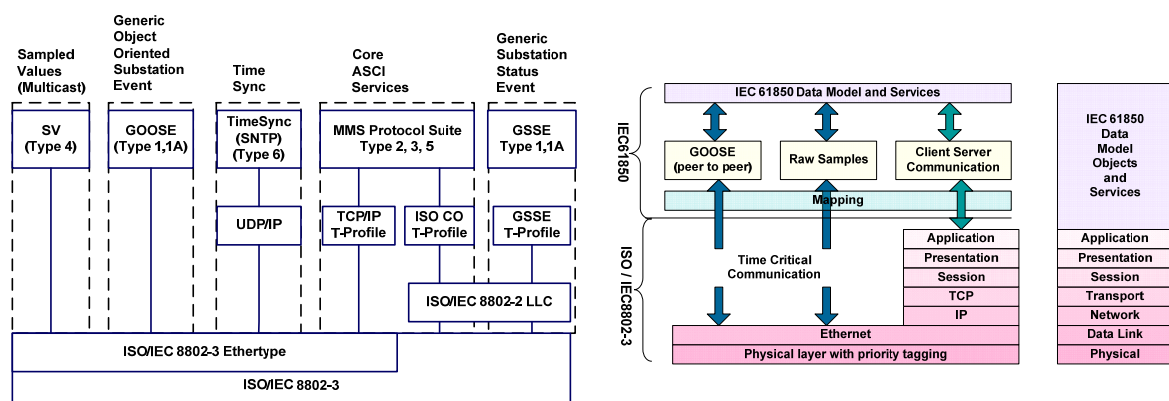


Figure 5.4. Overview of IEC 61850 functionality and associated communication profiles [58], [60]

4.4.7 Security and dependability

Functions in a power utility communications network are diverse and can range from less time-sensitive to time-sensitive applications. While traffic sources are heterogeneous, the service demands are always the same. The service must be dependable and secure, ensuring that the overall service is reliable. In a utility communications network, dependability is defined as the on-time delivery of traffic and in specific relay terms, as being able to trip when required to trip. Security is defined as the ability to deliver critical traffic and in relay terms as being able to refrain from tripping when not required to trip.

QoS (Quality of Service) is a method of providing controllable priorities to different applications. Therefore, the dependability concern can be mitigated by using high priorities for critical traffic and lowering the priorities for non-critical traffic. This feature becomes important when the network capacity is insufficient for the simultaneous transmission of real time streaming data along with non-critical data. Traffic classification is a function of the number of queues in the Ethernet switches and the flexibility provided to the user in directing traffic to the queues. Additionally, the security concern can be alleviated by means of VLAN (Virtual Local Area Networking) techniques, which restrict traffic flow of messages to a single individual LAN and therefore the devices within it. The IEEE 802.1Q standard defines a 4-byte extension to the standard Ethernet frame header, including a 12-bit field for VLAN identifier and a 3-bit priority tagging field for traffic classification, as illustrated in Figure 5.5 [64, 65, 60]. Conclusively, VLAN and CoS constitute key enabling Ethernet switch features to enhance the security and dependability required for protection applications over Ethernet technologies.

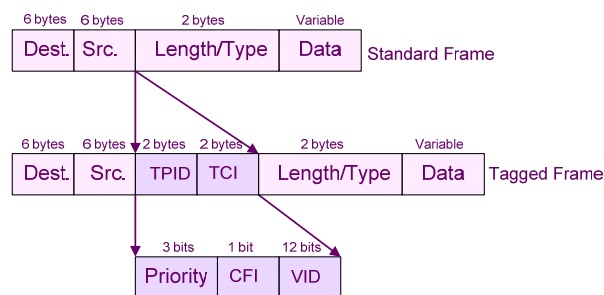


Figure 5.5. Tagged Ethernet frame structure [60]

4.5 Migration to totally integrated protection

As aforementioned, contemporary microprocessor relays have evolved to accomplish more and more protection functions for power apparatus within one protective device to provide main and backup protection as well as metering, automation, control, digital fault

recording and reporting [66]. However, the integration of functions has until now focused only on the protection of individual components, and not on multiple apparatuses.

Recent achievements in microprocessor, communication and sensor technologies permit the exploration of innovative concepts for centralized power system protection. Thus, interest is encouraged in new developments in the integrated protection. Research indicates that information obtained from multiple power system components can be used to derive new protection principles and schemes which could have significant benefits over the existing techniques (which are based on individual component protection) [67], [68], [69].

Therefore, the term "Integrated Protection" can be used to signify the integration of protective functions from multiple component items all over the distribution network into one protective relay within the substation [67]. Such an advanced integrated protection unit, integrates all network's protective functions into one relay in the main substation to form a totally centralized protection system. In this case, all the essential measured information obtained from multiple components in the network should be sent to the centralized integrated relay unit through a redundant communication network for the implementation of multi-layer protection functions. After decision making is accomplished, the trip commands and the control signals are sent back to the circuit breakers to trip the faulty zone in case of a fault event. Definitely, real time and dependable transmission of the sampled values and trip signals via the network constitutes the most significant part of the integrated protection communication system.

IEC61850 offers undoubtedly great benefits to conventional communications-aided protection schemes (such as fast bus tripping) with the use of GOOSE messaging. On the other hand, SV messaging is not directly related to traditional communications-aided protection scheme implementations. Formulation of a totally integrated protection system requires first of all that the process and station bus are merged [60]. This approach makes realization of a centralized protection concept feasible through:

- digitization of essential data by means of sensors which are wide-spread located all over the network,
- transfer of sampled values via communication system to the centralized multi-processor unit,
- overall processing of multi-component multi-layer protection functions locally in the substation rugged integrated unit,
- decision making and transfer of commands back to the actuators.

4.5.1 The SASensor system

An approach for full support of integrated protection scheme has been implemented in the Netherlands by Locamation (a company which specializes in smart grid solutions) in close cooperation with Alliander (a utility) and Phase to Phase (a software company) [70]. The developed system covers the functional requirements of a fully integrated substation

system, such as accurate data acquisition, remote and local control, alarm and event handling, power quality monitoring, digital fault recording, protection, revenue metering and IEC61850 compliance.

The system consists of a central processing unit and three types of process interface modules, one for a 3-phase current, one for a 3-phase voltage and one for indication and control, as depicted in Figure 5.6. The Current Interface Module (CIM) and the Voltage Interface Module (VIM) are connected to conventional instrument transformers CTs and VTs [70]. They measure and digitize the 3-phase currents and voltages supplied by the secondary windings of CTs and VTs respectively. The Breaker Interface Module (BIM) is a compact input/output interface to monitor and operate circuit breakers and switches. It is used for position and alarm indications of the circuit breaker as well as to trip/close the circuit breaker and/or other switching devices. All sensors dynamic specification ensures the support of an extreme wide value range. The CIM is equipped with two transformer cores (one for measurement and one for protection) per phase. It is additionally supplied with double A/D converters to obtain such a large measurement range from almost no-load currents (1% I_{nom}) up to large short-circuit currents ($100 \cdot I_{nom}$). Both CIM and VIM use Digital Signal Processing (DSP) techniques to digitize the analogue input signals. Conversion is done with high-speed A/D converters with a sampling frequency up to 900 kHz. CIM as well as VIM are calibrated to compensate for internal value and phase displacement errors. The errors of CTs and VTs are additionally compensated by means of software algorithms. All process interfaces are robustly designed for a long technical and functional lifetime, which is more or less equal to that of the primary equipment.

The heart of *SASensor* is the Central Control Unit (CCU), an “all-in-one-box” unit, consisting of a multiprocessor environment including industrial single board computers and a flexible number of fiber optic interface boards whose functionality act as an Ethernet switch device. For example, the CCU603 series has a maximum of 12 interface boards, supporting a maximum of 84 fiber optic ports [71]. All required functionalities (control, protection, power quality monitoring, revenue metering, etc) are executed by software in the MU. Therefore, other applications can be added to this system as long as they can be written in software. The CCU has compatible interfaces with IEC61850-8-1 and IEC61850-9-2 which enables the connection of specific third party apparatus. Therefore, in the present release of *SASensor*, multiple protection functions can be performed by external relays connected to the CCU by fibre optics. The central processing unit resamples the high speed, high precision samples of the data acquisition part to the lower speed of the IEC61850-9-2 process bus. These samples can be used by the third party protection and control devices to run their own applications according to their own specifications. In this case, possible trip messages are given directly to the actuators on the basis of the IEC61850-8-1 protocol. The interface modules are connected to the CCU with a simplex fiber optic connection using the standard 100Base-FX Ethernet protocol. The fibers guarantee electrical isolation and transmission over long distances up to 15 km. Additionally, signals transmitted over fiber optic cables are unaffected by interference.

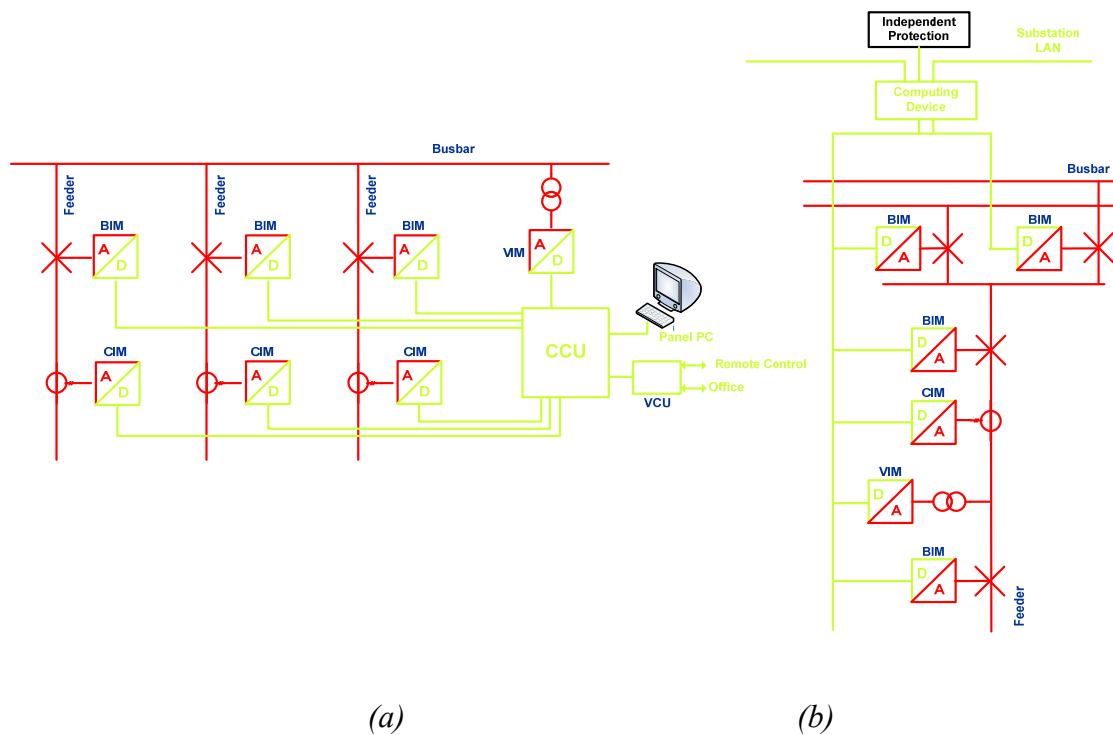


Figure 5.6. The SASensor system (a) Substation oriented hardware organization (b) Bay oriented hardware organization [70]

Since the CCU contains all functionality in its software, the system can be very easily duplicated by simply using a second identical CCU. Although the interface devices are single in the system, their Ethernet communication ports are redundant with a double set of fiber optic cables, one set for each CCU connection. This creates a complete redundant system, as illustrated in Figure 5.7(a). In the redundant system, one CCU can be turned off for repair or replacement without any degradation of functionality or shutdown of the substation. The other CCU simply continues to control the SASensor system.

The unique idea behind the SASensor technology is the separation between physical hardware (devices) and functionality (software) on one side, and the separation between the long life unalterable primary-process interface devices (sensors) and the fast ageing components (computing devices) on the other side [71]. This double separation within the SASensor technology, depicted in Figure 5.7(b), ensures its adaptation to the ever increasing requirements of the future grid, simply by software upgrades and/or computer performance improvements.

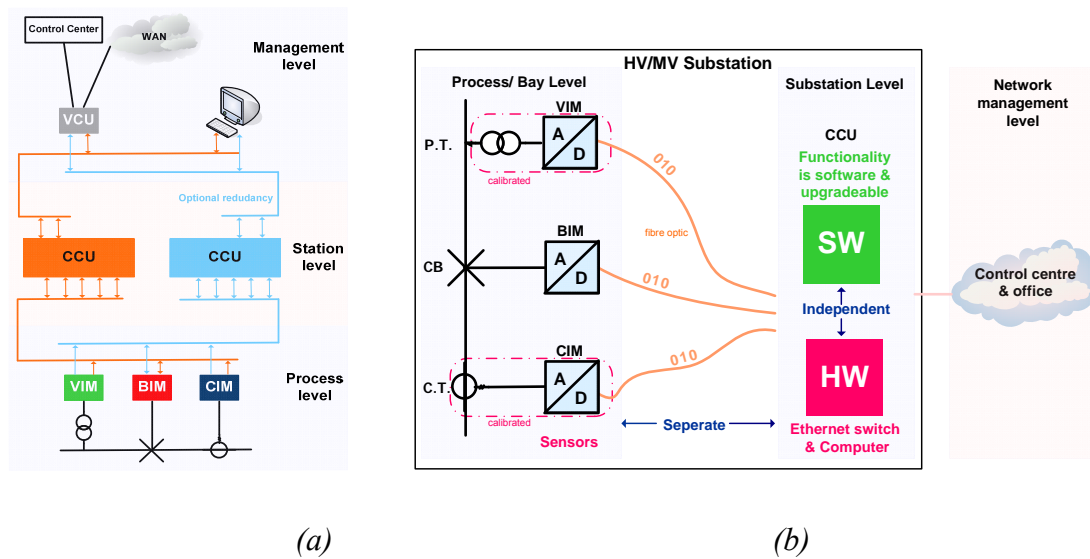


Figure 5.7. The SASensor system (a) Simple redundancy for central control units (b) Double partitioning of the essentials [72]

The Versatile Communication Unit (VCU) is the gateway that not only connects the SASensor's CCUs with the Remote Control Centre (RCC) for remote operation and maintenance, but also with the office for continuous access to all digital information from the substation [72]. The configuration of the VCU includes special ports for connection to RCCs and WAN, as well as fiber optic ports to enable 100Base-FX Ethernet communication with the CCUs. The VCU can also connect to an external GPS antenna to provide absolute time accuracy. Furthermore, the CCUs are connected by fibre optic to a local PC station. The PC can control locally the SASensor.

Integrated pilot projects are already realized and tested in dozens of substations of Alliander, Enexis and Stedin in the Netherlands. SASensor enables above all the smart grid revolution by enhancing the development of new applications (asset management, marketing support, maintenance, etc) for a better management of the distribution networks. All collected available digital data can be used to develop new algorithms and optimize current distribution grid performance. Therefore, the expected future functional upgrading is anticipated to transform SASensor into an excellent smart grid enabler.

The present release of SASensor supports the following ready available functions:

- Basic substation automation functions. The SASensor functionality includes all common substation automation functions like control, alarm and event handling, interlocking, automatic voltage regulation, automatic tap changer control and so forth.
- Protection. The SASensor software contains the functions for directional time overcurrent and earth fault protection. At the moment, other protection functions can be handled by external relays connected to the system on basis of IEC61850.

- Power quality. The sampling rate of the interface modules enables harmonic measurements up to the 50th harmonics. The power quality software in the control unit processes the data into a harmonic spectrum.
- Digital fault recording. It is triggered by user definable events and stores sampled data streams and half cycle RMS values of all relevant process variables.
- WAN communication. For remote access, the system supports secure connections with the outside world. The Virtual Private Network (VPN) technology enables accessibility for all authorized employees from any arbitrary location. Reading the on-line and stored data and even upgrading of the system and application software can be done remotely.
- Revenue metering. The CIM and VIM are calibrated to compensate for value and phase errors. Additionally, the errors of the conventional CTs and VTs can be measured as well and stored in a unique profile. The software in the computing devices uses these profiles to obtain revenue metering accuracy even on standard protection cores.

4.6 Summary

This chapter explains how the recent vast improvement in networking and sensor technology has dramatically changed what is nowadays feasible for power system substation automation. It illustrates how these technological advances impact the performance of traditional protection schemes and how development of innovative communications-assisted protection principles becomes possible. It discusses the scope of the new IEC61850 communications protocol for substation automation and explains why this standard is important, how it differs from legacy technology and what kind of benefits it offers to its users. Definitions and overview of the most important concepts in the standard are presented and it is explained how this results in significant improvements in both costs and performance of electric power systems. The benefits delivered by the standard are illustrated via description of its main features which include standardized service models, self-descriptive object data models, standardized configurability with SCL, high-speed performance requirements, and the promise of interoperability among IEDs from different manufacturers. Moreover, details of the novel peer-to-peer communications mechanisms as well as their applications on high-speed protection are discussed. Furthermore, the chapter examines from a protection engineers point of view what the standard cannot offer to traditional and non-traditional protection schemes that require communications assistance and how these problems can be solved with the implementation of totally integrated protection concepts, such as *SASensor* technology.

Communication infrastructures, standard communication protocols, sensor technologies, thoroughly explained in this chapter, are widely considered to be the precursor

to new horizons for protection related applications. All these technological advances have and will have the potential to be significant drivers of the pace and direction of change in electrical protection landscape now and in the near future.

Chapter 5

A novel concept of a smart protection strategy

5.1 Introduction

This chapter begins with a literature review of the proposed protection schemes for distribution networks supplied with DG-units. Then, it introduces a new intelligent protection algorithm, which guarantees the protection selectivity and is capable of enhancing the DG availability during and after fault occurrence. The algorithm applies a fully integrated protection concept. Conversion of the grid structure from radial to closed-loop and from closed-loop back to radial operation is involved in the steps towards the fault clearing process. Two different protection strategies that can accommodate the algorithm are thoroughly presented. The real-time organization of both the hardware architecture and communication infrastructure of the new communication-based protection strategies are illustrated in detail. An analytical description of the time delay components, which are comprised in the total fault clearing time is also given. It is demonstrated how the protection algorithm can be applied on any arbitrary distribution network, which is supplied with an arbitrary number of DG-units. The generic flowcharts of both protection strategies are displayed. The generic algorithm fundamentally makes use of intelligent blocking schemes. Nevertheless, different multi-functional protection principles can be accommodated in the real-time implementation. Finally, the application of the algorithm is illustrated on a simple test grid and illustrative examples of special scenario cases are depicted.

5.2 New concept of a fully-centralized protection philosophy

Different approaches have been proposed to overcome the potential problems caused by the DG integration in the distribution networks. These approaches range across distance protection [73, 74], transient directional overcurrent protection [75, 76, 77] adaptive overcurrent protection [78, 79], multi-agent protection [80], wide-area [81, 82] and relay-to-relay communication-based [83, 84] protection. In [79] an adaptive protection scheme for fuse-to-fuse and fuse-to-recloser coordination, which is independent of size, number and placement of DG-units is introduced. In this approach, the current setting is based on contributions from different sources and the tripping time is defined based on short circuit calculations and specific fuse characteristics. This brief summary of recent proposed solutions indicates that the research area is quite active since new ways should be developed to overcome the current protection malfunctions in distribution DG-supplied grids.

5.2.1 Utilized protection principles

The unique characteristic of the proposed protection algorithm is that the term ‘centralized protection’ refers to the concurrent processing of information originating from multiple points along each feeder. The concurrent processing can rely on either binary status decision signals or sampled values, as it will be explained in the following section of the chapter. The decision intelligence algorithm makes use of multi-layer protection principles; directional overcurrent, upstream blocking direction overcurrent, busbar differential, busbar interlocking directional overcurrent and line differential protection principles are included. In the proposed protection scheme many different multi-functional protection principles can be applied. Table 5.1 depicts the logical nodes related to both protection functions and primary equipment according to the acronyms used in IEC61850 terminology.

Table 5.1. Logical nodes related to protection functions and primary equipment in IEC61850

Protection function	Logical node
Differential line	PLDF
Differential busbar	PBDF
Directional overcurrent	PDOC
Primary equipment	Logical node
Circuit breaker	XCBR
Switch	XSWI
Current transformer	TCTR
Voltage transformer	TVTR

5.2.2 Proposed protection strategy I

The real time implementation of the sophisticated algorithm can be accommodated by two different protection philosophies. The key differences between the two proposed strategies are in the underlying distribution and/or integration of the required measurement and computation points.

This proposed protection philosophy relies on:

1. distributed measurement/digitization/time-stamping/Ethernet packet packaging of primary data values (current/voltages). This denotes the utilization of sensors at the selected measurement points,
2. fully integrated computation of the decision making process per feeder. This signifies that the computation of the algorithm is executed from a global perspective, covering the protection functionality of the whole feeder.

The protection strategy requires a high number of sensors units, “data” communication” and a low number of IEDs. The sensor layer (MUs in the IEC61850 terminology) is responsible for:

- the measurement of primary data (such as current and voltage measurements),
- digitization of primary data,
- the time stamping (synchronization) of the data and their formatting into Ethernet packets.

Furthermore, the Input/Output Units (I/OU) of the sensor layer (according to the IEC61850 terminology) are responsible for:

- the monitoring of the status of CBs and switches,
- the execution of tripping/closing commands for CBs and switches.

The formed Ethernet packets are propagated via redundant fiber-optic networks to the fully integrated computation point. This protection strategy requires “data” communication, thus a communication network featuring high bandwidth is needed. The decision intelligence layer is responsible for the processing of the multi-functional protection principles in a redundant pair of Central Protection Units (CPUs) (per feeder) located in the main HV/MV substation. The key characteristics of the protection strategy are as follows:

- the algorithm is intended for grid-connected distribution networks, whose grid structure is arranged in a radial operation,
- the data exchange between the interface units (sensors) and the CPUs is based on IEC61850 SV application. Thus, the protection scheme eliminates the use of GOOSE messaging. The data transfer between the interface units (located outside the borders of the main substation) and the CPUs is based on unicast point-to-point SV messages according to IEC61850-9-1. The data transfer between the interface units (located inside the borders of the main substation) should be founded on multicast SV messages according to IEC61850-9-2. Therefore, the topology of the communication network inside the borders of the main substation should form an Ethernet ring, as depicted in Figure 5.1,

- interface units produced from any manufacturer can be utilized for the implementation of the scheme, since IEC61850 guarantees the interoperability among components constructed from different manufacturers,

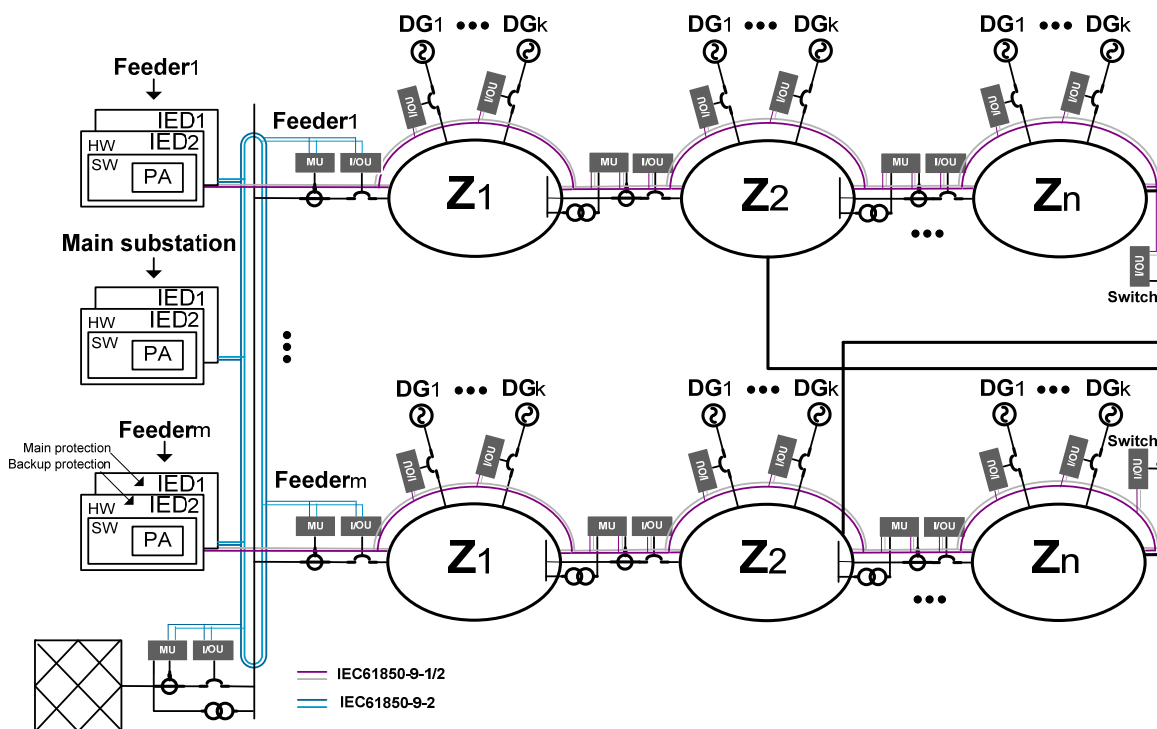


Figure 5.1. Demonstration of the protection strategy I (intended for any arbitrary Dutch MV grid supplied with an arbitrary number of DG-units) according to the IEC61850 terminology

- in the rest of the dissertation, the following terminology is adopted regarding the naming of sensor equipment. Three separate interface units are considered, each of them corresponding to current (CIU – Current Interface Unit), voltage (VIU – Voltage Interface Unit), and breaker (BIU – Breaker Interface Unit) sensors,
- the already existing locations of CT and CB equipment, can be directly used for the installation of the sensor interface units. Therefore, these locations delineate the borders of each zone. Due to the fact that each feeder in typical Dutch distribution grids is equipped with a small number of CT/CB locations, the feeder is subsequently segregated in a few number of zones ($n < 5$). Therefore, the borders of each zone are indicated by its equivalent pair of measurement points (interface unit locations). This zone definition will be adopted in the rest of the dissertation,
- Since Dutch grids are characterized by short feeder lengths (of maximum 15 km distance), it is not necessary to supply each feeder with more CT/CB locations. Each zone contains a part of the feeder, including both trunk feeders and laterals. An arbitrary number of DG-units (1 to k) can be connected to each zone. The algorithm is independent of the size, location and power rating of its DG-unit. From now on, the

installation of CIU, VIU and BIU equipment at its measurement point is assumed. VTs should be installed at the borders of the zones (at the measurement points where they do not already exist), in order to facilitate the processing of PDOC protection functionality. A pair of central protection units is responsible for the processing of the protection functions which correspond to a whole feeder. Figure 5.1 illustrates the protection scheme (intended for any arbitrary Dutch MV grid supplied with an arbitrary number of DG-units) according to the IEC61850 terminology. Figure 5.2 demonstrates the protection scheme according to the terminology adopted in this thesis,

- As aforementioned, a pair of CPUs is assigned per feeder. Each CPU of the pair runs the same protection functionality; thus, it acts as a backup protection, increasing the redundancy and reliability of the scheme. Each pair of CPUs is located in the control centre room of the main HV/MV substation. Furthermore, each pair of CPUs runs independently from the rest of the CPU pairs since there is no data exchange among CPUs. The number of functions allocated inside each pair of CPUs is identical to the number of zones protected by the associated pair of CPUs (for each separate feeder). Therefore, each faulty zone is isolated due to the activation of the corresponding function. Each function utilizes a sophisticated protection algorithm, processing PDOC blocks of all downstream measurement locations. This advanced functionality makes use of blocking signals among PDOC blocks that correspond to different measurement points along each feeder. The flowchart of the algorithm corresponding to the proposed strategy I is depicted in Figure 5.3(a). In special cases where tie switches exist between neighbouring feeders, advanced functionality can be supported which further enhances the protection selectivity by means of modification of the grid structure. The instant of the status change of the tie switch (between adjacent feeders) from radial to closed, denotes the moment when the operation of the grid converts from radial to closed-loop. The instant of the opening of the faulty zone-forming CB contacts, signifies the moment when the operation of the grid restores to its pre-disturbance radial arrangement,
- the CPU is defined as any device incorporating one or more processors with the capability to receive/send data/control to or from an external source. They are also able to time-align the processed data,
- The delay of the total clearing time D_{TCT} consists of:
 - a) the delay of the interface module (CIU or VIU). In general D_{IM} , which is a variable type of delay,
 - b) the delay of the packet-switched Ethernet Network - D_{EN} , which is a fixed-time delay type, depending on the distance of the fiber-optic cable,
 - c) the delay in the central protection unit – D_{CPU} , which consists of hardware and software delay types,
 - d) the delay of the packet-switched *Ethernet Network* - D_{EN}
 - e) the delay of the BIU interface module – D_{BIU} , which is in the order of 15 ms both for closing or opening a contact,

f) the delay of the Circuit Breaker contact opening - D_{CB} , which is in the order of 75 ms.

Thus, the total fault clearing time can be represented by the following latency components: $D_{TCT} = D_{IM} + D_{EN} + D_{CPU} + D_{EN} + D_{BIU} + D_{CB}$

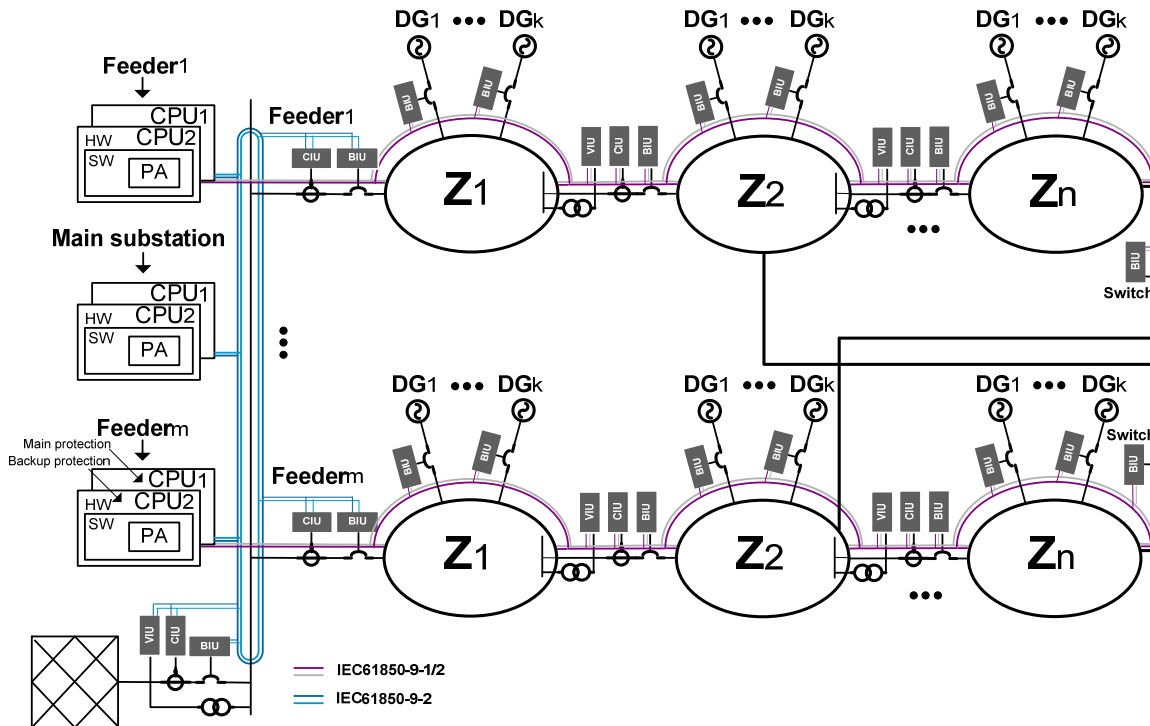


Figure 5.2. Demonstration of the protection strategy I (intended for any arbitrary Dutch MV grid supplied with an arbitrary number of DG-units) according to the terminology adopted in this thesis

5.2.3 Proposed protection strategy II

This proposed protection philosophy relies on:

- distributed computation of the binary decision signals of the processed PDOC blocks at each separate IED (CT/VT/CB) point (no interface units are required),
- central processing of the communication-transferred binary decision signals to determine the faulty zone. The faulty segment is identified and the required tripping and/or closing commands are issued. The proposed communication topology reduces the complexity of multiple IED-to-IED “logic” communications,
- the required communication network bandwidth is lower in this case of “data” communication and no sensor units are required. Nevertheless, redundant IEDs are needed at its measurement point to process locally the decision signal of the

processed PDOC block. The CPU runs the global blocking scheme and undertakes the process of decision making.

Figure 5.3(b) illustrates the generic flowchart of the protection algorithm corresponding to the protection strategy II. The strategy can be applied on any arbitrary distribution grid independent of the number, size and location of the DG-units. Figure 5.4 demonstrates the protection strategy according to the terminology adopted in this thesis,

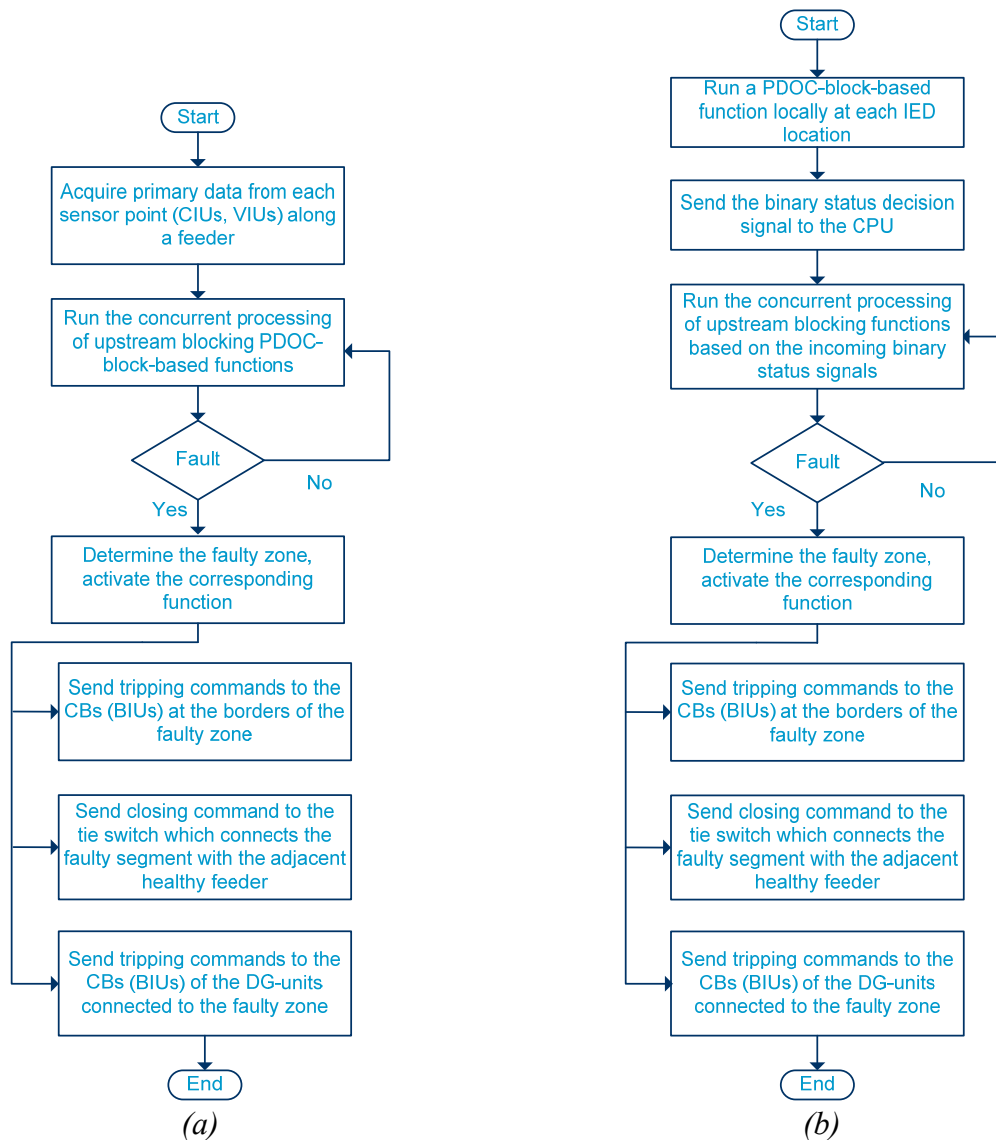


Figure 5.3. Generic flowchart of the protection algorithm that can be applied on any arbitrary distribution grid supplied with arbitrary number of DG-units per zone. (a) proposed protection strategy I, (b) proposed protection strategy II

Once again it is important to point out the fact that the protection algorithm remains identical in both cases. The difference between both strategies relies on the selection of distribution and/or integration of measurement and/or computation points. The undertaken strategy is a final selection of every power utility and it can be founded on a thorough cost

comparison. The scope of the thesis is within the algorithm and does not strictly recommend the adaptation of one of the proposed strategies. The strategy selection should be the outcome of the achieved decision among power, ICT and communication engineers.

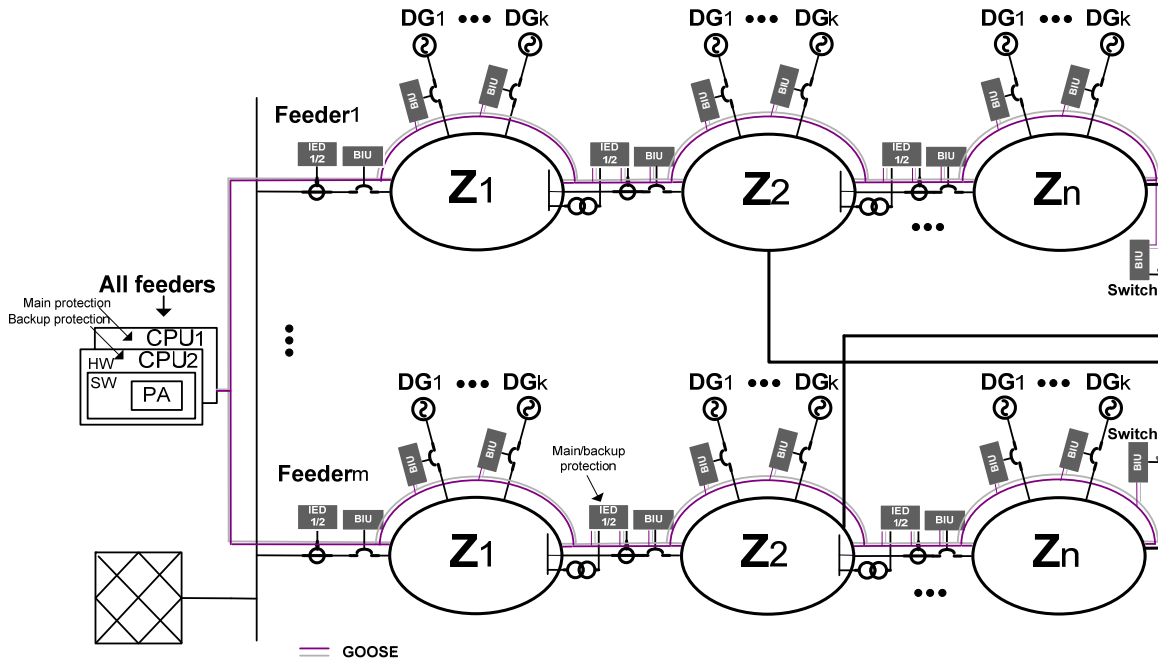


Figure 5.4. Demonstration of the protection strategy II (intended for any arbitrary Dutch MV grid supplied with an arbitrary number of DG-units) according to the terminology adopted in this thesis

5.3 Example case

In this section, an example of a simple test grid that consists of two feeders, Feeder 1 and Feeder 2 is considered. Feeder 1 and feeder 2 are divided in three zones (Z1, Z2 and Z3) and two zones (Z4 and Z5) respectively. DG1 is connected to zone Z1, DG3 to Z3 and DG5 to Z5. The ring architecture of the grid can be observed by the existence of two emergency ties, namely switch1 and switch2. However, the grid is radially operated since in the emergency ties the switches are open.

Figure 5.5 depicts the arrangement of the sensor and computation units in the main substation and along each feeder, according to the protection strategy I. It is assumed that for each measurement point, a PDOC block is processed, which triggers in the forward direction of the power flow. Table 5.2 presents the allocation of the functions in the CPUs, the associated input signals for each function and the utilization of blocking protection functionality. Table 5.3 shows the mapping among functions and corresponding BIUs.

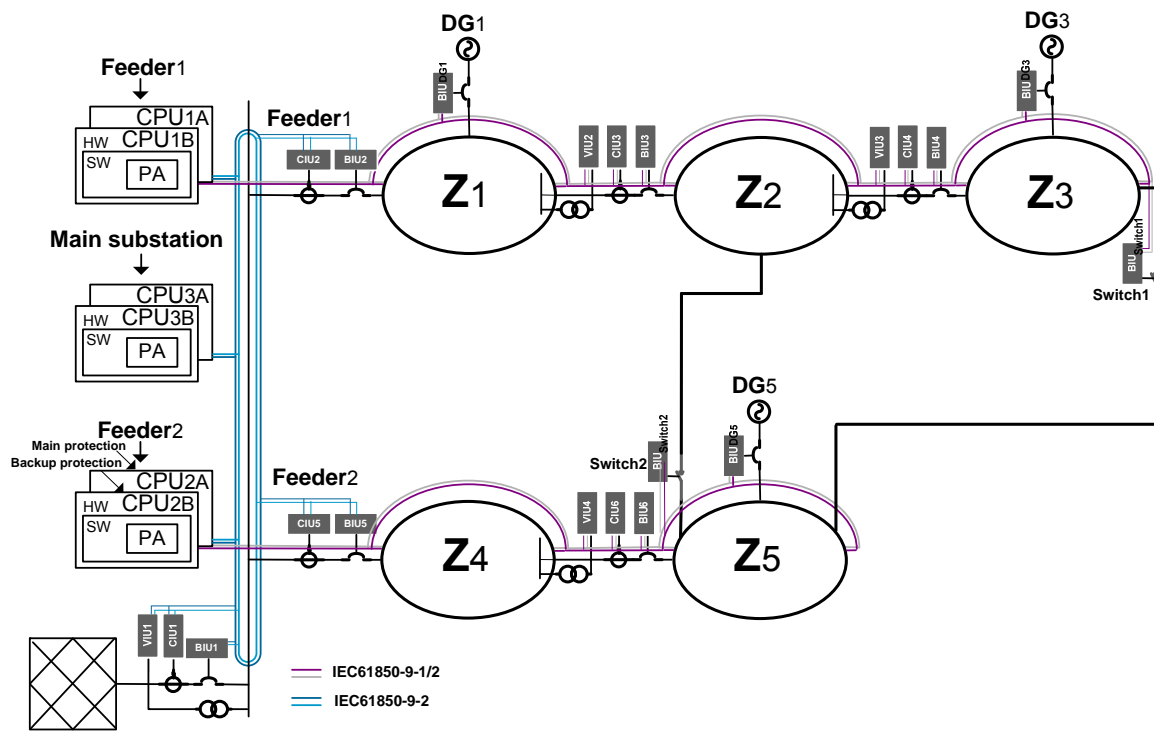


Figure 5.5. A case study of a simple grid with an illustration of the protection strategy I.

Table 5.2. Allocation of the functions in the CPUs, associated input signals and modeled protection principle of each function with the utilization of blocking protection logic

CUU	Function	Inputs		Protection principle	Blocking Function
		CIUs	VIUs		
CPU1A CPU1B	F1	CIU2, CIU3	VIU1	PDOC1	PDOC2 PDOC3
	F2	CIU3, CIU4	VIU2	PDOC2	PDOC3
	F3	CIU4	VIU3	PDOC3	-
CPU2A CPU2B	F4	CIU5, CIU6	VIU1	PDOC4	PDOC5
	F5	CIU6	VIU4	PDOC5	-
CPU3A CPU3B	F6	CIU1, CIU2, CIU5	-	PBDF	-

Table 5.3. An allocated function for each zone, mapping of functions to BIUs of grid, BIUs of DG-units and BIUs of switches

Function	BIUs of grid	BIUs of DGs	BIUs of switches	Zone
F1	BIU2, BIU3	BIU_DG1	BIU_switch1	Z1
F2	BIU3 BIU4	-	BIU_switch1	Z2
F3	BIU4	BIU_DG3	-	Z3
F4	BIU5, BIU6	-	BIU_switch2	Z4
F5	BIU6	BIU_DG5	-	Z5
F6	BIU1, BIU2, BIU5	BIU_DG1, BIU_DG3, BIU_DG5	-	Z6

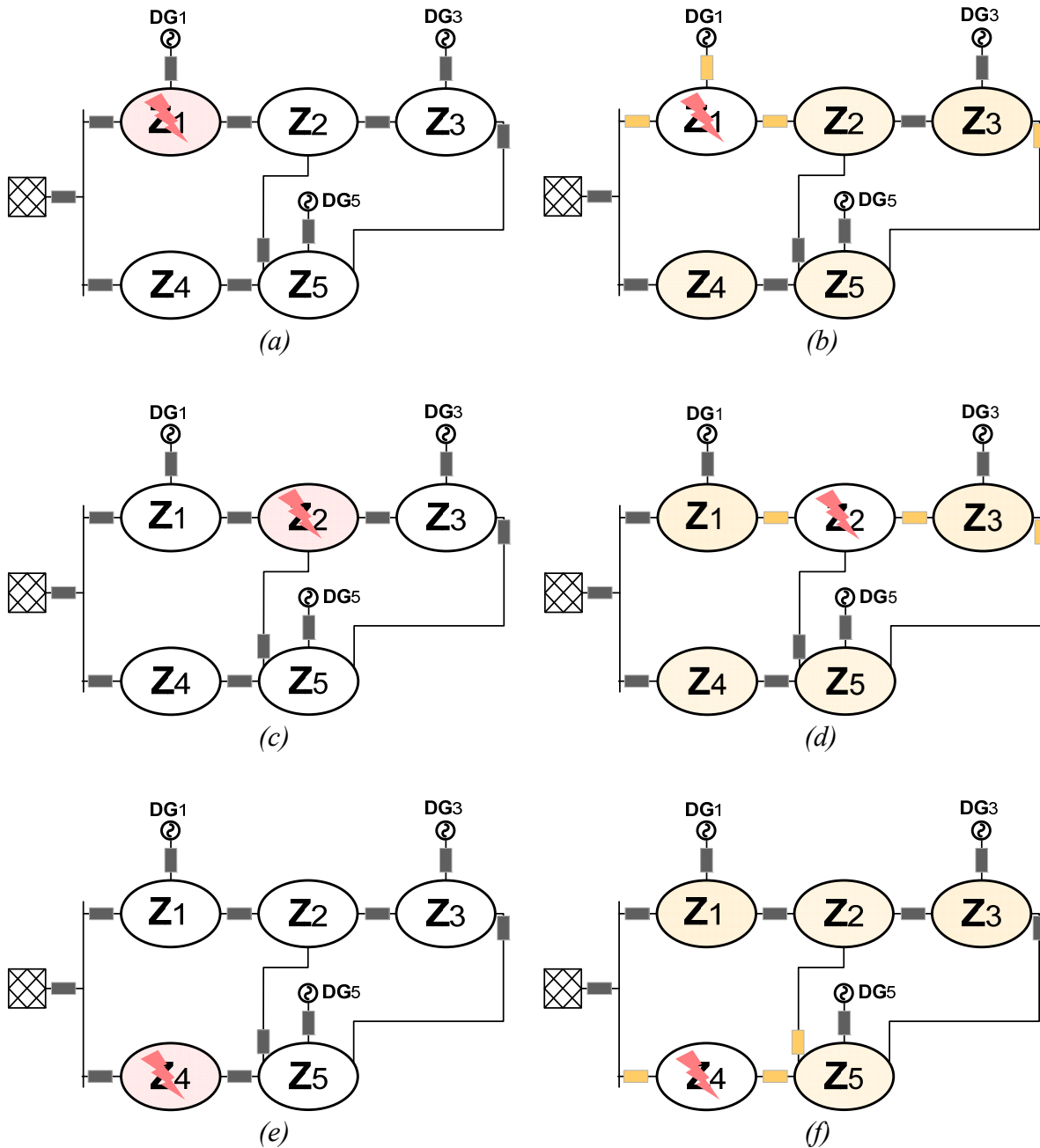


Figure 5.6. (a, b) Grid operation before and after the isolation of the faulty zone Z1. An illustration of activated circuit breakers and switches, (c, d) Grid operation before and after the isolation of the faulty zone Z2. An illustration of activated circuit breakers and switches, (e, f) Grid operation before and after the isolation of the faulty zone Z4. An illustration of activated circuit breakers and switches.

For a disturbance in zone 1, the fault clearing process presents the following tripping order:

- Function F1 is triggered and issues trip commands to the BIUs (BIU2 and BIU3) which are located at the borders of zone 1 and respectively to Z1-forming CBs. A

closing command is additionally issued to the BIU of switch1. Trip command is sent to the BIU of DG1.

- The distribution grid configuration is modified from radial to closed-loop by means of the change of the status of switch1 from open to closed.
- The grid remains in closed-loop operation for 15 ms because the opening time of the CBs is in the order of 75 ms whilst the closing time of the tie switch1 is approximately 60 ms. Faulty zone Z1 is isolated by its zone-forming CBs (CB2 and CB3). The disconnection of the faulty zone permits the continuity of operation of zone Z1 of Feeder 1 via Feeder 2. Therefore, the clearance of the faulty zone signifies the restoration of the grid configuration to a radial architecture.

The tripping order of the fault clearing process for a disturbance in zone 2 is as follows:

- The fault is detected by function F2. Trip commands are issued to the zone-forming CBs (CB3 and CB4) and a closing command is sent to the CB of switch1.
- The grid structure is transformed from radial to closed-loop arrangement by means of the conversion of the status of switch1 from open to closed.
- The faulty zone is isolated by the zone forming CBs, namely CB3 and CB4. DG1 is also disconnected. The grid structure restores to its pre-disturbance radial operation after the faulty zone and DG disconnection. Therefore, zone Z3 remains in operation due to the closing of tie switch1.

The tripping order of the fault clearing process for a disturbance in zone 4 includes the following steps:

- The activation of the associated function F4, which triggers closing command to switch2 and tripping commands to the zone-forming BIUs of Z4.
- The maintenance of the closed-loop grid architecture for 15 ms, the subsequent isolation of the faulty segment and the final grid restoration to its pre-fault radial arrangement. In this way, Z5 remains in operation by obtaining power supply through Feeder 1.

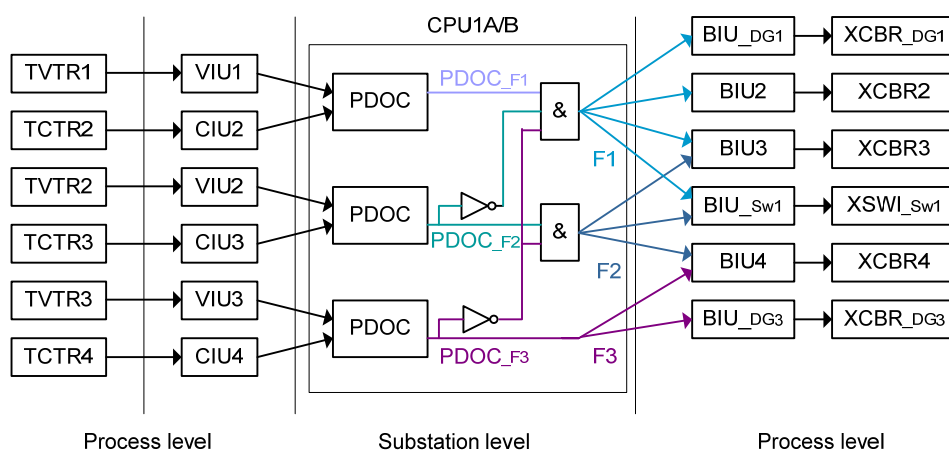


Figure 5.7. Decomposition of functions into interacting LDs on different levels.

Figure 5.7 displays the decomposition of the developed functions into interacting logical nodes across different levels (from process level to substation level and back to process level again). The figure additionally depicts the block representation of the functions of Feeder 1, which make use of blocking signals.

5.4 Conclusions

In this chapter, a protection algorithm, which can be applied to any arbitrary Dutch distribution grid supplied with arbitrary number of DG-units, is proposed. Two different protection strategies which can accommodate the developed algorithm are presented. The arrangement of the sensor, communication infrastructure, and IED organization are illustrated correspondingly for both protection strategies. The flowcharts which demonstrate the protection algorithm for both strategies are depicted and explained in detail. Fundamentally, the algorithm makes use of concurrent processing of directional overcurrent information, originating from multiple points along each feeder, in blocking scheme logic. The first proposed strategy suggests the implementation of SV communication protocol. The second protection strategy proposes the application of GOOSE communication protocol. In both protection philosophies functions are distributed across multiple devices, thus forming communication-based distributed functions. The functions are allocated across different physical devices, whilst the logical connections are mapped to the physical devices over the communication network with available transport mechanisms such as SV or GOOSE. Finally, the application of the algorithm is illustrated on a simple test grid and illustrative examples of special scenario cases are depicted.

Chapter 6

Application of the intelligent protection algorithm for Lelystad distribution network

6.1 Introduction

This chapter applies the new concept of protection philosophy for the Lelystad distribution network. The feeder/substation-oriented fully integrated protection strategy is illustrated. An analytical description is given of the time delay components, which are comprised in the total fault clearing time. The real-time organization of both the hardware architecture and communication infrastructure of the new communication-based protection algorithm is illustrated in detail. The intelligent protection algorithm is evaluated by the aid of Lelystad distribution network and meaningful conclusions are extracted. The discrete time dynamic simulations validate the correct performance and selectivity of the proposed protection scheme through various scenario cases. The algorithm implements different multi-functional protection principles supported by blocking schemes. Special emphasis is given to the network reconfiguration scenario cases and detailed simulation results of such illustrative studied cases are provided. The algorithm converts the grid structure from radial to closed-loop operation just before the isolation of the faulty segment of the network. It is demonstrated that in this way, the intelligent algorithm guarantees the protection selectivity and is capable of enhancing the availability of the DG-units during and after the fault. The numerous benefits of the proposed protection strategy are finally summarized.

6.2 Algorithm application for Lelystad distribution network

In this section, the feeder/substation-oriented fully centralized protection concept is analyzed for Lelystad distribution network. The feeders are equipped with instrument transformers and relay equipment at several locations along each of them, to accommodate the conventional protection scheme. The installation of primary interface units i.e. CIUs, VIUs and BIUs at the locations where instrument transformer equipment already exists is proposed. The designed scheme is based on the proposed algorithm I, explained in chapter 5. Therefore, time-stamped digital samples of current and voltage measurements acquired from multiple locations are provided to create a sophisticated protection algorithm. This proposed strategy implies that there is no need of installation of additional instrument transformers, except for the cases in which VT equipment is required.

The hardware and communication infrastructure organization of the fully centralized protection scheme for Lelystad distribution network is depicted in detail in Figures 6.1 and 6.2. The red dots indicate the location of the sensors and the circuit breakers. Each feeder is divided into zones and the locations of the primary interface units indicate the borders of each separate zone.

The assumptions taken into consideration regarding the time delay components of the total fault clearing time are defined according to Figure 6.3. The following assumptions have been considered regarding the latency values of each separate delay component:

- Sensor delay (CIU, VIU): 5 ms
- Communication delay: 5 μ s/km
- CPU delay: variable type of delay, dependent on the modeled protection principle
- BIU delay: 15 ms
- CB delay due to contact opening: 75 ms
- Switch delay due to contact closing (applied for the tie switches): 60 ms

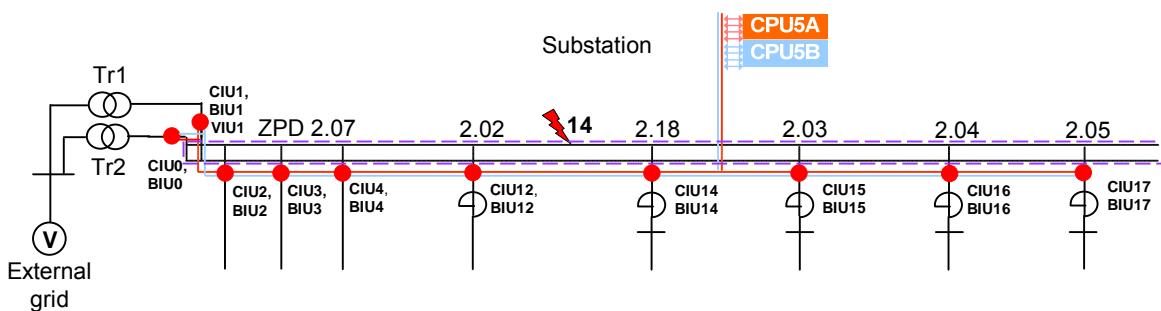


Figure 6.1. Substation-oriented hardware organization for Lelystad distribution network

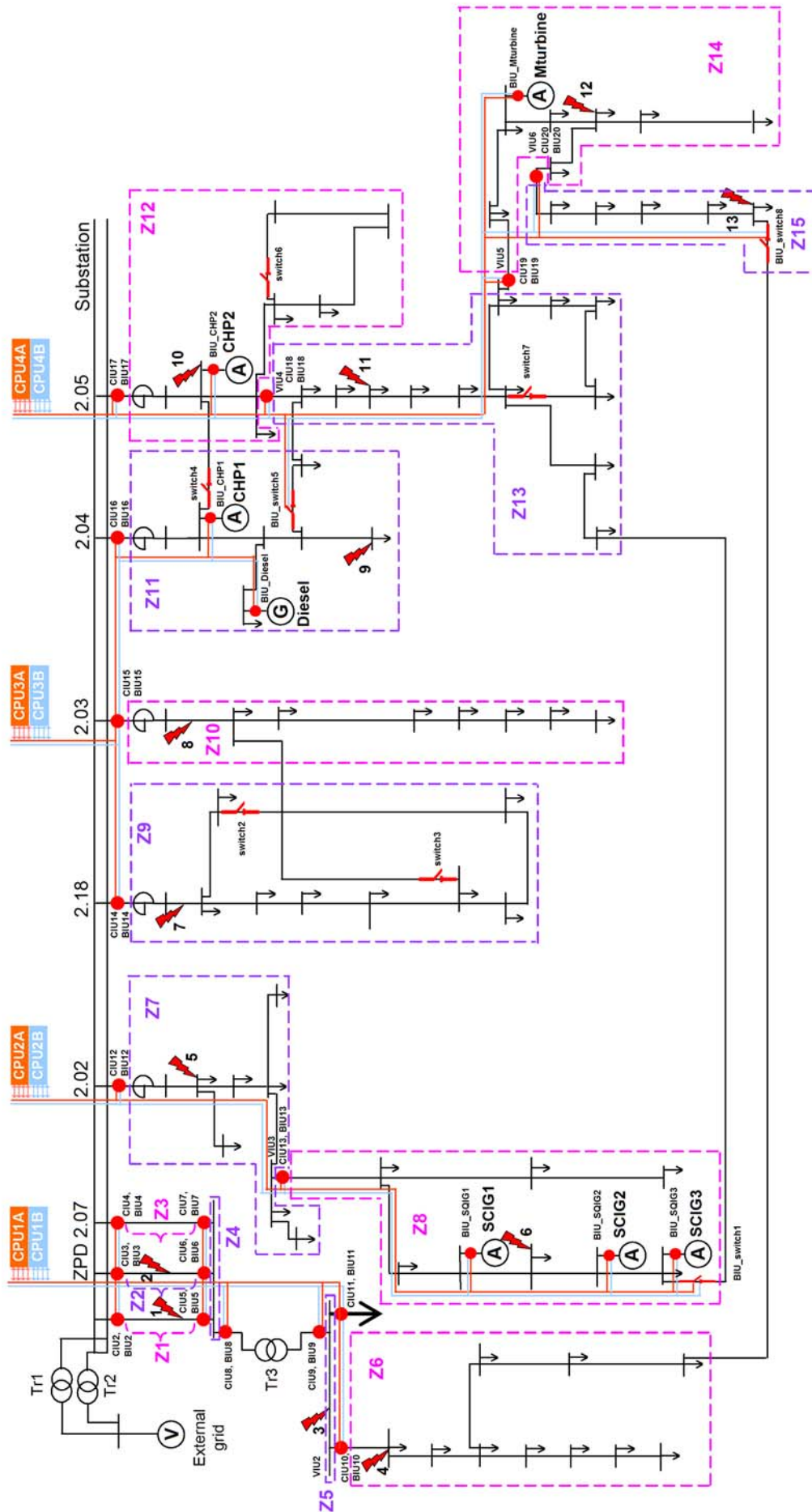


Figure 6.2 Feeder-oriented hardware organization for Lelystad distribution network

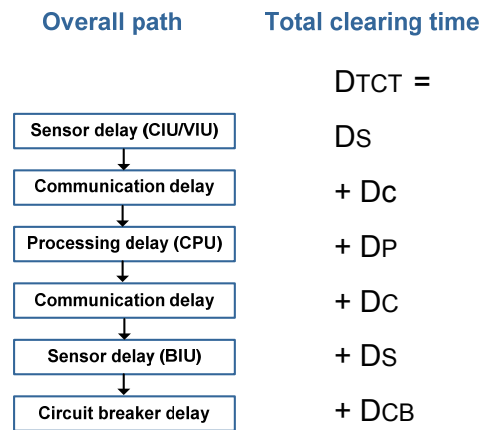


Figure 6.3. Delay components of the total fault clearing time

Tables 6.1 and 6.2 present the allocation of the functions in the CPUs. The associated input signals and modeled protection principle for each function are displayed as well. The implementation of blocking protection logic in the developed functions is additionally depicted. Table 6.2 shows the mapping among functions and BIUs. The BIUs correspond to interface units coupled to CBs of the grid, the DG-units and the tie switches.

Table 6.1. Allocation of the functions in the CPUs, associated input signals and modeled protection principle of each function, utilization of blocking protection logic

CUU	Function	Inputs		Protection principle	Blocking function
		CIUs	VIUs		
CPU1A CPU1B	F1	CIU2, CIU5	-	PLDF	-
	F2	CIU3, CIU6	-	PLDF	-
	F3	CIU4, CIU7	-	PLDF	-
	F4	CIU5, CIU6, CIU7, CIU8	-	PBDF	-
	F5	CIU9, CIU10, CIU11	-	PBDF	-
	F6	CIU10	VIU2	PDOC	-
CPU2A CPU2B	F7	CIU12	VIU1	PDOC	PDOC8
CPU3A CPU3B	F8	CIU13	VIU3	PDOC	-
	F9	CIU14	VIU1	PDOC	-
	F10	CIU15	VIU1	PDOC	-
CPU4A CPU4B	F11	CIU16	VIU1	PDOC	-
	F12	CIU17	VIU1	PDOC	PDOC13, PDOC14, PDOC15
	F13	CIU18	VIU4	PDOC	PDOC14, PDOC15
	F14	CIU19	VIU5	PDOC	PDOC15
CPU5A CPU5B	F15	CIU20	VIU6	PDOC	-
		F16	CIU0, CIU1, CIU2, CIU3, CIU4, CIU12, CIU14, CIU15, CIU16, CIU17	-	PBDF

Table 6.2. Allocated function for each zone, mapping of functions to BIUs of grid, BIUs of DG-units and BIUs of switches

Function	BIUs of grid	BIUs of DGs	BIUs of switches	Zone
F1	BIU2, BIU5	-	-	Z1
F2	BIU3 BIU6	-	-	Z2
F3	BIU4, BIU7	-	-	Z3
F4	BIU5, BIU6, BIU7, BIU8	-	-	Z4
F5	BIU9 BIU10, BIU11	-	-	Z5
F6	BIU10	-	-	Z6
F7	BIU12, BIU13	-	BIU_switch1	Z7
F8	BIU13	BIU_SCIG1, BIU_SCIG2, BIU_SCIG3	-	Z8
F9	BIU14	-	-	Z9
F10	BIU15	-	-	Z10
F11	BIU16	BIU_CHP1, BIU_Diesel	-	Z11
F12	BIU17, BIU18	BIU_CHP2	BIU_switch5	Z12
F13	BIU18, BIU19	-	BIU_switch8	Z13
F14	BIU19, BIU20	BIU_Mturbine	BIU_switch8	Z14
F15	BIU20	-	-	Z15
F16	BIU0, BIU1, BIU2, BIU3, BIU4, BIU12, BIU14, BIU15, BIU16, BIU17	BIU_SCIG1, BIU_SCIG2, BIU_SCIG3, BIU_CHP1, BIU_Diesel, BIU_CHP2, BIU_Mturbine	-	Z16

6.2.1 Protection settings of the implemented functions

The sensors provide (by communication-based transmission) the overcurrent and the directional blocks (which run in the central integrated algorithm) with voltages and currents values obtained by the current and voltage transformers. Directional overcurrent functionality has been developed for specific measurement points. The overcurrent block detects an overcurrent and provides instantaneously an active signal when a threshold value is exceeded. The directional block detects whether the direction of the power that belongs to the fault current is in forward or reverse direction. The relays are set in forward direction, thus active signals are generated when the fault is in forward direction.

In this scheme, blocking signals have been applied among the different blocks to enhance the protection reliability. The binary signals generated by PDOC block are used for blocking the function of upstream PDOC blocks. The overall binary status signals of the blocks generate the final trip signals, which are transferred back. Figure 6.4 depicts the block representation of the functions, that make use of the blocking signals.

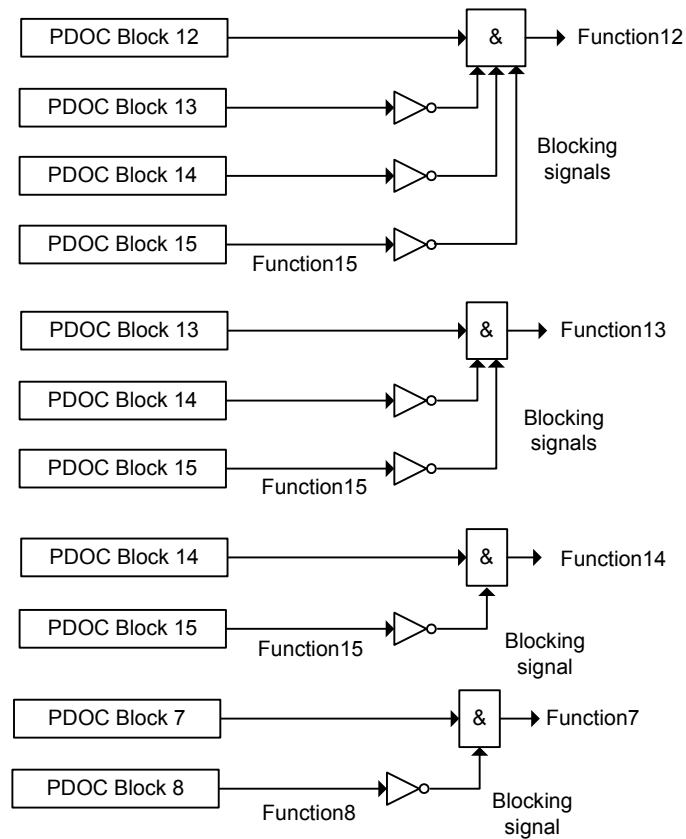


Figure 6.4. Block representation of the functions that make use of blocking signals

Table 6.3 gives an overview of the settings of the directional overcurrent based functions. The pickup value of the definite overcurrent relays is set to 50% of the end-of-line phase to phase fault. The short-circuit currents are calculated without the contribution of the plants. Furthermore, I_{pickup} should be higher than 200% of the feeder maximum load current. The DG-unit interconnect protection is also taken into account. Therefore, the DG connection point is equipped by typical protection devices for under and overvoltage detection.

Table 6.3. Settings of the directional overcurrent-based functions

Function	CT ratio	$I_{>>}$ [A] [Primary side]	$t_{>>}$ [s]
F6	300/5	2000	0.045
F7	200/5	2000	0.045
F7	200/5	1800	0.045
F9	300/5	2000	0.045
F10	100/5	2000	0.045
F11	400/5	2000	0.045
F12	400/5	2000	0.045
F13	400/5	2000	0.045
F14	200/5	1500	0.045
F15	100/5	1000	0.045

The applied functions based on the differential protection principle utilize percentage restraint differential protection logic and particularly make use of a single –slope characteristic. The applied differential protection functions are separated into two categories. Line differential protection functions represented by F1, F2 and F3 are applied to detect the section of the parallel connected cables located in feeder ZPD 2.07, namely zones 1, 2 and 3. The typical recommended value for the pickup current of the line differential protection logic ranges between 20 to 50% of the nominal current value. The setting of the pickup current used in the simulations is set to 30% of the nominal line current.

The busbar differential protection functions represented by F4, F5 and F16, are applied to protect the busbars corresponding to the protection zones 4, 5 and 16. The recommended value of the pickup current of the busbar differential protection logic is between 80 and 100% of the highest nominal primary current of all current transformers connected to the protected busbar. The setting of the pickup current used in the performed short-circuit calculations is 90% of the maximum CT primary nominal current connected to the busbar. Table 6.4 gives an overview of the settings of the functions based on differential protection principle. Figure 6.5 depicts the single-slope differential characteristics corresponding to the settings of the differential functions F1, F2, F3, and F16.

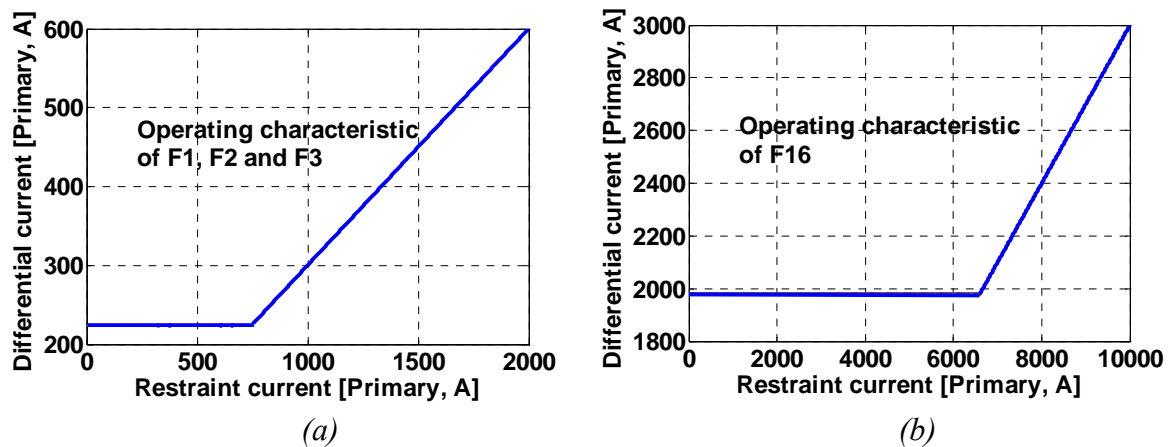


Figure 6.5. Single-slope characteristic of the differential protection principle-based functions a) F1, F2, F3 b) F16

Table 6.4. Overview of the settings of the differential-based functions

Function	CT ratio	$I_{pickup}[A]$ [Primary side]	Bias coefficient
F1	750/5	225	0.3
F2	750/5	225	0.3
F3	750/5	225	0.3
F4	750/5	675	0.3
F5	750/5	675	0.3
F16	2200/5	1980	0.3

6.2.2 Simulation results

In order to validate the selectivity and speed performance of the proposed smart protection algorithm, detailed simulation studies are carried out. The smart protection concept is verified for the Lelystad test grid. The fully centralized communication-based protection scheme and its corresponding settings are applied on the investigated network and simulations are performed to evaluate the proper operation of the proposed protection algorithm. Therefore, the simulation results are obtained after having applied the network protection settings displayed in Tables 6.3 and 6.4.

The system is subjected to various three-phase and two-phase faults (the choice is made for the same reasons explained in chapter 3) at different locations, as shown in Figures 6.1 and 6.2. Tables 6.5, 6.6, 6.7 and 6.8 depict the simulated results for two different scenario cases:

- Scenario case 1: fully centralized protection scheme with PL1
- Scenario case 2: fully centralized protection scheme with PL2

for which the corresponding DG penetration levels are:

- PL1=37%
- PL2=74%, (double penetration level) by keeping the same share of DG and decreasing the load by 50% ($L2=L1/2$).

*Table 6.5. Scenario case I: centralized protection scheme, PL1
Triggered function-CBs, total fault clearing time and network reconfiguration*

Fault location / type	Triggered function	Triggered CBs	Network reconfiguration
1 / 3L	F1: 0.106	CB2, CB5: 0.196	-
2 / LL	F2: 0.107	CB3, CB6: 0.197	-
3 / LL	F5: 0.108	CB9, CB10, CB11: 0.198	-
4 / 3L	F6: 0.157	CB10: 0.247	-
5 / LL	F7: 0.156	CB12, CB13: 0.246	CB_switch1: 0.231
6 / LL	F8: 0.158	CB13: 0.248	-
7 / LL	F9: 0.158	CB14: 0.248	-
8 / 3L	F10: 0.153	CB15: 0.243	-
9 / LL	F11: 0.158	CB16: 0.248	-
10 / 3L	F12: 0.154	CB17, CB18: 0.244	CB_switch5: 0.229
11 / LL	F13: 0.156	CB18, CB19: 0.246	CB_switch8: 0.231
12 / LL	F14: 0.157	CB19, CB20: 0.247	CB_switch8: 0.232
13 / LL	F15: 0.157	CB20: 0.247	-
14 / LL	F16: 0.109	CB0, CB1, CB2, CB3, CB4, CB12, CB14, CB15, CB16, CB17: 0.199	-

In chapter 3, the reasons why protection blinding is not an issue for typical Dutch underground cable distribution networks have been thoroughly explained. However, it was demonstrated that false tripping of the network protection and nuisance tripping of the DG-

units (which are connected to healthy zones of the grid) cause significant potential problems for the case of the currently applied conventional time-graded protection schemes. This section gives an opportunity to observe the occurrence of similar protection problems for the new protection scheme.

Fault initiation is at 100 ms for all case scenarios. Fault clearing time is the total time covering the time delays of the total path from the instant of the fault inception (sensor time delay) to the instant of the fault clearance (circuit breaker contact opening time delay). The fault locations and types, the triggered functions, the triggered circuit breakers and their corresponding tripping and total fault clearing times (all in seconds) are presented for all case scenarios. Additionally, the disconnection time of the DG-units (all in seconds) and the corresponding triggered function, which initiates this disconnection are shown in the given tables.

The protection scheme has been tested for three and two phase faults at the borders of each separate protection zone (covering both DG penetration levels) and the accuracy of the new protection algorithm has been validated. In this section the scenario cases corresponding to the fault locations presented in tables 6.5, 6.6, 6.7 and 6.8 have been analyzed.

*Table 6.6. Scenario case I: centralized protection scheme, PLL
DG availability during and after fault*

Fault location / type	SCIG1	SCIG2	SCIG3	CHP1	CHP2	Diesel	Mturbine
1 / 3L	-	-	-	-	-	-	-
2 / LL	-	-	-	-	-	-	-
3 / LL	-	-	-	-	-	-	-
4 / 3L	-	-	-	-	-	-	-
5 / LL	-	-	-	-	-	-	-
6 / LL	F8: 0.248	F8: 0.248	F8: 0.248	-	-	-	-
7 / LL	-	-	-	-	-	-	-
8 / 3L	-	-	-	-	-	-	-
9 / LL	-	-	-	F11: 0.248	-	F11: 0.248	-
10 / 3L	-	-	-	-	F12: 0.244	-	-
11 / LL	-	-	-	-	-	-	-
12 / LL	-	-	-	-	-	-	F14: 0.247
13 / LL	-	-	-	-	-	-	-
14 / LL	F16: 0.199						

The evaluation of the intelligent protection scheme shows that for all fault locations and for both DG penetration levels correct functions are executed and corresponding circuit breakers are triggered. It is additionally observed that for all scenario cases, the faulty

section is isolated in less than 160 ms, permitting a high percentage of the DG-units to remain connected to the network and support it during and after the disturbance. Simulation results verify that the innovative protection scheme is highly beneficial in case of a high number of DG-units connected to the network. Since the protection scheme speed performance has been significantly improved, the faulty zone of the network is isolated quickly and there is no problem of interference related to the coordination between the network protective functions and the interconnect protection of the DG-units. The reason for this is that the protection scheme is so fast that only the DG-units which are included in the faulty section are disconnected, while the other DG-units (connected to the sound parts of the grid) remain in operation. For all the studied cases, DG-units are disconnected by the transferred trip command of the activated function and not by the locally installed DG interconnect protection (undervoltage protection). Therefore, the locally installed DG interconnect protection units (under/over voltage) can be mainly used as backup, in case the remote communication-based trip command fails.

*Table 6.7. Scenario case II: centralized protection scheme, PL2
Triggered function-CBs, total fault clearing time and network reconfiguration*

Fault location / type	Triggered function	Triggered CBs	Network reconfiguration
1 / 3L	F1: 0.106	CB2, CB5: 0.196	-
2 / LL	F2: 0.107	CB3, CB6: 0.197	-
3 / LL	F5: 0.107	CB9, CB10, CB11: 0.197	-
4 / 3L	F6: 0.154	CB10: 0.244	-
5 / LL	F7: 0.155	CB12, CB13: 0.245	CB_switch1: 0.23
6 / LL	F8: 0.158	CB13: 0.248	-
7 / LL	F9: 0.158	CB14: 0.248	-
8 / 3L	F10: 0.153	CB15: 0.243	-
9 / LL	F11: 0.157	CB16: 0.247	-
10 / 3L	F12: 0.154	CB17, CB18: 0.244	CB_switch5: 0.229
11 / LL	F13: 0.156	CB18, CB19: 0.246	CB_switch8: 0.231
12 / LL	F14: 0.157	CB19, CB20: 0.257	CB_switch8: 0.232
13 / LL	F15: 0.157	CB20: 0.257	-
14 / LL	F16: 0.109	CB0, CB1, CB2, CB3, CB4, CB12, CB14, CB15, CB16, CB17: 0.199	-

As it can be seen, the DG-units connected to the sound sections of the grid always remain connected to the network because the total fault clearing time is shorter than the DG disconnection time of its interconnect protection. Another significant observation is that false tripping does not take place for both cases of DG penetration level. The problem of false tripping is completely eliminated by applying directional elements in the protection logic of the software-based protection functionality, which runs in the CCUs.

Table 6.8. Scenario case II: centralized protection scheme, PL2
DG availability during and after fault

Fault location / type	SCIG1	SCIG2	SCIG3	CHP1	CHP2	Diesel	Mturbine
1 / 3L	-	-	-	-	-	-	-
2 / LL	-	-	-	-	-	-	-
3 / 3L	-	-	-	-	-	-	-
4 / 3L	-	-	-	-	-	-	-
5 / LL	-	-	-	-	-	-	-
6 / LL	F8: 0.248	F8: 0.248	F8: 0.248	-	-	-	-
7 / LL	-	-	-	-	-	-	-
8 / 3L	-	-	-	-	-	-	-
9 / LL	-	-	-	F11: 0.247	-	F11: 0.247	-
10 / 3L	-	-	-	-	F12: 0.243	-	-
11 / LL	-	-	-	-	-	-	-
12 / LL	-	-	-	-	-	-	F14: 0.247
13 / LL	-	-	-	-	-	-	-
14 / LL	F16: 0.199						

We can also see that the fully integrated protection algorithm enables a uniform fault clearing time in the order of maximum 160 ms for all the geographically dispersed circuit breaker locations. One of the most significant observations is that the protection algorithm is designed in such a way that it prevents the loss of a complete feeder. A feeder is divided into several zones and the algorithm is additionally capable of keeping the healthy zones of a feeder in operation. This is done by changing the status of the switch ties between neighboring feeders from radial to closed-loop operation, 15 ms before the isolation of the faulty segment. This grid conversion from radial to closed-loop operation (just before the isolation of the faulty zone) increases the DG availability during and after fault. The grid structure restores to its pre-fault radial operation, after the successful fault clearance.

The disconnection of all the feeders and subsequent loss of all the generators connected to the grid is noticed only for fault location #14. Figure 6.6 depicts the variation of terminal voltage, terminal current, active and reactive power of the DG-units for a two-phase fault at location #14 corresponding to scenario case 1. Function F16 (allocated in CPU5A/B) detects the fault and gets triggered at 0.109 sec. Therefore, it sends the trip commands to the BIUs of the DGs via the communication network. Trip commands are additionally transferred through the fiber-optic network to the BIUs of all CBs, which connect the grid feeders to the main substation. The CBs of the DG-units trip at 0.199 sec and it can be seen in Figure 6.6 that at the instant of DG disconnection, active/reactive powers become zero. Additionally, it can be observed that the terminal voltage and current of the DG-units connected to the isolated feeders become zero approximately one cycle after the fault isolation, since the

extraction of the RMS values of the current and voltage measurements is based on DFT calculations.

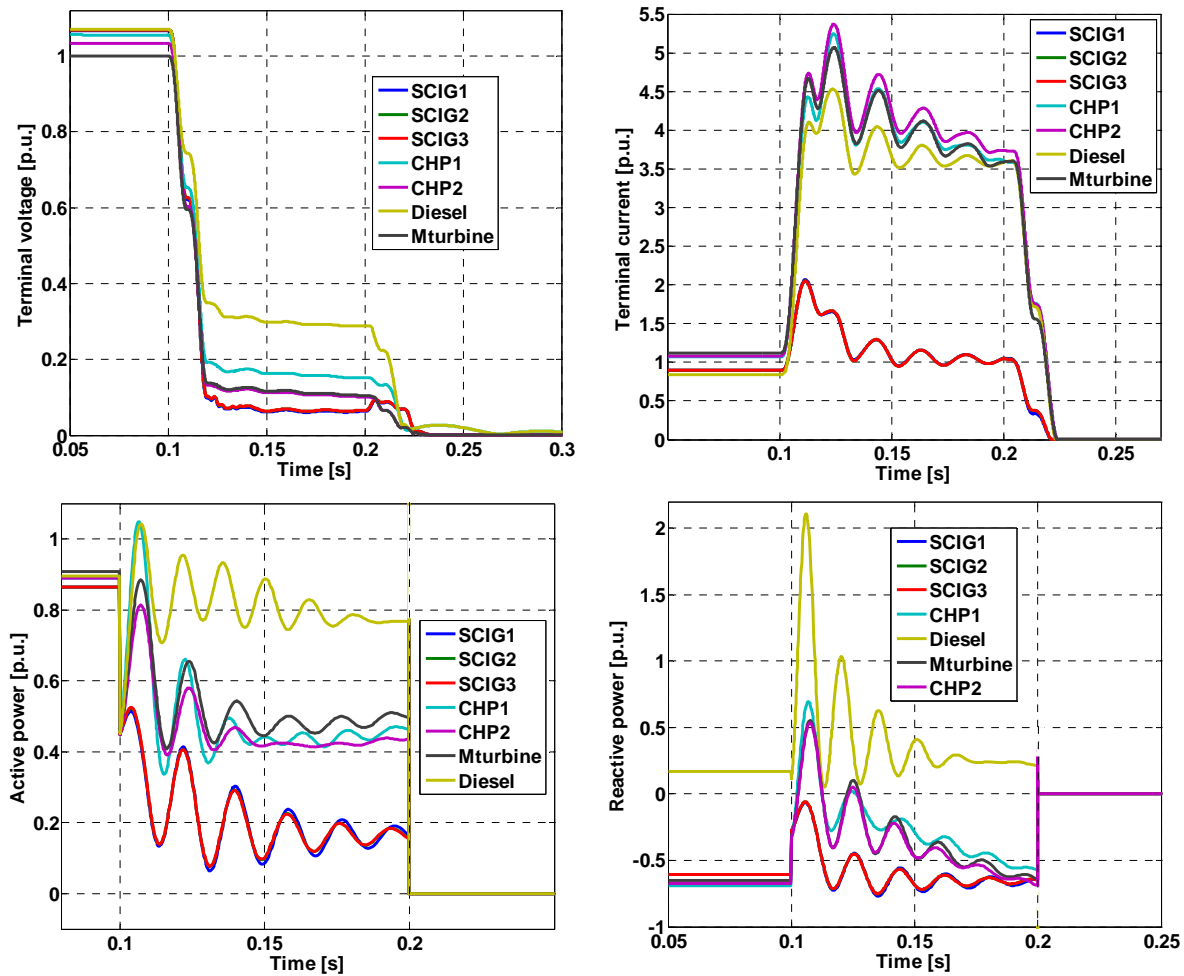
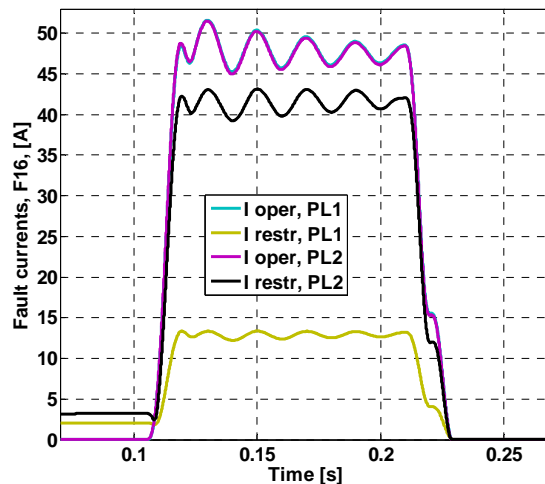


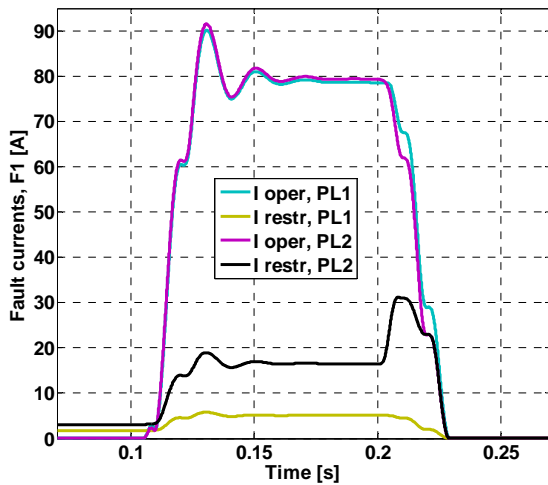
Figure 6.6. Terminal voltage, terminal current, active power and reactive power (all in [p.u.]) of DG-units following a two-phase fault at fault location #14 for scenario case I

Figure 6.7(a) illustrates the operating and restraint currents monitored by the differential function F16 following a two-phase fault at location #14 and covering both scenario cases I, II. As aforementioned, F16 triggers at 0.109 sec and issues trip commands to the CBs of all feeders connected to the faulty main busbar. It can be seen that during the disturbance, the restraint current component stays below the fault current magnitude of the operating current component. One can additionally observe that the operating and restraint current components of F16 become zero at around one cycle after the isolation of all the feeders (at 0.199 sec) connected to the faulty busbar. In a similar way, Figures 6.7(b) and (c) depict the fault current magnitudes of the differential and bias current components monitored by the functions F1 and F2 following correspondingly a three-phase fault at location #1 (at a 60% distance from the main busbar) and a two-phase fault at location #2 (at a 5% distance from the main busbar) for scenario cases I, II. For disturbances in the cable section ZPD 2.07a (zone 1), function F1 gets activated at approximately 0.106 sec and trip

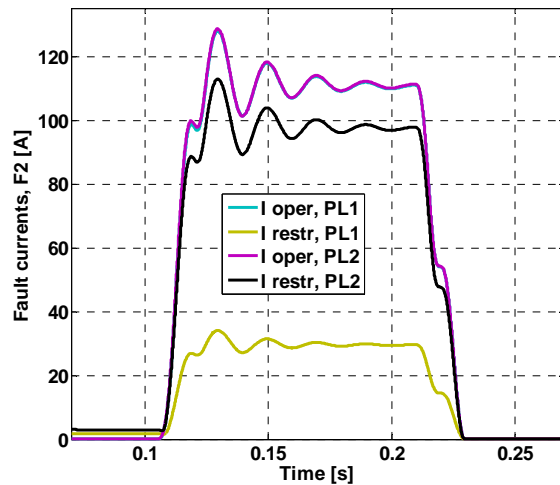
signals are issued to the BIUs, BIU2 and BIU5. The faulty cable section is finally disconnected at 0.196 sec through triggering of CB2 and CB5. Correspondingly, short-circuits in cable section ZPD 2.07b (zone 2) are detected by function F2. The associated CBs, CB3 and CB6 isolate the faulty segment Z2 upon receipt of remote communication-based trip signals from BIU3 and BIU6. The depicted curves in Figures 6.7(b,c) validate the fact that short-circuits are reliably isolated by F1 and F2 for all the studied cases.



(a)



(b)



(c)

Figure 6.7. I_k'' of the operating and restraining components (a) of F16 following a two-phase fault at location #14 for scenario cases I and II (b) of F1 following a three-phase fault at location #1 for scenario cases I and II (c) of F2 following a two-phase fault at location #2 for scenario cases I and II

6.3 Network reconfiguration scenario cases

In the previous sections it was highlighted the fact that the most significant advantage of the proposed protection scheme is that it provides an isolation of the least number of faulty zones. At the same time it ensures the avoidance of islanding problems in the remaining healthy grid zones by converting the network configuration from radial to closed loop arrangement between adjacent feeders. The most representative scenario cases for this issue cover the fault locations in zones 12, 13, 14, and 7. In this section, detailed analysis is provided for faults located in the aforementioned protection zones.

6.3.1 Fault detection and isolation in zone 12

For a short-circuit current in zone 12, the fault clearing process presents the following tripping order:

- Function F12 detects the fault and gets triggered around 55 ms after the fault inception. F12 issues trip commands to the BIUs, BIU17 and BIU18, which are located at the borders of zone 12. It additionally issues trip commands to the BIU which supervises the CB of switch5. Trip command is sent to the BIU (connected at the PCC of the DG-unit to the network) of CHP2.
- The status of switch 5 is converted from open to closed facilitating the modification of the distribution grid configuration from radial to closed-loop.
- The faulty segment Z12 is isolated by the CBs (CB17 and CB18) located at the borders of Z2. CHP2 is also disconnected. The faulty segment and DG isolation is achieved 15 ms after the network reconfiguration from radial to closed-loop operation. The grid remains in closed-loop operation for 15 ms.
- The fault is cleared. The closing of the tie switch5 permits the continuity of operation of the remaining healthy zones (Z13, Z14, and Z15) of feeder 2.05 via feeder 2.04. The operation of the grid structure restores to radial.

The sequence of closing and tripping events in case of a fault located in zone 12 is demonstrated through the representative example of fault 10. For a three-phase fault at location #10, function F12 generates a trip signal at 0.154 sec and issues closing command to switch5 and trip commands to CB17 and CB18. Functions F13, F14, and F15 (featuring a forward-set directional overcurrent protection principle) do not generate any trip signal and therefore unblock the selective operation of F12. The triggered CBs, CB17 and CB18 trip at 0.244 sec.

This sequence of events validates the fact that the DG-units connected to the healthy parts of the feeder will remain connected to it, and only the DG-units connected to the faulty segment will be isolated. Figure 6.8 depicts the variation of the terminal voltage, terminal current, active and reactive power of the DG-units following this three-phase fault at location #10 that corresponds to scenario case I. It is clearly seen that all the DG-units

which are connected to the sound zones of the grid, remain connected to it and all their terminal parameters regain their nominal values. It is additionally observed that only CHP2, which is connected to the faulty zone of the network, gets disconnected at 0.244 sec; therefore, all its terminal parameters become zero. The disconnection of the CHP2 plant is initiated by the activation of F12. In case of a communication failure in the remote trip command, the DG interconnect protection can serve as a backup to provide the desirable disconnection.

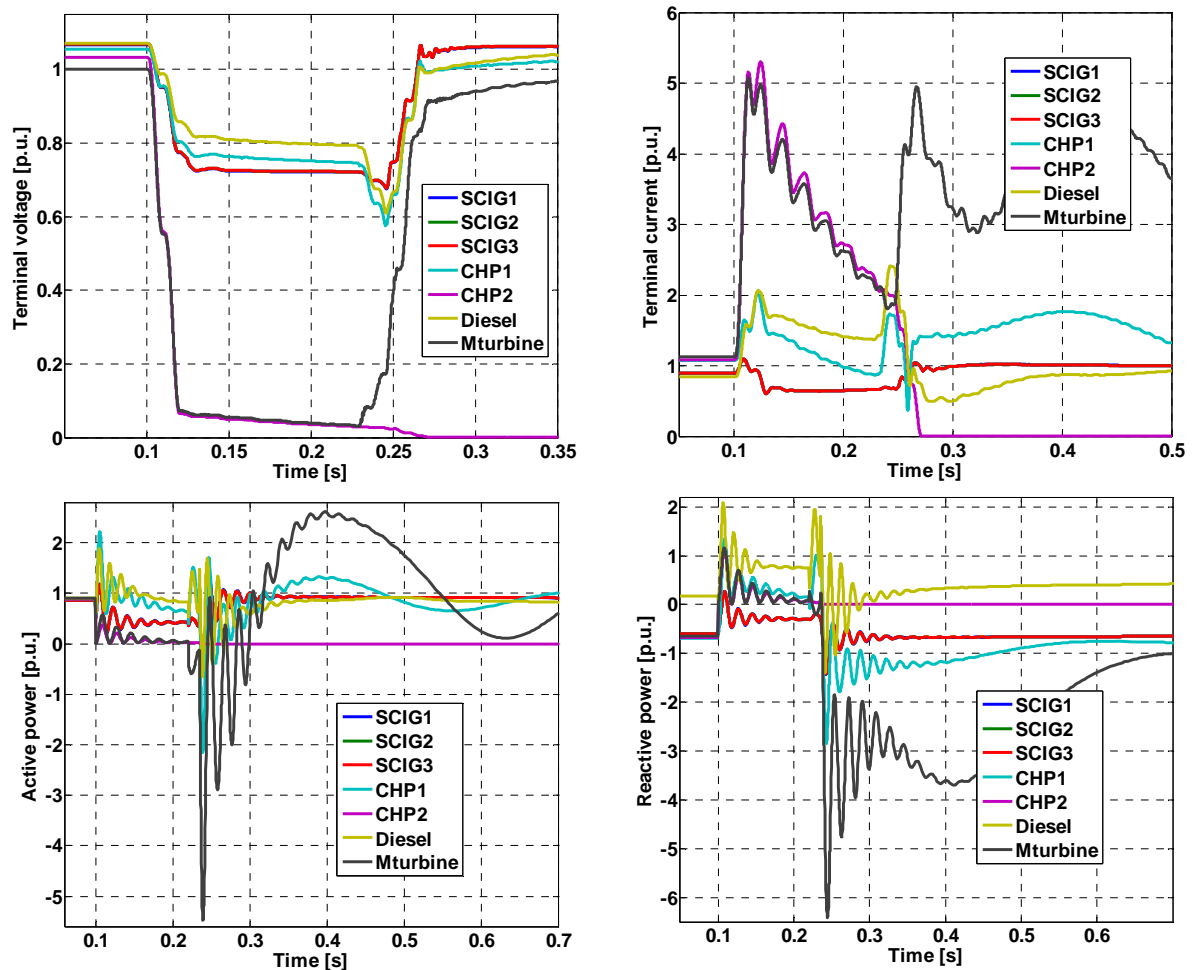


Figure 6.8. Terminal voltage, terminal current, active power and reactive power (all in [p.u.]) of DG-units following a three-phase fault at fault location #10 for scenario case I

Furthermore, it is remarkable to observe that during the 15 ms of closed-loop operation (when the status of the tie switch5 gets closed) the voltage collapse at the terminals of CHP1 and Diesel gets deepened, since the path of fault current contribution to the disturbance location is shortened. During the same period, the short-circuit current contributions of CHP1 and Diesel to the fault increase.

Figure 6.9 shows the current and voltage measurements recorded at switch5 following the disturbance at location #11 for both DG penetration levels. These figures let us to observe the order of the conversions of the grid structure arrangement:

- Initially the grid operates in a radial structure. Since the tie switch is open, the monitored current is zero.
- The grid structure converts to a closed-loop operation after the closing of switch5. During the 15 ms of the closed-loop operation of the network, the circulating current via switch5 constitutes the fault current contribution from the neighboring feeder. After the isolation of the faulty zone and the subsequent grid structure restoration to a radial operation, the monitored current obtains a steady state value.

The figure depicts the primary current monitored by switch5. It can be additionally observed that the voltage seen at one of the poles of switch5 (that belongs to feeder 2.04) recovers as soon as the faulty zone is isolated.

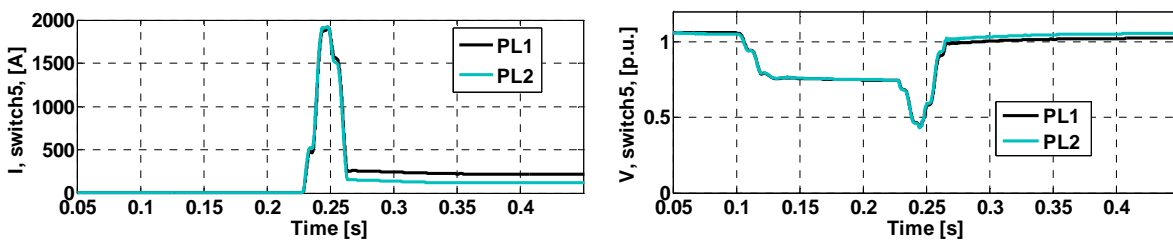


Figure 6.9. Monitored current and voltage measurements at switch5 following a three-phase fault at fault location #10 for scenario case I and II

6.3.2 Fault detection and isolation in zone 13

The tripping order of the fault clearing process for a short-circuit current in zone 13, is as follows:

- The fault is detected by function F13 within 55 ms after the fault initiation. Trip commands are issued to the zone-forming CBs (CB18 and CB19). A closing command is additionally sent to the CB of switch8.
- The status of switch 8 is converted from open to closed, thus transforming the grid structure from radial to closed-loop operation.
- The grid remains in closed-loop operation for 15 ms. The faulty segment Z13 is isolated by its zone-forming CBs (CB18 and CB19). The faulty zone isolation is carried out 15 ms after the network reconfiguration from radial to closed-loop operation.
- The clearance of the faulty zone implies the restoration of the grid structure to a radial operation. The closed switch8 permits the continuity of operation of the sound zones (Z14, and Z15) of feeder 2.05 via feeder 2.07.

The representative example of fault 11 is used to describe the sequence of closing and tripping events in the case of disturbances located in zone 13. The trip signals of functions F12, F13 and F14 following a two-phase fault at location #11 for scenario cases I and II are illustrated in Figure 6.10. It is observed that F13 generates a trip signal at 0.156 sec and therefore blocks F12. F13 issues closing command to switch8 (which closes at 0.231 sec)

and trips the equivalent CBs of the faulty zone CB18 and CB19 at 0.246 sec. Figure 6.12 depicts the short-circuit currents monitored by the overcurrent part of the modeled PDOC blocks 12, 13 and 14 for the scenario cases I and II. It can be clearly observed that the recorded fault currents seen by PDOC13 and PDOC14 become zero approximately one cycle after the zone isolation by CB18 and CB19. However, the current measurement seen by PDOC12 regains its pre-disturbance current nominal value.

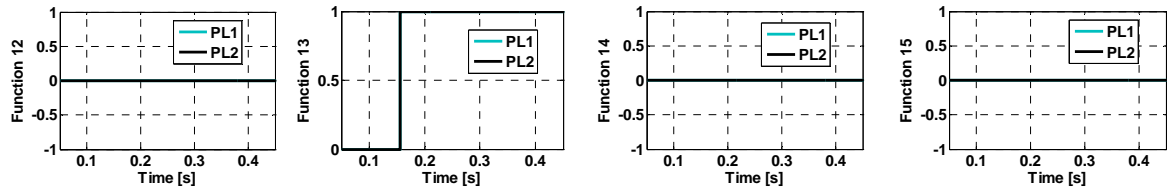


Figure 6.10. Trip signals of functions F_{12} , F_{13} , F_{14} and F_{15} following a two-phase fault at fault location #11 for scenario case I

The most significant outcome of the sequence of events following a short-circuit in zone 13, is that for this specific case all DG-units remain connected to the grid. The downstream healthy parts of the feeder 2.05, namely Z14 and Z15, are supplied from the adjacent feeder 2.07 through the closed switch8. This issue is demonstrated in Figure 6.13 where the terminal voltage, current, active/reactive power of the DG-units are depicted following a two-phase fault at location #11 corresponding to penetration level 1. The results show that all DG terminal parameters regain their initial nominal values and no DG-unit is disconnected. During the 15 ms of the closed-loop operation, we observe a small reduction and correspondingly a slight increase in the voltage dip magnitudes and the fault current contributions at the DG-unit terminals.

The current and voltage measurements monitored by switch8 following a disturbance at location #11 for penetration level 1, are shown in Figure 6.11. It is illustrated that the voltage seen at the pole of switch8 that belongs to feeder 2.07 recovers after the fault isolation. The current in switch8 obtains a steady state value after restoration of the configuration of the grid structure from closed-loop to radial.

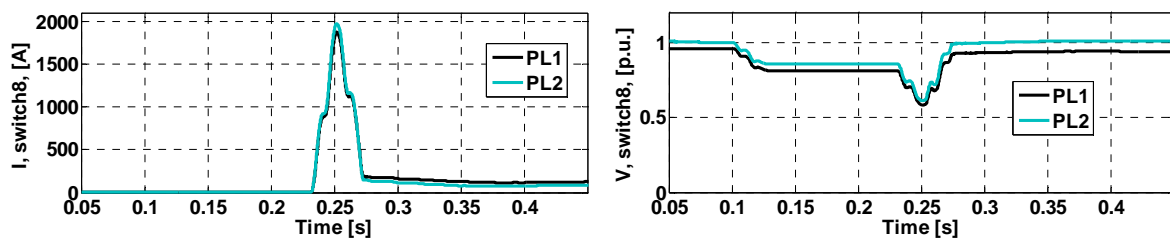


Figure 6.11. Monitored current and voltage measurements at switch8 following a two-phase fault at fault location #12 for scenario case I and II

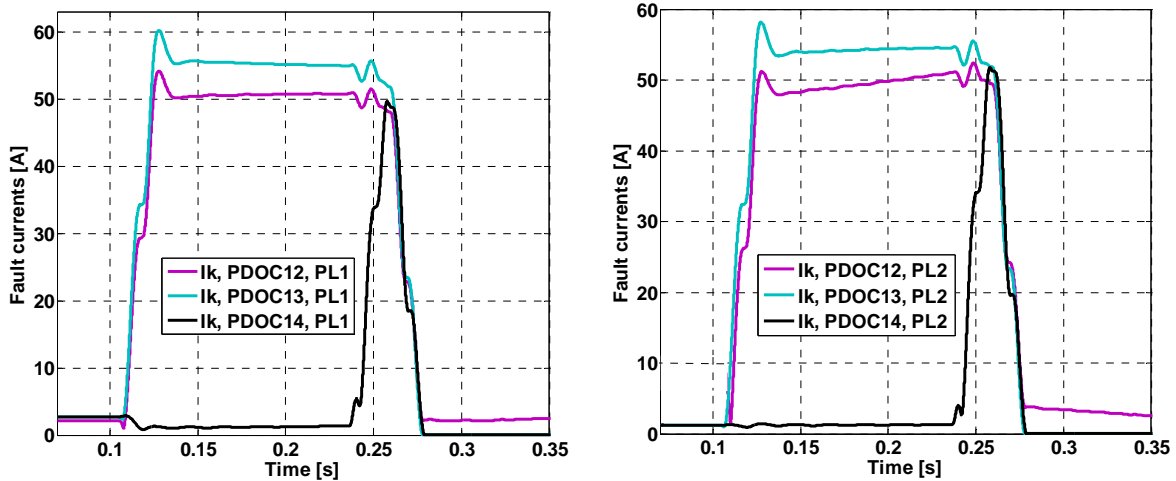


Figure 6.12. I_k of PDOC12, PDOC13 and PDOC14 following a two-phase fault at location #11 for scenario case I

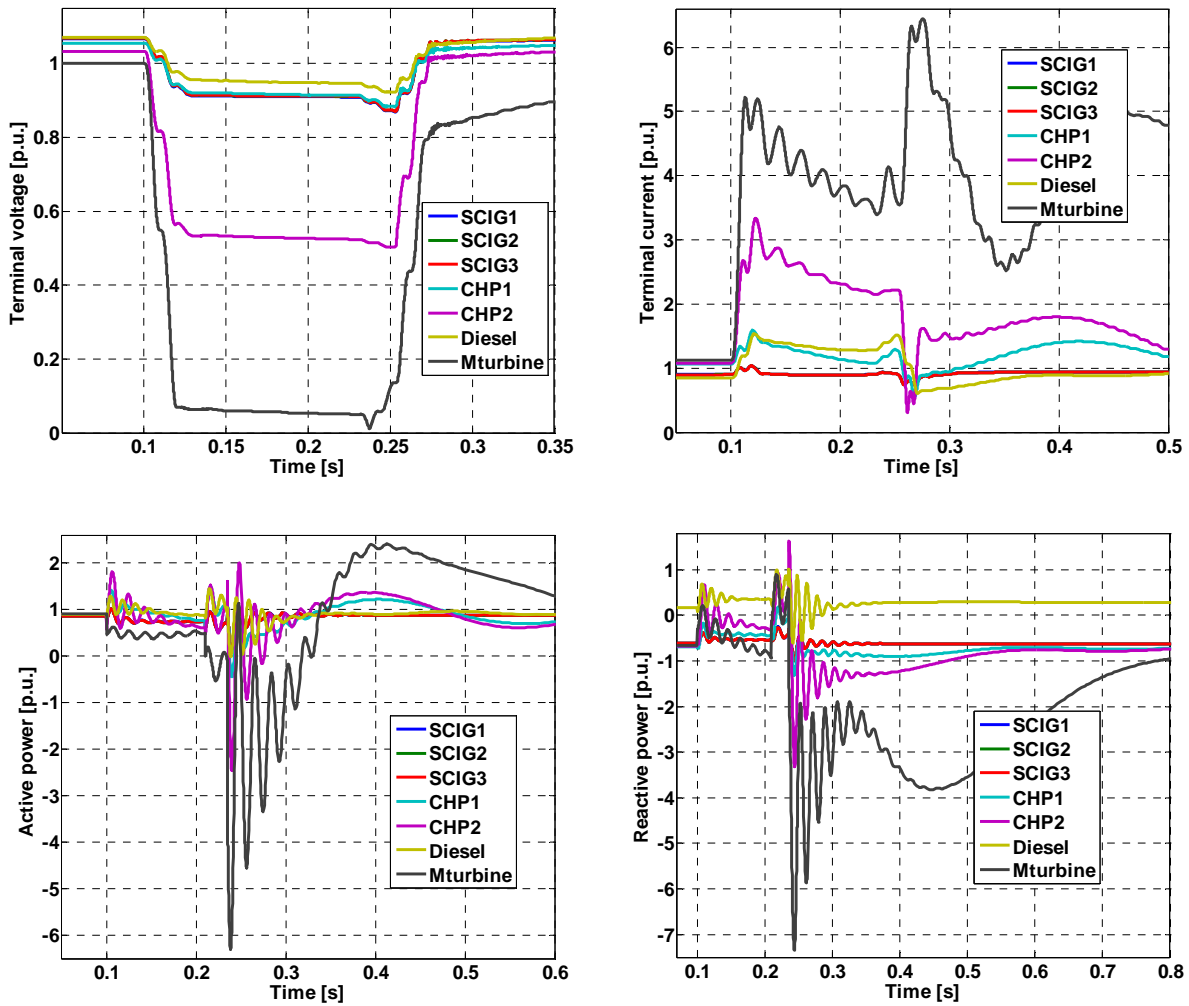


Figure 6.13. Terminal voltage, terminal current, active power and reactive power (all in [p.u.]) of DG-units following a two-phase fault at fault location #11 for scenario case I

6.3.3 Fault detection and isolation in zone 14

For the scenario case covering disturbances located in zone 14, the tripping order of the fault clearing process includes the closing of the tie switch8 and the subsequent isolation of the faulty zone 14 through the tripping of the equivalent zone-forming CBs, CB19 and CB20. In this way, Z15 remains in operation. The illustrative example of fault12 is thoroughly examined and plots derived from the simulation results are provided in this part. The trip signals of functions F12, F13, F14 and F15 following a two-phase fault at location #12 for scenario cases I and II are presented in Figure 6.14. It is seen that F14 generates a trip signal at 0.157 sec and consequently blocks F12 and F13. F14 issues closing command to switch8, which closes at 0.232 sec. CB19 and CB20 of the faulty zone are tripped at 0.247 sec. The achievement of the grid reconfiguration from radial to closed-loop just before the fault isolation facilitates the increase of the DG availability during and after the disturbance. The closed status of the tie switch8 permits the continuity of operation of the zone 15 by obtaining power supply through feeder ZPD 2.07.

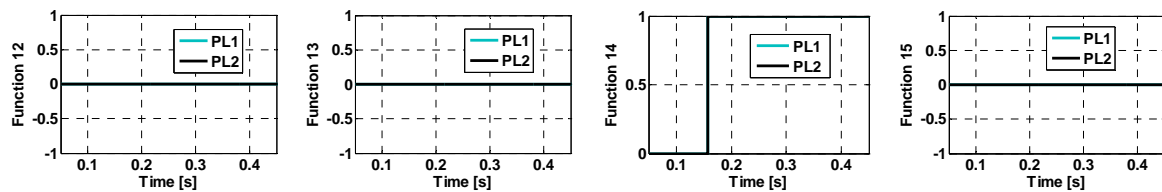


Figure 6.14. Trip signals of functions F12, F13, F14 and F15 following a two-phase fault at fault location #12 for scenario cases I and II

Figure 6.15 depicts the short-circuit currents monitored by the overcurrent part of the modeled PDOC blocks 12, 13 and 14 for the scenario cases I and II. It is demonstrated that the current measurements seen by PDOC12 and PDOC13 regain their pre-fault nominal current values after the clearance of the fault. However, the recorded fault currents seen by PDOC14 become zero at around one cycle after the zone isolation by CB19 and CB20. The terminal voltage, current, active/reactive power of the DG-units following a two-phase fault at location #12 corresponding to PL1 are depicted in Figure 6.16.

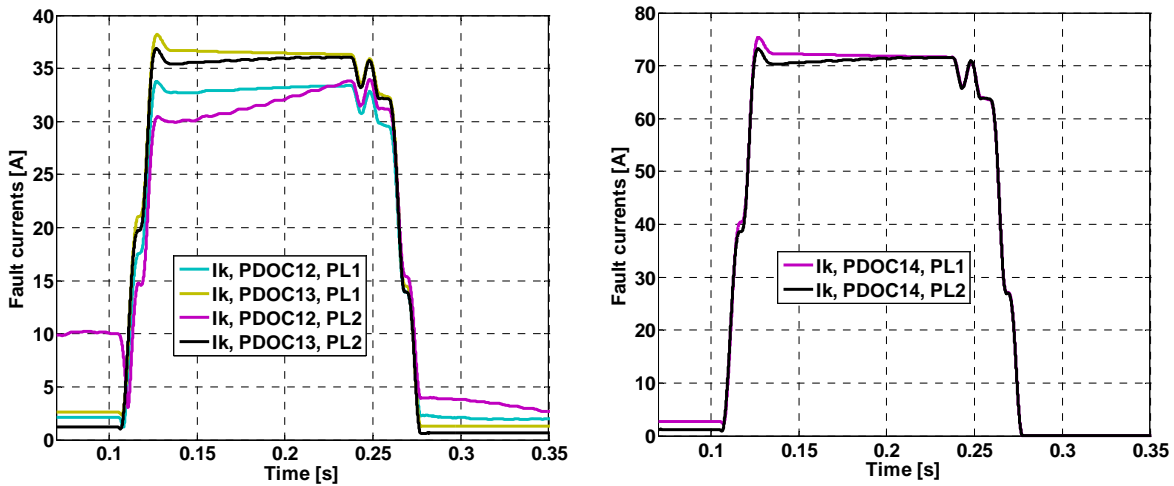


Figure 6.15. I_k of PDOC12, PDOC13 and PDOC14 following a two-phase fault at location #12, for scenario cases I and II

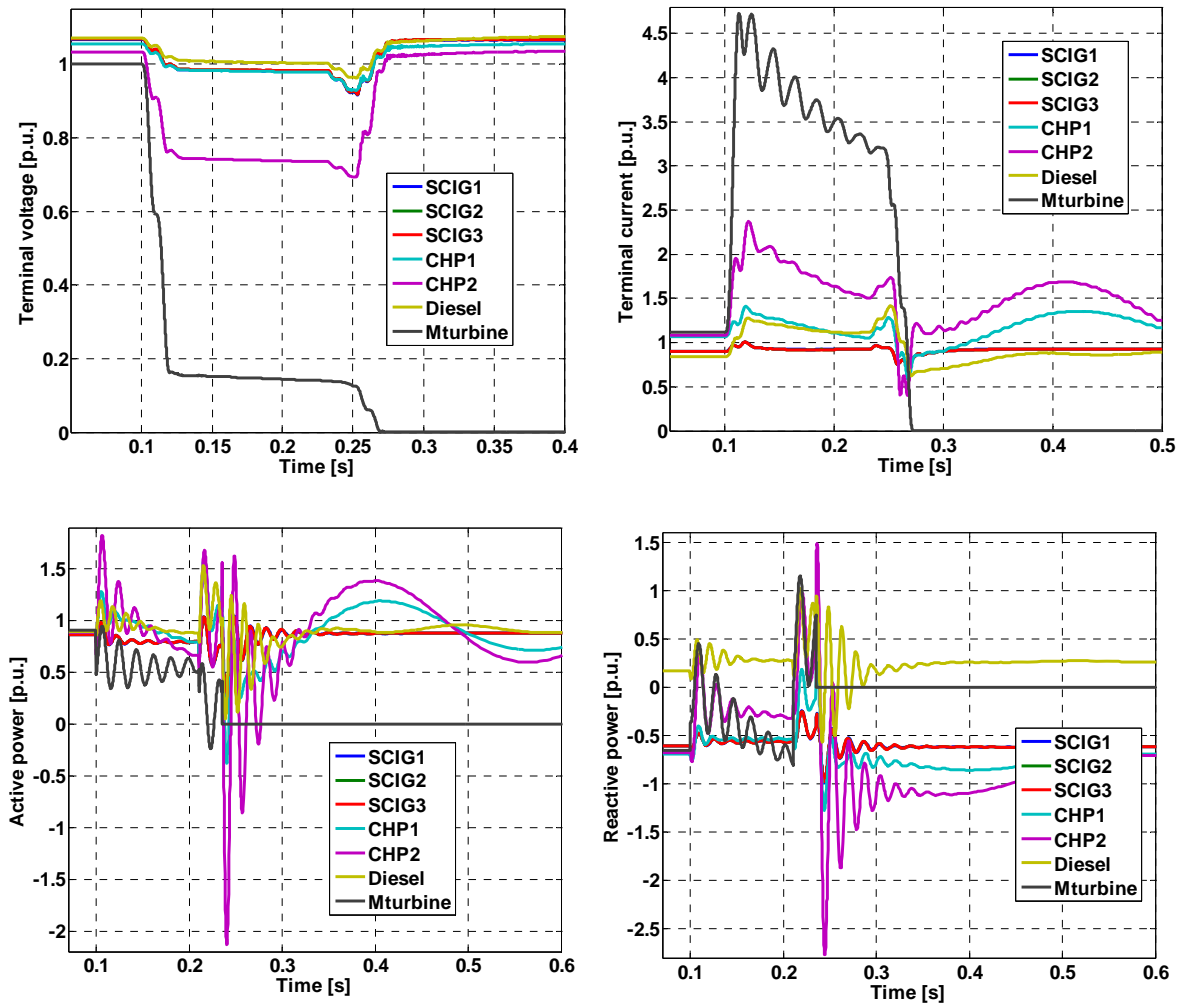


Figure 6.16. Terminal voltage, terminal current, active power and reactive power (all in [p.u.]) of DG-units following a two-phase fault at fault location #12 for scenario case I

6.3.4 Fault detection and isolation in zone 7

In a similar way, Figure 6.17 illustrates the terminal voltage, current, active/reactive power of the DG-units following a two-phase fault at location #5 corresponding to PL1.

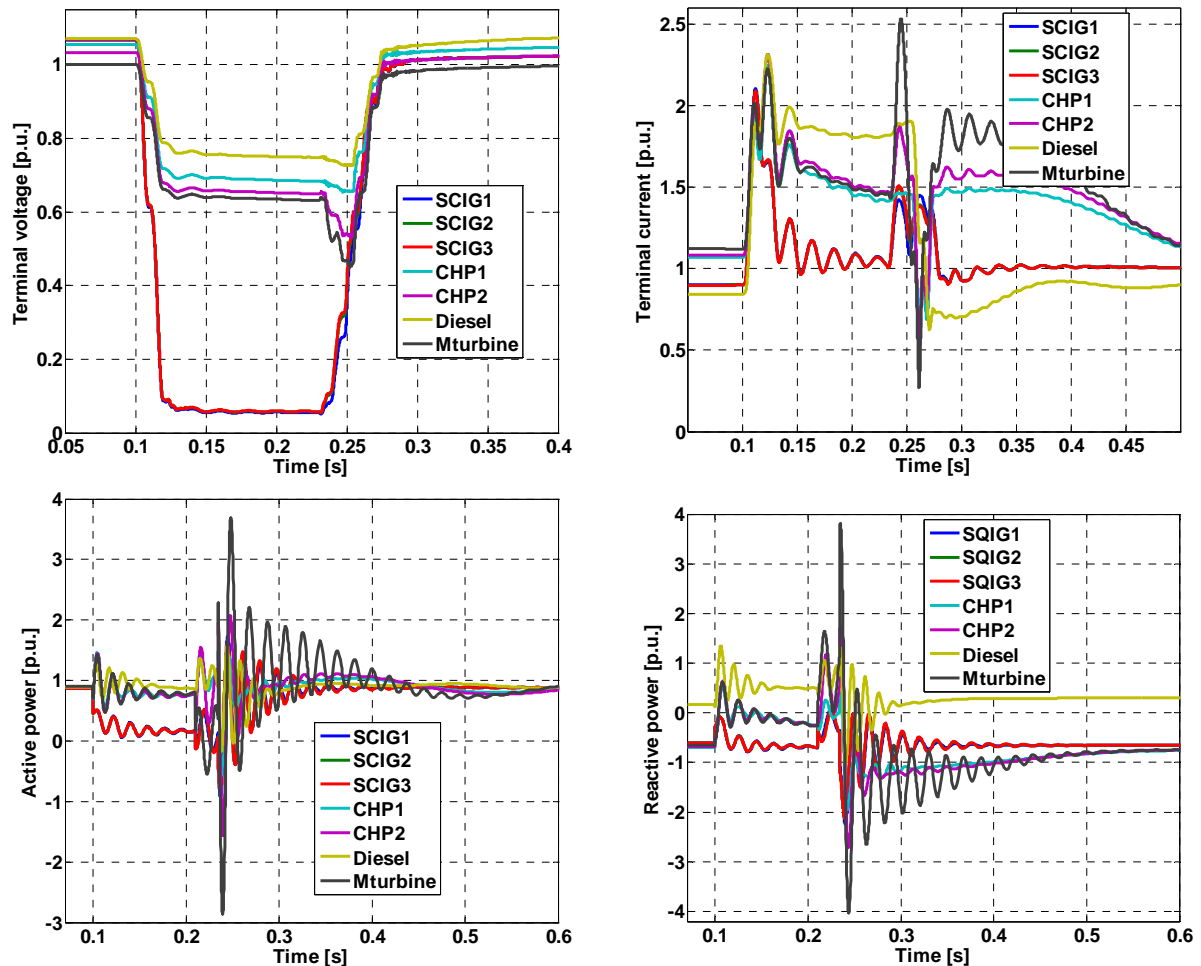


Figure 6.17. Terminal voltage and terminal current (all in [p.u.]) of DG-units following a two-phase fault at fault location #5 for scenario case I

6.4 Non-reconfiguration network scenario cases

6.4.1 Fault detection and isolation in zone 15

For the scenario case of disturbances located in zone 15, no event of network reconfiguration occurs. The fault is in this case cleared through the tripping process of CB20. It is interesting to observe the proper operation of the sophisticated protection functionality (upstream blocking directional overcurrent principle) for this specific case study. Figure 6.18 displays the trip signals of functions F12 through F15. Figure 6.19

depicts the short-circuit currents monitored by the overcurrent part of the modeled PDOC blocks 12, 13, 14 and 15 for the scenario cases corresponding to both DG penetration levels. It is observed that F15 generates a trip signal at 0.157 sec and consequently blocks the (upstream blocking directional overcurrent based) functions F12, F13 and F14, thus assuring a selective fault clearance. Current measurements recorded by PDOC12, PDOC13 and PDOC14 all regain their pre-fault current nominal value, while PDOC15 becomes zero at approximately one cycle after the zone isolation by CB20.

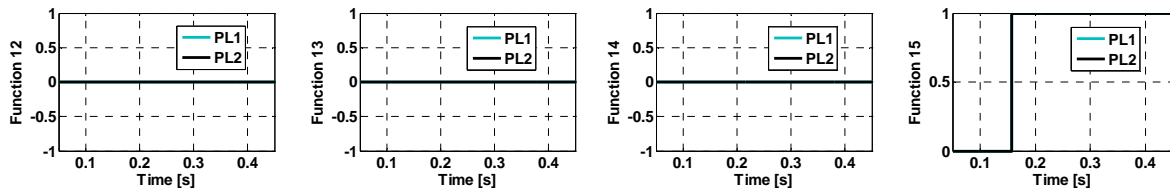


Figure 6.18. Trip signals of functions F12, F13, F14 and F15 following a two-phase fault at fault location #14 for scenario cases I and II

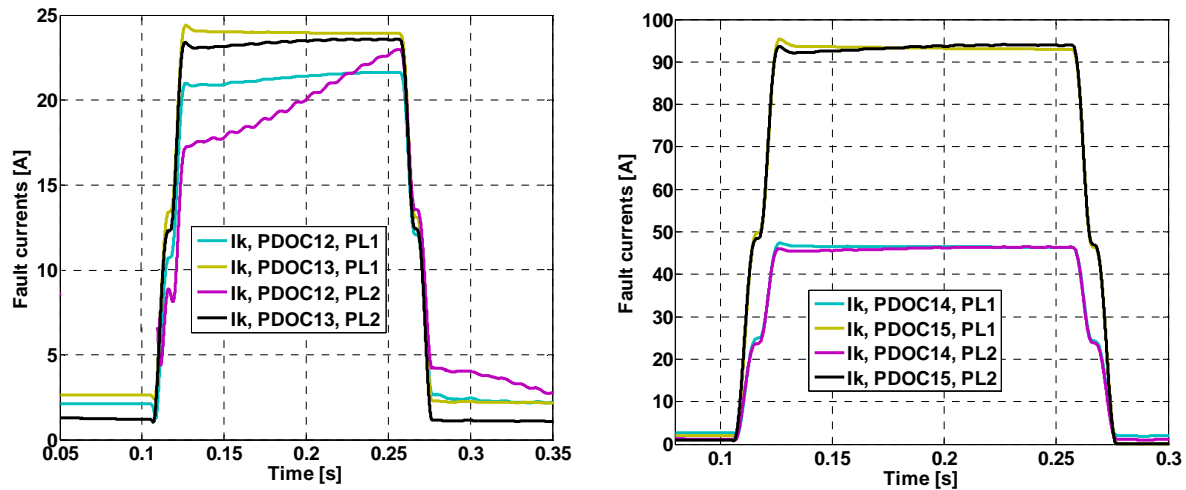


Figure 6.19. I_k'' of PDOC12, PDOC13, PDOC14, and PDOC15 following a two-phase fault at location #14, for scenario cases I and II

6.5 Acceptance and cost efficiency of the new technology

Generally, a period of reservations precedes the acceptance of a new technology. Protection specialists will be faced with a decades-old dilemma of providing reliable protection through communication channels. Seemingly, the acceptance of fully centralized or distributed protection functions based on high-speed peer-to-peer communications will only become attainable when protection specialists are convinced that the adoption of the

new technology will enhance overall system dependability and performance. This can be accomplished by careful design of the communication-aided protection system. Presently, it seems that protection specialists lack confidence in the communication network reliability.

The installation of communication channels in existing distribution grids entails large investments. These expenses can be hardly justified only for protection issues, in comparison with the benefits of ameliorating DG-units availability. However, the need for more accurate grid operation, smart metering and introduction of microgrids and virtual power plants also asks for communication links. The installation of communication channels will become attractive when they are shared by the various services in the active distribution grid. Various services which can share the communication channels are dispatch center control signals, metering data transfer, control of virtual power plants in the future, etc. In this way, new developments will be done, which are hardly feasible when each individual development is justified by its own.

Additionally, the large investment in the substitution of the existing coordination logics infrastructure seems ineluctable, since the problem of loss of protection coordination becomes more and more urgent and modifications in the existing protection philosophy are imperatively required.

6.6 Summary

This chapter proposes an innovative feeder/substation-oriented fully centralized protection scheme, which is capable of solving the current protection problems faced by Dutch DG-supplied distribution networks. The real-time implementation of the proposed protection strategy reflects an intelligent protection scheme, which makes use of smart hardware sensors, redundant communication infrastructure, standard communication protocols, and flexible multi-functional software algorithms. A thorough analysis of the delay components, which contribute to the total fault clearing time is provided. The hardware architecture and communication infrastructure organization of the new scheme is demonstrated. The performance of the algorithm is validated by the aid of Lelystad distribution network. The simulation results show that the protection scheme achieves a very fast fault clearing time, which assures the elimination of false tripping problems of the network protective functions and of the nuisance tripping of the DG-units. The observed significantly increased DG availability (during and after the disturbance) ensures the maintenance of the transient stability of the remaining connected to the grid DG-units. Furthermore, the application of multi-functionality in the software of the CCUs reflects an unprecedentedly flexible environment, which further enhances the development of smart grid functions in the future.

6.7 Conclusions

From the simulation results of the feeder/substation-oriented fully centralized protection concept, meaningful conclusions can be summarized:

- increases and assures the protection scheme selectivity by converting the grid structure from radial to loop operation just before the fault isolation. After the isolation of the faulty zone, the grid structure restores to a radial operation and the healthy zones maintain their operation,
- eliminates the problem of nuisance tripping of the DG-units by ensuring the availability of all the DG-units (during and after fault), which are connected to the sound zones of the grid,
- ensures a fast protection speed performance by minimizing the fault clearing time, which satisfies the needs of grid transient stability,
- prevents DG transient instabilities,
- eliminates the problem of false tripping by means of incorporating directional elements in the protection functionality,
- enables an enhanced flexibility of the protection logic, by means of supporting multi-functional software-based protection principles; thus it boosts the decision intelligence in the CPUs. It additionally enables the adaptivity of the protection settings via the software. This unprecedented flexibility raises up the development of various smart grid functions,
- eliminates the conventional relay time coordination via utilization of redundant and reliable communication links,
- enables more or less a uniform fault clearing time (in the order of maximum 200 ms) for all the geographically dispersed circuit breaker locations,
- gives the opportunity of immediate implementation of the protection scheme in Dutch MV networks due to the already feasible hardware and software required by the new system architecture.

Chapter 7

General conclusions and future possible work

7.1 General conclusions and thesis contribution

The main goal of this research was to investigate the effect of the distributed generation on distribution grid protection and to design a new protection philosophy, which overcomes the current protection mal-operations. The new algorithm provides high speed protection performance, increased protection selectivity and enhanced DG availability during disturbances. This has been realized for a typical Dutch distribution network supplied with DG units with a high penetration level. This section provides a detailed overview of the key contributions and conclusions, as well as ideas for future possible work.

- Exploration and presentation of arguments, which justify the need for migration towards intelligent protection strategies.

It has been demonstrated that conventional protection concepts lead to high fault clearing times, unselective relay operations and massive DG disconnections which are unacceptable in deregulated energy markets. A low degree of protection selectivity due to massive DG disconnection for disturbances located everywhere in the network is observed. It is additionally indicated that the maximum permissible fault clearing times should be shortened in order to accommodate increased DG availability and to guarantee post-fault grid stability. Furthermore, it is highlighted that in the future, new protection coordination principles should be developed which allow concurrent processing of information from multiple locations. Thus, new protection coordination strategies are needed, that will overcome protection selectivity problems, avoid unacceptable high fault clearing times and maximize the number of DG-units that remain connected to the distribution grid. The new software algorithms should be capable of increasing the protection speed performance and the DG during-fault availability, while simultaneously assuring the protective device selectivity. Directional

protection and concurrent processing of multi-origin information will be necessary to guarantee the protection selectivity.

- The derivation of enhanced FRT requirements for each specific DG-unit.
It is concluded that the generator tolerance depends on the type of the DG-unit, implying that different FRT requirements can be derived for different types of DG. These FRT capabilities should be within the limits of the CCT and the transient stability criteria of the DG-unit. Moreover, the fault clearing time of the future protection schemes should be reduced in order to accommodate an increased DG-availability during and after disturbances.
- Description and demonstration of how recent technological advances revolutionize conventional protection strategies and permit the real implementation of fully integrated or distributed communication-aided protection schemes.
These technological advances permit the migration from today's strictly local-information-based relay protection to innovative smart communication-assisted centralized or distributed protection schemes. Such intelligent protection strategies exhibit a high degree of flexibility, a high level of protection selectivity and a fast performance. It has been demonstrated that this innovation is achieved by means of:
 - The universal adoption of IEDs.
 - The unprecedented advances in sensor and communication technologies as well as infrastructure.
 - The emergence of new standard communication protocols (IEC61850 is the international communication standard targeting interoperability and enhancing the goals of substation automation). The unique characteristics and key features' architecture of IEC 61850, the performance requirements of the supported distributed or integrated functions, the architecture of the developed protection schemes, the included real-time peer-to-peer communication messaging protocols and the required time synchronization issues are described in detail.
- Design and development of a smart protection philosophy which guarantees protection selectivity and enhances the DG during-fault availability.
An intelligent algorithm is developed and two different architectures, which can accommodate such a protection philosophy, are proposed. The protection philosophy can be applied on any arbitrary distribution network. The results of the used protection algorithm verify that the protection scheme is particularly beneficial when DG with high penetration level is connected to the network. The protection scheme is so fast that only the DG-units which are included in the faulty zone are disconnected, whilst the rest of the DG-units (connected to the healthy parts of the network) remain in operation. The DG-units are disconnected by the remote communication-based trip commands of the corresponding activated functions. It is shown that for all scenario cases the faulty

zone is isolated in less than 150 ms thus permitting a high percentage of the DG-units to remain connected to the network. The new protection algorithm eliminates the problem of false tripping by means of incorporating directional elements in the protection strategy. The proposed protection philosophy increases and assures the protection selectivity by applying intelligent blocking functionality. The minimization of the fault clearing time eliminates the problem of nuisance tripping of the DG-units by ensuring the availability of the DG-units (during and after the fault) which are connected to the sound parts of the grid. The influence of the intelligent algorithm on the grid transient stability is additionally examined. It is also shown that the minimization of the fault clearing time prevents grid and DG transient instabilities. It is demonstrated that the algorithm enables a uniform fault clearing time (in the order of 150 ms) for all the geographically dispersed circuit breaker locations. Furthermore, the protection strategy is designed in a way that it prevents the loss of a complete feeder. Each feeder is divided in zones and the healthy zones of each feeder remain in operation due to the change of the status of the tie switch between neighboring feeders from radial to closed-loop operation just before the isolation of the faulty segment. The grid arrangement restores to its pre-fault radial operation after the successful isolation of the faulty zone. Therefore, the DG availability is significantly enhanced due to the grid conversion from radial to closed-loop operation. In this scheme, the conventional relay time coordination is substituted by making use of communication links. Moreover, the actual implementation of the protection scheme in Dutch MV grids is feasible due to the fact that the required hardware and software equipment is available. Furthermore, the new protection strategy enables enhanced flexibility of the protection logic. The support of multi-functional protection principles in the software boosts the decision intelligence in the CPUs. Therefore, the acquired flexibility increases the development of various smart grid functions.

7.2 Recommendations for future work

Investigation of autonomously operated distribution grids. In autonomously operated distribution grids, voltage and frequency controllers are needed to maintain the voltage and frequency level. Besides, the fault current level is significantly lower compared to that of the grid-connected case, and this affects the fault current during disturbance. Therefore, to guarantee successful protection of autonomously operated distribution grids more research on the short-circuit behavior and the ability of the protection system to detect fault currents is required. Additionally, the reduced system inertia makes larger impact on the stability of the distribution grid and associated DG units. To keep the distribution grid stable and maintain the power balance, FRT criteria for DG for autonomous distribution grids should be developed.

Testing of communication-based protection schemes with the aid of real time digital simulator (RTDS). RTDS simulator, which is a facility used by TU Delft allows closed-loop testing of IEC 61850 compliant protection devices and protection schemes. Therefore, RTDS can be used for testing the reliability of both traditional and non-traditional communication-aided protection schemes whose real time implementation involves the exchange of GOOSE and SV messages among IEDs.

Appendix A

Parameters of the Lelystad distribution network

The scheme of Lelystad distribution network is illustrated in Figure A.1. Parameters of the network are given in the tables below.

Table A.1. Parameters of different types of cables

Cable type	R_1 , [m Ω /m]	R_0 , [m Ω /m]	L_1 , [μ H/m]	L_0 , [μ H/m]	C_1 , [nF/m]	C_0 , [nF/m]
AL630XLPE(d)	0.047	0.134	0.286	0.430	0.640	0.640
AL240GPLK8	0.125	0.835	0.248	0.471	0.500	0.300
AL185GPLK8	0.164	1.080	0.242	0.484	0.450	0.270
AL150GPLK8	0.206	1.325	0.248	0.497	0.420	0.252
AL095GPLK8	0.320	2.095	0.271	0.541	0.340	0.204
CU095GPLK8	0.193	1.160	0.271	0.407	0.340	0.204
AL050GPLK8	0.641	3.980	0.290	0.579	0.280	0.168

R_1 and R_0 – positive- and zero-sequence resistances,
 L_1 and L_0 – positive- and zero-sequence inductances,
 C_1 and C_0 – positive- and zero-sequence capacitances.

Parameters of the external grid:

- Rated voltage: 150 kV
- Short-circuit power at rated voltage: 5321 MVA
- X/R ratio: 10.

Table A.2. Cable types and lengths

Cable between buses	Cable type	Cable length [m]
Substation – G01 a	AL630XLPE(d)	7 370
Substation – G01 b	AL630XLPE(d)	7 370
Substation – G01 c	AL630XLPE(d)	7 370
G02 – G03	AL240GPLK8	1 000
G03 – G04	AL240GPLK8	810
G04 – G05	AL240GPLK8	245
G05 – G06	AL240GPLK8	231
G06 – G07	AL240GPLK8	68
G07 – G08	AL240GPLK8	390
G08 – G09	AL240GPLK8	187
G05 – G10	AL240GPLK8	203
G10 – G11	AL240GPLK8	200
G11 – G12	AL240GPLK8	146
G12 – E32	AL240GPLK8	150
B01 – B02	AL240GPLK8	640
B02 – B12	AL185GPLK8	30
B02 – B03	AL150GPLK8	440
B03 – B04 a	AL240GPLK8	60
B03 – B04 b	AL150GPLK8	1 360
B04 – B13	AL095GPLK8	720
B04 – B05 a	AL240GPLK8	80
B04 – B05 b	CU095GPLK8	2 240
B05 – B14	AL185GPLK8	30
B05 – B06 a	CU095GPLK8	213
B05 – B06 b	AL240GPLK8	410
B06 – B07	AL240GPLK8	790
B07 – B08	AL240GPLK8	510
B08 – B09	AL240GPLK8	350
B09 – B10	AL240GPLK8	1 010
B10 – B11	AL240GPLK8	270
B11 – E16	AL240GPLK8	115
B06 – B15 a	AL240GPLK8	375
B06 – B15 b	CU095GPLK8	750
B06 – B15 c	AL240GPLK8	100
B15 – B16 a	CU095GPLK8	2 500
B15 – B16 b	AL240GPLK8	100

Table A.2. Cable types and lengths (continued)

Cable between buses	Cable type	Cable [m]
R01 – R02	AL240GPLK8	250
R02 – R03	AL240GPLK8	250
R03 – R04	AL240GPLK8	290
R04 – R05	AL240GPLK8	175
R05 – R06	AL240GPLK8	290
R06 – R07	AL240GPLK8	525
R07 – R08	AL240GPLK8	355
R08 – R09	AL240GPLK8	355
R02 – R09	AL240GPLK8	355
R06 – C02	AL150GPLK8	1 000
C01 – C02	AL240GPLK8	2 115
C02 – C03	AL240GPLK8	410
C03 – C04 a	AL240GPLK8	465
C03 – C04 b	AL150GPLK8	445
C03 – C04 c	AL240GPLK8	40
C04 – C05	AL240GPLK8	70
C05 – C06	AL150GPLK8	300
C06 – C07	AL150GPLK8	300
C07 – C08	AL150GPLK8	730
D01 – D02	AL240GPLK8	1 860
D02 – D03	AL240GPLK8	1 000
D03 – D04	AL240GPLK8	1 000
D03 – D05	AL095GPLK8	1 000
D04 – D06	AL240GPLK8	1 000
D02 – E02	AL240GPLK8	10
D04 – E05	AL240GPLK8	710
E01 – E02	AL240GPLK8	1 860
E02 – E03	AL240GPLK8	1 600
E03 – E04	AL240GPLK8	1 600
E04 – E05	AL240GPLK8	500
E03 – E17	AL240GPLK8	1 000
E17 – E18	AL240GPLK8	1 000
E18 – E19	AL240GPLK8	1 000
E19 – E20	AL240GPLK8	1 000
E17 – E20	AL240GPLK8	1 000
E04 – E06	AL240GPLK8	535

Table A.2. Cable types and lengths (continued)

Cable between buses	Cable type	Cable length [m]
E06 – E07	AL240GPLK8	150
E07 – E08	AL240GPLK8	180
E08 – E09	AL240GPLK8	400
E09 – E10	AL240GPLK8	647
E10 – E15	AL240GPLK8	260
E15 – E16	AL240GPLK8	290
E10 – E11	AL240GPLK8	635
E11 – E12	AL240GPLK8	800
E12 – E13	AL240GPLK8	210
E13 – E14	AL240GPLK8	300
E10 – E14	AL240GPLK8	529
E14 – E21	AL095GPLK8	293
E21 – E22	AL095GPLK8	479
E22 – E23	AL095GPLK8	112
E23 – E24	AL095GPLK8	420
E24 – E25	AL095GPLK8	253
E25 – E26	AL095GPLK8	370
E24 – E27	AL150GPLK8	897
E27 – E28	AL050GPLK8	210
E28 – E29	AL050GPLK8	333
E29 – E30	AL050GPLK8	318
E30 – E31	AL050GPLK8	298
E31 – E32	AL050GPLK8	191

Table A.3. Load parameters

Bus	P [MW]	Q [MVA _r]	Bus	P [MW]	Q [MVA _r]
G02	18.0000	8.7180	B02	0.2550	0.1580
G03	0.1157	0.0560	B03	0.0675	0.0327
G04	0.2165	0.1049	B04	0.0675	0.0327
G05	0.3090	0.1497	B05	0.2400	0.1800
G06	0.2561	0.1240	B06	0.1080	0.0523
G07	0.1826	0.1132	B07	0.0675	0.0327
G08	0.3619	0.1753	B09	0.1689	0.0813
G09	0.2622	0.1625	B11	0.1080	0.0523
G10	0.1322	0.0640	B12	0.2700	0.1308
G11	0.6492	0.4023	B13	0.1688	0.0817
G12	0.3090	0.1497	B14	0.2126	0.103
E03	0.0156	0.0075	B15	0.1080	0.0523
E04	0.0449	0.0217	B16	0.0100	0.0010
E05	0.0779	0.0377	R02	0.3600	0.1744
E06	0.1559	0.0755	R03	0.3600	0.1744
E07	0.1140	0.0552	R04	0.3600	0.1744
E08	0.0720	0.0540	R05	0.3600	0.1744
E09	0.1272	0.0616	R06	0.3600	0.1744
E10	0.1871	0.0906	R07	0.3600	0.1744
E11	0.2843	0.1377	R08	0.3600	0.1744
E12	0.0980	0.0735	R09	0.3600	0.1744
E13	0.0100	0.0010	C02	0.0925	0.0448
E14	0.2593	0.1256	C03	0.0611	0.0296
E15	0.1160	0.0870	C04	0.1350	0.0654
E16	0.0480	0.0360	C05	0.0900	0.0436
E17	0.0156	0.0075	C06	0.1373	0.0851
E20	0.0100	0.0010	C07	0.0900	0.0436
E21	0.1422	0.0689	C08	0.0083	0.0040
E22	0.3510	0.2175	D05	0.0100	0.0010
E23	0.1422	0.0689	D06	0.0100	0.0010
E24	0.1347	0.0652	E29	0.1160	0.0562
E25	0.1197	0.0580	E30	0.1122	0.0543
E26	0.1347	0.0652	E31	0.1085	0.0525
E27	0.1571	0.0761	E32	0.1610	0.0998
E28	0.1422	0.0689			

Reactor parameters (Reactor02 = Reactor18 = Reactor03 = Reactor04 = Reactor05):

- Rated voltage: 10 kV
- Resistance and inductance: 0.01 Ω and 0.956 mH.

Transformer parameters:

Tr1 = Tr2:

- Rated power: 47 MVA
- Primary winding: Rated voltage: 150 kV, Resistance: 0.002383 p.u., Inductance: 0.101472 p.u., Winding connection: Yg
- Secondary winding: Rated voltage: 11 kV, Resistance: 0.002383 p.u., Inductance: 0.101472 p.u., Winding connection: Δ
- Magnetizing branch: Resistance: 1700 p.u., Inductance: 2000 p.u.

Resistances and inductances for a winding are given in p.u. based on the transformer rated power and the rated voltage of the winding. Magnetizing branch is referred to the primary winding.

Tr3:

- Rated power: 20 MVA
- Primary winding: Rated voltage: 10 kV, Resistance: 0.00013 p.u., Inductance: 0.03 p.u., Winding connection: Yn
- Secondary winding: Rated voltage: 10 kV, Resistance: 0.00013 p.u. Inductance: 0.03 p.u., Winding connection: Yn
- Magnetizing branch: Resistance: 17000 p.u., Inductance: 20000 p.u.

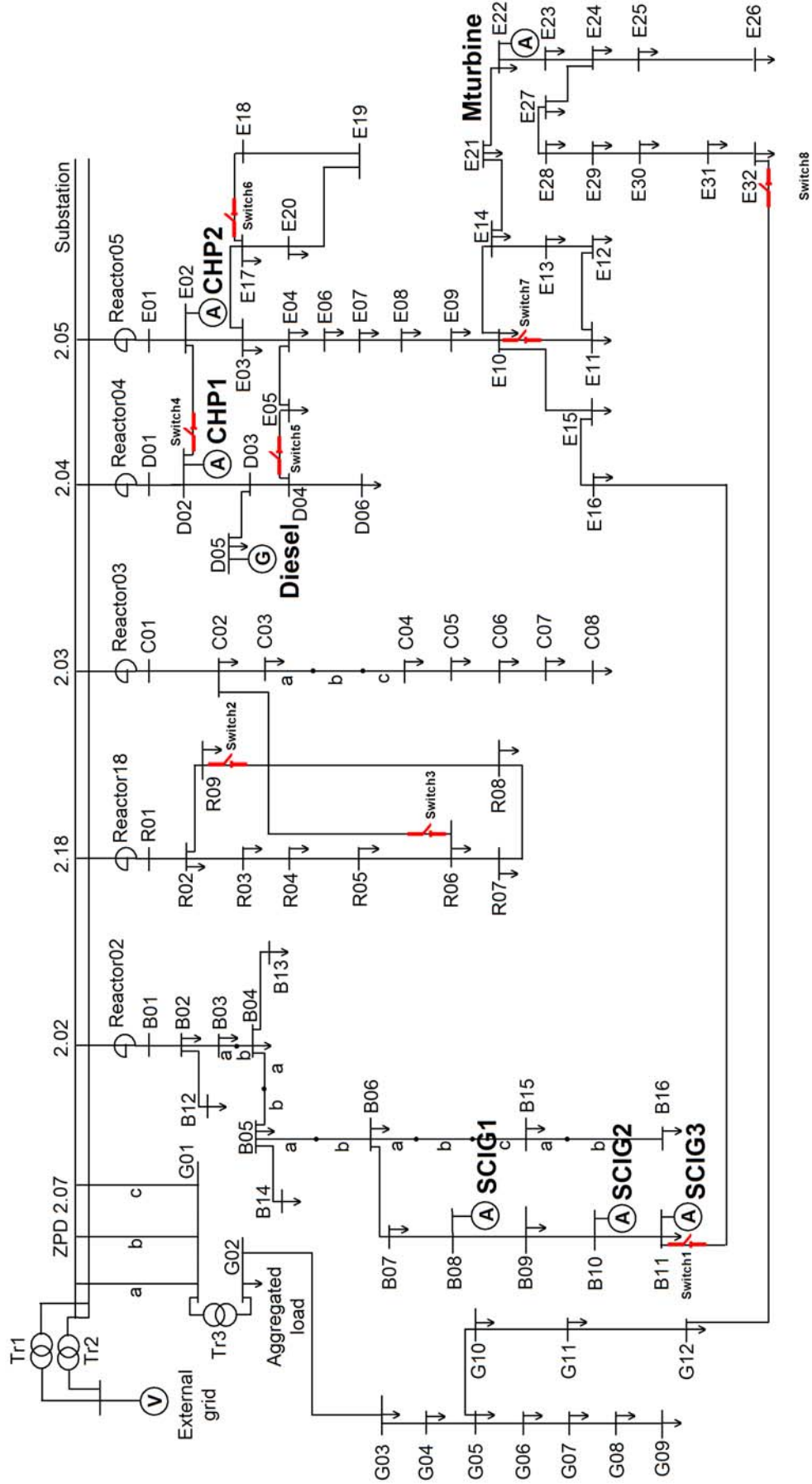


Figure A.1. Lelystad distribution network

Appendix B

Dynamic modeling of power systems with distributed generation

B. 1 Introduction

The dynamic models of DG presented in this Appendix are utilized in the chapters for power system protection and stability analysis. The DG models that have been used for simulation are experimentally validated by different authors. Representative models of a squirrel-cage induction generator wind turbine, a split-shaft microturbine and a Diesel synchronous machine plant are explained in detail.

B. 2 Dynamic modeling of power systems

In this dissertation, the modeling and the simulations have been performed in Matlab/Simulink environment. Simulink is a program that is integrated with Matlab. It provides a graphical user interface that is used for building block diagrams, performing simulations as well as analyzing results. There are different toolboxes that can be used in Simulink for power system analysis. Among all, SimPowerSystems (SPS) is a powerful and visual toolbox, which comprises most of the electrical elements for power systems. SPS is a modern design tool that allows scientists and engineers to rapidly and easily model, simulate and analyze power systems. SPS runs in the Simulink environment and it can include a comprehensive built-in block library of sinks, sources, linear and nonlinear components, and connectors in addition to the power system blocksets. The simulation speed of the modeled power system significantly depends on the type of mathematical tool applied to solve the algebraic and differential equations. One important feature of SPS

software is its ability to simulate electrical systems either with continuous variable-step integration algorithms or with a fixed-step using a discretized system.

Every time a simulation is started, a special initialization mechanism is called. This initialization process computes the state-space model of the electric circuit and builds the equivalent system that can be simulated by Simulink software. This process follows the following steps [85]:

- Sorts all SPS blocks, gets the block parameters and evaluates the network topology. The blocks are separated into linear and nonlinear blocks, and each electrical node is automatically given a node number.
- Network topology is obtained and the state-space model of the linear part of the network is computed. All steady-state calculations and initializations are performed at this stage. When the circuit is chosen to be discretized, the discrete state-space model is computed from the continuous state-space model. In the case of phasor solution method, the state-space model is replaced by the complex transfer matrix $H(j\omega)$ relating inputs and outputs (voltage and current phasors) at the specified frequency. This matrix defines the network algebraic equations.
- Builds the Simulink model of the circuit and stores it inside the Powergui block located at the top level of the model.

Figure B.1 represents the interconnections between the different parts of the complete Simulink model. The non-linear models are connected in feedback between voltage outputs and currents inputs of the linear model. The non-linear elements are simulated by predefined Simulink models. These models can be found in the SPS powerlib_models library [85].

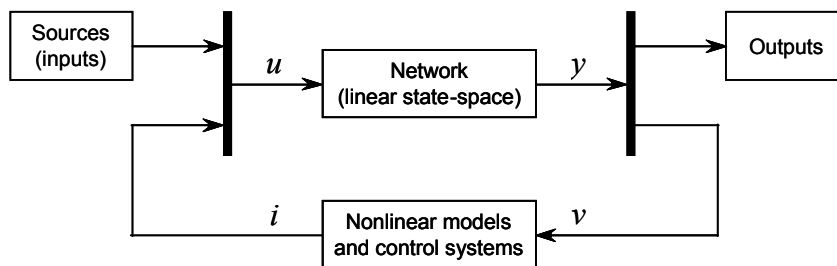


Figure B.1. Overall dynamic system model [85]

B. 3 Dynamic models of the DG-units

B.3.1 Dynamic model of a squirrel cage induction generator wind turbine

The squirrel cage induction generator (SCIG) wind turbine is a fixed-speed wind turbine. The generator used is asynchronous and has a short-circuited rotor. The stator is directly connected to the grid. The machine operates at a rotating speed higher than the synchronous. The equations which characterize each subsystem of the wind turbine model are described in this section. The SCIG wind turbine model consists of an induction generator subsystem, an electrical and a mechanical part, the pitch control and the wind turbine subsystems [86], [87], [88].

The electrical part of the generator is described by a fourth order state space model while the mechanical part by a second order system. All variables are referred to the stator and all stator and rotor quantities are given in the dq reference frame. The stator and rotor voltage equations in dq reference frame are:

$$\begin{aligned}
 V_{qs} &= R_s i_{qs} + \frac{d}{dt} \varphi_{qs} + \omega \varphi_{ds} \\
 V_{ds} &= R_s i_{ds} + \frac{d}{dt} \varphi_{ds} - \omega \varphi_{qs} \\
 V'_{qr} &= R'_r i'_{qr} + \frac{d}{dt} \varphi'_{qr} + (\omega - \omega_r) \varphi'_{dr} \\
 V'_{dr} &= R'_r i'_{dr} + \frac{d}{dt} \varphi'_{dr} - (\omega - \omega_r) \varphi'_{qr}
 \end{aligned} \tag{B.1}$$

The relevant fluxes are:

$$\begin{aligned}
 \varphi_{ds} &= L_s i_{qs} + L_m i'_{qr} \\
 \varphi_{qs} &= L_s i_{ds} + L_m i'_{dr} \\
 \varphi'_{qr} &= L'_r i'_{qr} + L_m i_{qs} \\
 \varphi'_{dr} &= L'_r i'_{dr} + L_m i_{ds} \\
 L_s &= L_{ls} + L_m \\
 L'_r &= L'_{lr} + L_m
 \end{aligned} \tag{B.2}$$

where:

R_s and L_{ls} are the stator resistance and leakage inductance,
 R'_r and L'_{lr} are the rotor resistance and leakage inductance,
 L_m is the magnetizing inductance,
 L_s and L'_r are the total stator and rotor inductances,
 V_{qs} and i_{qs} are the q axis stator voltage and current,
 V'_{qr} and i'_{qr} are the q axis rotor voltage and current,
 V_{ds} and i_{ds} are the d axis stator voltage and current,

V'_{dr} and i'_{dr} are the d axis rotor voltage and current,
 φ_{qs} and φ_{ds} are the stator q and d axis fluxes,
 φ'_{qr} and φ'_{dr} are the rotor q and d axis fluxes,
 ω_r is the electrical angular velocity ($\omega_m p$) where p is the number of pole pairs

The differential equation representing the mechanical part of the SCIG wind turbine is:

$$\begin{aligned}\frac{d}{dt}\omega_m &= \frac{1}{2H}(T_e - F\omega_m - T_m) \\ \frac{d}{dt}\theta_m &= \omega_m\end{aligned}\quad (B.3)$$

where:

ω_m is the angular velocity of the rotor,
 θ_m is the rotor angular position, p is the number of pole pairs,
 ω_r is the electrical angular velocity,
 T_e is the electromagnetic torque,
 T_m is the shaft mechanical torque,
 F is the rotor viscous friction coefficient,
 H is the inertia coefficient.

The wind turbine block represents the relationship between the generator speed, pitch angle, wind speed and the mechanical power of the turbine.

The mechanical energy extracted from the wind is:

$$P_m = C_p(\lambda, \beta) \frac{\rho A}{2} v_{wind}^3 \quad (B.4)$$

where P_m is the mechanical output power of the turbine (W), C_p is the power coefficient as a function of λ and β , ρ is the air density (kg/m^3), A is the turbine swept area, λ is the tip speed ratio of the rotor blade tip speed to wind speed, β is the blade pitch angle (deg). Dynamic stall, the wind shear and the tower shadow effects are neglected. The general equation describing the power coefficient is:

$$c_p(\lambda, \beta) = c_1 \left(\frac{c_2}{\lambda_i} - c_3 \beta - c_4 \right) e^{\frac{-c_5}{\lambda_i}} + c_6 \lambda \quad (B.5)$$

where:

$$\lambda_i = \frac{1}{\frac{1}{\lambda + 0.08\beta} - \frac{0.035}{\beta^3 + 1}} \quad (B.6)$$

The turbine power characteristics of a 1.5 MW SCIG are depicted in Figure B.2.

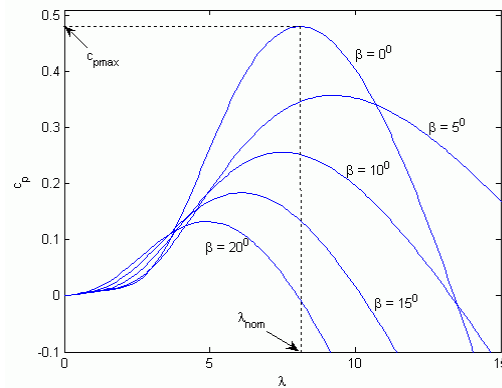


Figure B.2. Turbine power characteristics of a 1.5 MW SCIG

B.3.2 Dynamic model of a split-shaft microturbine

A microturbine is a typical example of a controllable DG. Turbines of this type are small in size and contain mostly simple-cycle gas turbines, generating electric power in the range of 25 kW to 500 kW. There are essentially two types of microturbines. One is a high-speed single shaft unit with a compressor and a turbine mounted on the same shaft as the electrical generator. The turbine speed ranges from 50 000 to 120 000 rpm. The other type of microturbines is a split-shaft design that has its generator connected via a gearbox [47]. The schematic diagram of a split-shaft microturbine is illustrated in Figure B.3. The split-shaft turbine mainly involves an air compression section, a recuperator, a burner or combustor, and a power turbine driving the load. The exhaust gas from the combustion chamber forces the high-pressure compressor turbine that drives the compressor. The power turbine drives the generator. A special heat exchanger unit and a recuperator, which captures the exhausted thermal energy from the power turbine, preheat the compressed air. This improves the overall efficiency. The waste heat recovery or heat exchanger captures the exhaust energy, which significantly improves power generation efficiency. The microturbine dynamic model makes use of an induction generator model which is already described in Section B.3.1.

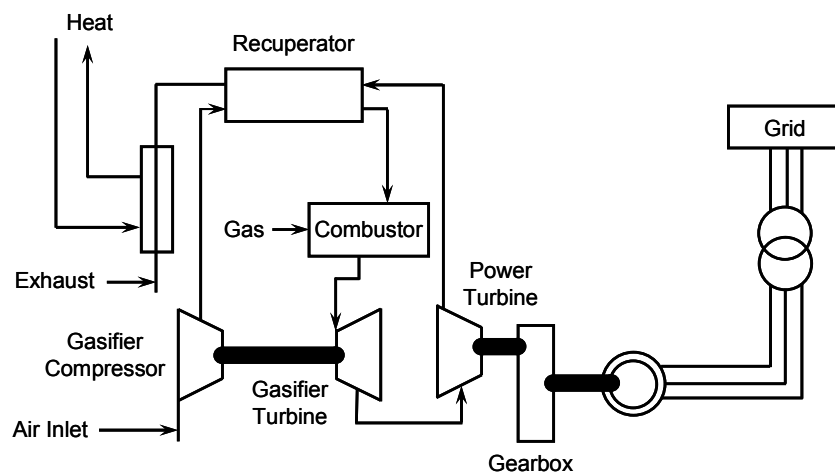


Figure B.3. Schematic diagram of a split-shaft microturbine [47]

In this dissertation, the slow dynamic performance of the microturbine is of main interest. Based on this fact, the simplified microturbine model is founded on the following assumptions:

- System operation is under normal operating conditions, whilst start-up and fast dynamics are not included.
- The microturbine's electromechanical behavior is the main interest. The recuperator is not included in the model as it is only a heat exchanger to raise the engine efficiency. Moreover, due to the recuperator's very slow response time, it has little influence on the time-scale of the dynamic simulations.
- The gas turbine's temperature control and accelerator control are of no significance under normal system conditions. They can be omitted in the turbine model.
- Most turbines do not have governors and therefore a governor model is not considered.

The main blocks in the microturbine model are shown in Figure B.4.

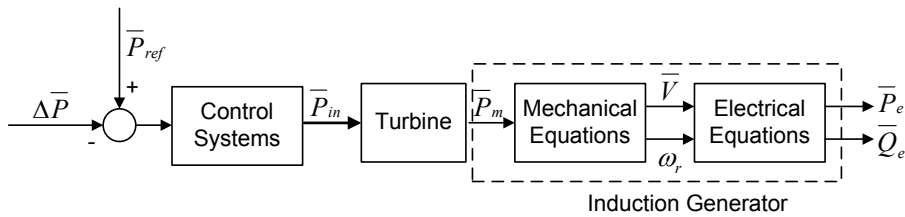


Figure B.4. Main blocks in microturbine model [47]

The control system block comprises of a real power proportional-integral (PI) control function as depicted in Figure B.5. The controlled real power P_{in} is applied to the turbine. The split-shaft turbine is modeled as a simple-cycle, single-shaft gas turbine.

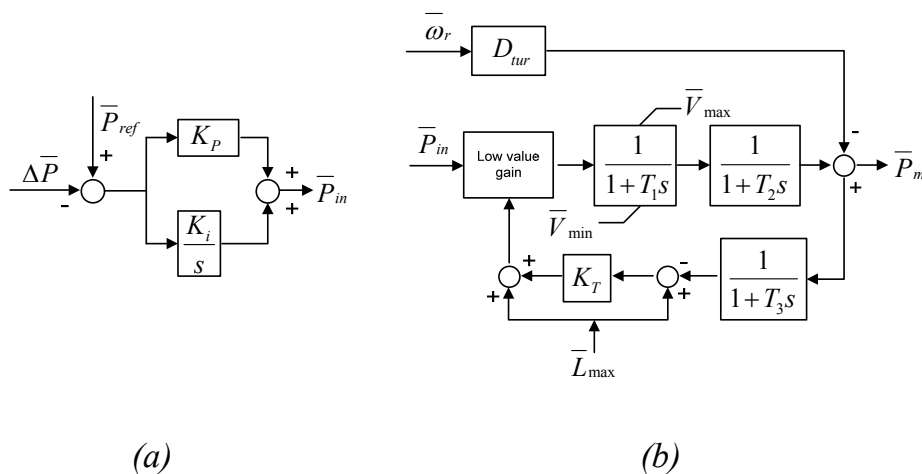


Figure B.5. a) Control system model, b) Turbine model [47]

The microturbine which is used in this dissertation has the rated power of 250kW and rated line voltage 660V. The detailed parameters of the whole model can be found in [47].

B.3.3 Dynamic model of a diesel synchronous generator

A diesel generator is the combination of a diesel engine with a synchronous electrical generator. Usually, diesel generating units are situated in places without grid connection or used for emergency power supply when the grid fails. Except emergency power supply, they support the grid during peak periods and during periods with shortage of large power production. The engine works with all the crude oil distillates, from natural gas, gasoline, wood gas to fuel oils from diesel oil to residual fuels. Their great advantage is they can start up very quickly, normally in a few minutes. The model used for the diesel synchronous generator is the synchronous machine together with a diesel's engine voltage and speed control. The diesel generator consists of the synchronous generator, the governor and diesel engine system, and the excitation subsystem. The complete block modeling diagram is shown in Figure B.6.

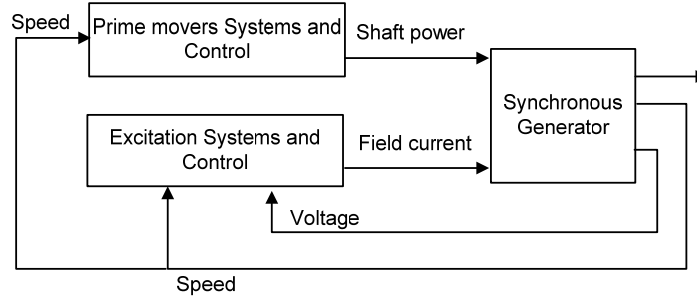


Figure B.6. Synchronous machine block modeling diagram

The electrical part of the generator is described by a sixth-order state-space model. All variables are referred to the stator and all stator and rotor quantities are given in a dq reference frame. The model takes into account the dynamics of the stator, field and damper windings. The stator and rotor voltage equations in dq reference frame are:

$$\begin{aligned}
 V_d &= R_s i_d + \frac{d}{dt} \varphi_d - \omega_R \varphi_q \\
 V_q &= R_s i_q + \frac{d}{dt} \varphi_q + \omega_R \varphi_d \\
 V'_{fd} &= R'_{fd} i'_{fd} + \frac{d}{dt} \varphi'_{fd} \\
 V'_{kd} &= R'_{kd} i'_{kd} + \frac{d}{dt} \varphi'_{kd} \\
 V'_{kq1} &= R'_{kq1} i'_{kq1} + \frac{d}{dt} \varphi'_{kq1} \\
 V'_{kq2} &= R'_{kq2} i'_{kq2} + \frac{d}{dt} \varphi'_{kq2}
 \end{aligned} \tag{B.7}$$

The relevant fluxes are:

$$\begin{aligned}
 \varphi_d &= L_d i_d + L_{md} (i'_{fd} + i'_{kd}) \\
 \varphi_q &= L_q i_q + L_{mq} i'_{kq} \\
 \varphi'_{fd} &= L'_{fd} i'_{fd} + L_{md} (i_d + i'_{kd}) \\
 \varphi'_{kd} &= L'_{kd} i'_{kd} + L_{md} (i_d + i'_{fd}) \\
 \varphi'_{kq1} &= L'_{kq1} i'_{kq1} + L_{mq} i_q \\
 \varphi'_{kq2} &= L'_{kq2} i'_{kq2} + L_{mq} i_q
 \end{aligned} \tag{B.8}$$

where:

R_s : stator resistance

L_{md} , L_{mq} : d- and q-axis magnetizing inductances

V_q , i_q : q-axis stator voltage and current

V_d , i_d : d-axis stator voltage and current

R'_{fd} , L'_{fd} : field resistance and leakage inductance,

$V'_{kq1,2}$, $i'_{kq1,2}$: q-axis damper windings voltage and current

V'_{kd} , V'_{fd} : d-axis damper and field windings voltages

φ_q , φ_d : q- and d-axis stator fluxes

φ'_{fd} , φ'_{kd} : d-axis field and damper windings fluxes

$\varphi'_{kq1,2}$: q-axis damper windings fluxes

i'_{kd} , i'_{fd} : d-axis damper and field winding currents

R'_{kd} , L'_{kd} : d-axis damper resistance and leakage inductance

R'_{kq1} , L'_{kq1} : q-axis damper 1 resistance and leakage inductance

R'_{kq2} , L'_{kq2} : q-axis damper 2 resistance and leakage inductance (only in round rotor)

The differential equation representing the mechanical part of the synchronous machine is:

$$\begin{aligned}
 \Delta\omega(t) &= \frac{1}{2H} \int_0^t (T_m - T_e) dt - K_d \Delta\omega(t) \\
 \omega(t) &= \Delta\omega(t) + \omega_0
 \end{aligned} \tag{B.9}$$

In equation (B.9), T_m is the mechanical torque, T_e is the electromagnetic torque, K_d is the damping factor representing the effect of damper windings, $\omega(t)$ is the mechanical speed of the rotor, ω_0 the speed of operation, and $\Delta\omega$ is the speed variation with respect to speed of operation.

Figure B.7 illustrates the excitation control system modeled. The excitation system controls the terminal voltage and provides the DC current to the field winding. The used parameters are taken from [46].

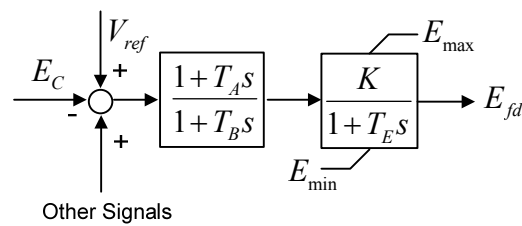


Figure B.7. Excitation system model [46]

The governor system is responsible for the speed control of the synchronous generator. The output of the system is the mechanical power at the machine's shaft. When the machine operates as a generator, the mechanical power is positive. Figure B.8 depicts the governor system model. The modeled Diesel plant has a rated power of 3.125MVA and rated voltage of 2400V.

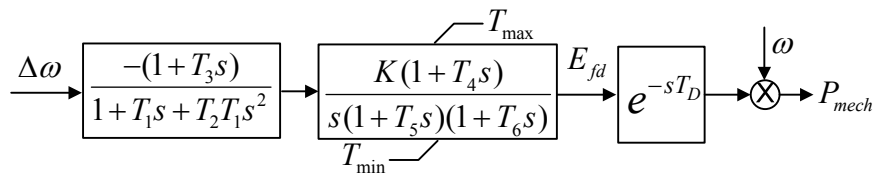


Figure B.8. Governor model [46]

References

- [1] P.H. Schavemaker and L. van der Sluis, “Electrical power systems essentials”, *Wiley & sons*, Chichester, United Kingdom, 2008.
- [2] A. Ishchenko, “Dynamics and stability of distribution networks with dispersed”, Ph.D. Thesis, *Eindhoven University of Technology*, the Netherlands, 2008.
- [3] N. Jenkins, R. Allan, P. Crossley, D. Kirschen, G. Strbac, “Embedded generation”, *The Institution of Electrical Engineers*, London, 2000
- [4] CIRED preliminary report of CIRED Working Group 04, “Dispersed generation”, *CIRED Conference*, Nice, June, 1999.
- [5] A. Schweer, “Special Report Session 3”, *Proc. of CIGRE Symposium on Impact of demand side management, integrated resource planning and distributed generation*, Neptum, Romania, 1997.
- [6] G. Papaefthymiou, “Integration of stochastic generation in power systems”, Ph.D. Thesis, *Technische Universiteit Delft*, 2007.
- [7] P. Vermeyen, “Effect of distributed generation on fault detection and ripple control” Ph.D. Thesis, *Katholieke Universiteit Leuven*, 2008.
- [8] M. Reza. “Stability analysis of transmission systems with high penetration of distributed generation”, Ph.D. thesis, *Technische Universiteit Delft*, 2006.
- [9] F. Provoost, “Intelligent distribution network design”, Ph.D. thesis, *Technische Universiteit Eindhoven*, 2009.
- [10] J. Morren, “Grid support by power electronic converters of distributed generation units”, Ph.D Thesis, *Technische Universiteit Delft*, 2006.
- [11] 1547 IEEE standard for interconnecting distributed resources with electrical power systems, *IEEE*, 2003.
- [12] G. Pepermans, J. Driesen, D. Haeseldonckx, R. Belmans and W. D’ haeseleer, “Distributed generation: definition, benefits and issues”, in *Energy Policy* 33, pages 787-798, 2005.
- [13] T. Ackermann, G. Andersson, L. Soder, “Distributed generation: a definition”, in *Electric Power Systems Research* 57, pages 195-204. Elsevier, 2001.

- [14] T. Ackermann and V. Knyazkin, "Interaction between distributed generation and the distribution network: operational aspects", in *IEEE transmission and distribution conference and exhibition, Asia Pacific*, Yokohama, Japan Oct 6-10. 2002.
- [15] E.J. Coster, "Distribution grid operation including distributed generation", Ph.D. Thesis, *Technische Universiteit Eindhoven*, 2010.
- [16] G. Celli, F. Pilo, G. Pisano, V. Allegranza, R. Cicoria, and A. Iaria, "Meshed vs. radial MV distribution network in presence of large amount of DG", in *IEEE Power Systems Conference and Exposition*, October 10-13, 2004.
- [17] US Department of energy (2008), the smart grid: an introduction, [Online]. Available: <http://www/oe.energy.gov/SmartGridIntroduction.htm>.
- [18] European Commission, "European smart grid technology platform" Luxembourg, 2006.
- [19] Joint US-China Cooperation on Clean Energy, "JUCCCE), "Smart grid-future grid?-A basic information report on smart grid", Dec. 18, 2007.
- [20] J. Berst, "Why the smart grid industry can't talk the talk", *Smart Grid News*, Mar. 5, 2009.
- [21] E. Santacana, G. Rackliffe, L. Tang, X. Feng, "Getting smart", *IEEE Power and Energy Magazine*, vol. 8, no. 2, pp. 41-48, March-April 2010.
- [22] U.S. House of Representatives, (H.R. 6) "Energy independence and security act of 2007", 2007.]
- [23] Edison Electric Institute, "Understanding smart grid. From definition to deployment", Washington, D.C., Mar. 2009.
- [24] National Institute of Standards and Technology (Sept. 2009), "NIST framework and roadmap for smart grid interoperability standards", Release 1.0 (Draft), [Online]. Available: http://www.nist.gov/public-affairs/releases/smartgrid_interoperability.pdf.
- [25] A. Vaccaro, M. Popov, D. Villaci, and V. Terzija, "An integrated framework for smart microgrids modeling, monitoring, control, communication, and verification", *Proceedings of the IEEE*, vol. 99, no. 1, pp. 119-132, January 2011.
- [26] V. Terzija, G. Valverde, D. Cai, P. Regulski, V. Madani, J. Fitch, S. Skok, M.M. Begovic, A. Phadke, "Wide-area monitoring, protection, and control of future electric power networks", *Proceedings of the IEEE*, vol. 99, no. 1, pp. 80-93, January 2011.
- [27] P.M. Anderson, "Power system protection", *IEEE Press series on power engineering*, McGraw-Hill, New York, 1999.

- [28] A.G. Phadke, J.S. Thorp, Computer relaying for power systems. *Research Studies Press, Ltd.*, 1988.
- [29] J.M. Gers, E.J. Homes, "Protection of electricity distribution networks", *IEE Power & Energy Series 47*, London, 2nd edition, 2004.
- [30] S.G.A. Perez, "Modeling relays for power system protection studies", Ph.D. Thesis, *University of Saskatchewan*, Canada, 2006.
- [31] B. Hadzi-Kostova, "Protection concepts in distribution networks with decentralized energy resources", Ph.D. Thesis, *Otto-von-Guericke-Universitat Magdeburg*, 2005.
- [32] H. Wihartady, "Modeling of short-circuit fault arcs in 150kV system and its influence on the performance of distance protection" Msc thesis, *Delft University of Technology*, the Netherlands, June, 2009.
- [33] E. Lakervi, E.J. Homes, "Electricity distribution network design", *IET Power & Energy Series 21*, London, 1995.
- [34] H.B. Funmilayo, K.L. Butter-Purry "An approach to mitigate the impact of distributed generation on the overcurrent protection scheme for radial feeders". In *IEEE Power Systems Conference and Exposition*, pages 1-11, 2009.
- [35] M.T. Doyle, "Reviewing the impact of distributed generation on distribution system protection", In *IEEE Power Engineering Society Meeting*, 2002.
- [36] N. Hadjsaid, J.-F. Canard and F. Dumas, "Dispersed generation impact on distribution networks", In *IEEE computer applications in power*, vol. 12, pp. 22-28, 1999.
- [37] K. Kauhaniemi and L. Kumpulainen, "Impact of distributed generation on the protection of distribution networks", In *Eight IEE international conference on developments in power system protection*, 2004, vol. 1, pp. 315-318, 2004.
- [38] K. Maki, S. Repo and P. Jarventausta, "Effect of wind power based distributed generation on protection of distribution", In *Eight IEE international conference on developments in power system protection*, 2004, vol. 1, pp. 327-330, 2004.
- [39] I. Xyngi, M. Popov, "Smart protection in Dutch medium voltage distributed generation systems", *IEEE PES Innovative Smart Grid Technologies Conference Europe*, October 2010, Gothenburg, Sweden.
- [40] L.K. Kumpulainen and K.T. Kauhaniemi, "Analysis of the impact of distributed generation on automatic reclosing", In *IEEE Power Systems Conference and Exposition*, vol. 1, pp. 603-608, 2004.

- [41] O. Abarategui, I. Zamora and D.M. Larruskain, "Comparative analysis of islanding detection methods in networks with dg", in *19th international conference on electricity distribution*, May 21-24, Vienna, 2007.
- [42] S.M. Brahma and A.A. Girgis, "Microprocessor-based reclosing to coordinate fuse and recloser in a system with high penetration of distributed generation", in *IEEE Power Engineering Society Winter Meeting*, pp. 453-458, 2002.
- [43] "Protective relays application guide" 3rd edition, *GEC ALSTHOM*, Protection & Control Ltd., Stafford, UK, 1987.
- [44] I. Xyngi, A. Ishchenko, M. Popov, L. van der Sluis, "Protection and transient stability issues in medium voltage grids with distributed generation", *6th Mediterranean Conference on Power Generation, Transmission and Distribution (MEDPOWER)*, 2-5 November, 2008, Thessaloniki, Greece.
- [45] N.W. Miller, J.J. Sanche-Gasca, W.W. Price and R.W. Delmerico, "Dynamic modeling of GE 1.5 and 3.6 MW wind turbine generators for stability simulations", GE Power Systems Energy Consulting, *IEEE WTG Modeling Panel*, July 2003.
- [46] E. Yeager and J.R. Willis, "Modeling of emergency Diesel generators in an 800 MW nuclear power plant", *IEEE transactions on energy conversion*, vol. 8, no. 3, September, 1993.
- [47] Y. Zhu and K. Tomsovic, "Development of analyzing the load-following performance of microturbines and fuel cells", *Elsevier Electric Power Systems Research*, no. 62, pp. 1-11, 2002.
- [48] C.J. Mozina "Distributed generator interconnect protection practices", *IEEE Power Engineering Society Power System Conference and Exposition, 2006*.
- [49] I.Xyngi, A. Ishchenko, M. Popov, L. van der Sluis, "Transient stability analysis of a distribution network with distributed generators", *IEEE Transactions on Power Systems*, PES letter, May 2009.
- [50] I. Xyngi, A. Ishchenko, M. Popov, L. van der Sluis, "Coordination between distributed generation stability and undervoltage protection at DG interconnection point", *International Conference on Power Systems Transients (IPST)*, 3-6 June, 2009, Kyoto, Japan.
- [51] I. Xyngi, A. Ishchenko, M. Popov, L. van der Sluis, "Protection, transient stability and fault ride-through issues in distribution networks with dispersed generation, *43rd International Universities Power Engineering Conference (UPEC)*, 1-4 September, 2008, Padova, Italy.

- [52] European standard, prEN 50438, "Requirements for the connection of micro-generators in parallel with public low voltage distribution networks, Cenelec.
- [53] E. Coster, A. Ishchenko, J.M.A. Myrzik, W.L. Kling, "Comparison of practical fault ride-through capability for MV-connected DG-units", *Power System Computations Conference (PSCC)*, Glasgow, Scotland, July 2008.
- [54] E.on Netz, "Grid code for high and extra high voltage". August 2003.
- [55] R. Piwko, N. Miller, R. Girard, J. MacDowell, K. Clark, A. Murdoch, "Generator fault tolerance and grid codes", *IEEE Power and Energy Magazine*, vol. 8, no. 2, pp. 18-26, March-April 2010.
- [56] D. Hou, D. Dolezilek, "IEC 61850-what it can and cannot offer to traditional protection schemes". Available: <http://www.selinc.com/techpprs.htm>
- [57] G.W. Scheer, D.J. Dolezilek, "Selecting, designing and installing modern data networks in electrical substations", Available: <http://www.selinc.com/techpprs.htm>.
- [58] International standard of IEC61850, First Edition.
- [59] T.S. Sidhu, P.K. Gangadharan, "Control and automation of power system substation using IEC 61850 communication", *Proceedings of IEEE Conference on Control Applications*, 2005.
- [60] I. Xyngi, M. Popov, "IEC61850 overview – where protection meets communication", *the IET International Conference on Developments in Power System Protection (DPSP 2010)*, 29th March – 1st April, 2010, Manchester, UK.
- [61] R.E. Mackiewicz, "Overview of IEC 61850 and benefits", *IEEE Power Engineering Society General Meeting*, 2006.
- [62] V. Skendzic, I. Ender, G. Zweigle, "IEC 61850-9-2 process bus and its impact on power system protection and control reliability", Available: <http://www.selinc.com/techpprs.htm>
- [63] V. Skendzic, R. Moore, "Extending the substation LAN beyond substation boundaries: current possibilities and potential and protection applications of wide-area Ethernet", *Proceedings of the 8th Annual Western Power Delivery and Automation Conference*, 2007. Available: <http://www.selinc.com/techpprs.htm>
- [64] K. Fodero, A. Silgado, "Protection and the communications network: can you hear me now?" Available: <http://www.selinc.com/techpprs.htm>
- [65] V. Skendzic, A. Guzman, "Enhancing power system automation through the use of real-time Ethernet", *Power Systems Conference: Advanced Metering, Protection, Control, Communication, and Distributed Resources*, 2006

- [66] A. Apostolov, D. Tholomier, "Impact of IEC 61850 on power system protection", *Power Systems Conference and Exposition*, 2006.
- [67] I. Xyngi, M. Popov, "Integrated busbar protection scheme based on IEC61850-9-2 process bus concept", *IEEE PES General Meeting*, July 25-29, 2010, Minneapolis, Minnesota, USA.
- [68] Z. Bo, "A integrated protection scheme for distribution systems based on overcurrent relay principle" *19th International Conference on Electricity Distribution (CIRED)*, 2007.
- [69] Y. Ren, J. He, Z.Q. Bo, S. Richards, A. Klimek, "Research on real time communication capacity of IEC 6850 applied in integrated protection systems", *IET 9th International Conference on Developments in Power System Protection*.
- [70] F.L. Baldinger, T. Jansen, M.J.M. van Riet, F. Volberta, F.J.T. van Erp, M. Dorgelo, W.M. van Buitenen, "Advanced secondary technology to evoke the power of simplicity", *9th IET International Conference on Developments in Power System Protection*, 2008.
- [71] M.J.M. van Riet, F.L. Baldinger, W.M. van Buitenen, F.J.T. van Erp, F. Volberta, F. Provoost, "Alternative approach for a total integrated secondary installation in MV substations covering all possible and required functions", *18th International Conference and Exhibition on Electricity Distribution*, 2005.
- [72] F.L. Baldinger, T. Jansen, M.J.M. van Riet, F. Volberta, "Nobody knows the future of Smart Grids, therefore separate the essentials in the secondary system", *10th IET International Conference on Developments in Power System Protection*, 2010.
- [73] I. Chilvers, N. Jenkins and P. Crossley, "The use of 11kV distance protection to increase generation connected to the distribution network", In *Eight IEE international conference on developments in power system protection*, 2004.
- [74] I. Chilvers, N. Jenkins and P. Crossley, "Distance relaying of 11kV circuits to increase the installed capacity of distributed generation", In *IEE Proceedings Generation, Transmission and Distribution*, vol. 152, pp. 40-46, 2005.
- [75] Z.Q. Bo, A. Klimek, X.Z. Dong, J.H. He, B.H. Zhang, "Developments of transient and integrated protection for power system", *DRPT 2008*, 6-9 April, China.
- [76] H.Y. Li, P.A. Crossley, N. Jenkins, "Transient directional protection for distribution feeders with embedded generators", *Power System Computation Conference*, 2004.

- [77] N. Perera, A.D. Rajapakse, and T.E. Buchholzer “Isolation of faults in distribution networks with distributed generators”, In *IEEE Transactions on power delivery*, vol. 23, pp. 2347-2355, October 2008.
- [78] Mesut Baran and Ismail El-Markabi, “Adaptive overcurrent protection for distribution feeder with distributed generation”, in *IEEE Power Systems Conference and Exposition*, vol. 2, pp. 715-719, 2004.
- [79] S.M. Brahma, and A.A Girgis, “Development of adaptive protection scheme for distribution systems with high penetration of distributed generation”, In *IEEE Transactions on power delivery*, vol. 19, pp. 56-63, 2004.
- [80] T. Kato, H. Kanamori, Y. Suzuoki, T. Funabashi, “Multi-agent based control and protection of power distribution system”, *International Conference on Intelligent Application to Power Systems (ISAP)*, 2005.
- [81] M.G. Adamiak, A.P. Apostolov, M.M. Begovic, C.F. Henville, K.E. Martin, G.L. Michel, A.G. Phadke and J.S. Thotp, “Wide-area protection-technology and infrastructures”, *IEEE Transactions on power Delivery*, vol. 21, April 2006.
- [82] S.H. Horowitz and A.G. Phadke, “Blackouts and relaying considerations-relaying philosophies and the future of relay systems”, *IEEE power and energy magazine*, vol. 4, no. 5, September-October 2006.
- [83] M. Prica, M. Ilic, “A novel fault-dependent-time-settings algorithm for overcurrent relays”, In *IEEE Proceedings Generation, Transmission and Distribution*, vol. 152, pp. 40-46, 2005.
- [84] I. Xyngi, M. Popov, “Power distribution protection scheme enhanced with communication”, *IEEE PES/IAS Conference on Sustainable Alternative Energy*, 28-30 September, 2009, Valencia, Spain
- [85] “SimPowerSystems User’s Guide”, *The Mathworks*, 2004.
- [86] S. Heier, “Grid integration of wind energy conversion systems”, *John Wiley&Sons*, 1998.
- [87] J.G. Slootweg, “Wind power: modeling and impact on power system dynamics”, PhD thesis, *Delft University of Technology (TUD)*, Delft, Netherlands, December 2003.
- [88] V. Akhmatov, “Analysis of dynamic behaviour of electric power systems with large amount of wind power”, PhD thesis, *Technical University of Denmark (DUT)*, Kgs. Lyngby, Denmark, April 2003.

List of articles published prior to thesis printing

1. N.H.V. Phuong, I. Xyngi, M. Popov, L. van der Sluis, "Influence of distributed generation on protection schemes of medium voltage grids", *International Conference on Power Systems Transients (IPST)*, 14-17 June, 2011, Delft, the Netherlands.
2. E.J. Coster, P. Karaliolios, I. Xyngi, J.G. Sloopweg, M. Popov, W. Kling, L. van der Sluis, "Short-circuit behavior of distribution grids with a large share of distributed generation units", *21st International Conference on Electricity Distribution (CIRED)*, 6-9 June, 2011, Frankfurt, Germany.
3. I. Xyngi, M. Popov, "Smart protection in Dutch medium voltage distributed generation systems", *IEEE PES Innovative Smart Grid Technologies Conference Europe*, October 2010, Gothenburg, Sweden.
4. I. Xyngi, M. Popov, "Integrated busbar protection scheme based on IEC61850-9-2 process bus concept", *IEEE PES General Meeting*, July 25-29, 2010, Minneapolis, Minnesota, USA.
5. I. Xyngi, M. Popov, "Transient directional busbar protection scheme for distribution networks", *the 10th IET International Conference on Developments in Power System Protection (DPSP 2010)*, 29th March – 1st April, 2010, Manchester, UK.
6. I. Xyngi, M. Popov, "IEC61850 overview – where protection meets communication", *the IET International Conference on Developments in Power System Protection (DPSP 2010)*, 29th March – 1st April, 2010, Manchester, UK.
7. I. Xyngi, M. Popov, L. van der Sluis, "Hybrid transient based protection scheme for distribution grids supplied with distributed generation", *European EMTP-ATP Users Group (EEUG) meeting*, 26-28 October, Delft, the Netherlands.
8. N. Farkhonden Jahromi, I. Xyngi, G. Papaefthymiou, M. Popov, L. van der Sluis, "An approach to the real-time power balancing for enhancing the security of electrical networks", *Proceedings of North American Power Symposium (NAPS)*, 4-6 October, 2009, Mississippi, USA.

9. I. Xyngi, M. Popov, "Power distribution protection scheme enhanced with communication", *IEEE PES/IAS Conference on Sustainable Alternative Energy*, 28-30 September, 2009, Valencia, Spain.
10. I. Xyngi, M. Popov, "Transient based protection scheme for distribution grids supplied with distributed generation", *the 44th International Universities' Power Engineering Conference (UPEC)*, 1-4 September, 2009, Glasgow, Scotland.
11. I. Xyngi, A. Ishchenko, M. Popov, L. van der Sluis, "Coordination between distributed generation stability and undervoltage protection at DG interconnection point", *International Conference on Power Systems Transients (IPST)*, 3-6 June, 2009, Kyoto, Japan.
12. I. Xyngi, A. Ishchenko, M. Popov, L. van der Sluis, "Transient stability analysis of a distribution network with distributed generators", *IEEE Transactions on Power Systems*, PES letter, May 2009.
13. I. Xyngi, A. Ishchenko, M. Popov, L. van der Sluis, "Protection and transient stability issues in medium voltage grids with distributed generation", *6th Mediterranean Conference on Power Generation, Transmission and Distribution (MEDPOWER)*, 2-5 November, 2008, Thessaloniki, Greece.
14. I. Xyngi, A. Ishchenko, M. Popov, L. van der Sluis, "Protection, transient stability and fault ride-through issues in distribution networks with dispersed generation", *43rd International Universities Power Engineering Conference (UPEC)*, 1-4 September, 2008, Padova, Italy.
15. I. Xyngi, M. Popov, L. van der Sluis, "Protection coordination analysis of distribution network with dispersed generation", *Young Researcher Symposium (YRS)*, 7-8 February, 2008, Eindhoven, the Netherlands.
16. I. Xyngi, M. Popov, L. van der Sluis, "Research in power system protection on networks supplied with embedded generation", *Young Researcher Symposium (YRS)*, 7-8 February, 2008, Eindhoven, the Netherlands.

Acknowledgements

First of all, I would like to thank my promotor Prof. ir. Lou van der Sluis for providing me an opportunity to work in the Electrical Power Systems Group of Delft University of Technology. I am grateful to my copromotor and daily supervisor Dr. Marjan Popov for his guidance, support and stimulating discussions. I appreciate the freedom I was given in making my own choices along the way.

Many thanks to all employees in the power systems group for their support. I experienced a highly stimulating and pleasant working atmosphere during these years. Special thanks to Ralph Hendriks, Arjen van der Meer, Freek Baalbergen and Gerben Hoogendorp for translating some English text to Dutch.

The research presented in this thesis was supported financially by Senter Novem in the framework of the IOP-EMVT research program (Innovatiegericht Onderzoeks-Programma ElektroMagnetische VermogensTechniek). I wish to thank the IOP-EMVT program committee members and especially Prof. ir. M. Antal and ir. G.W. Boltje.

I am grateful to all committee members for their valuable comments and suggestions regarding the thesis. In addition, I would like to thank Locamation B.V., Phase-to-Phase and Alliander for our collaboration within the project. I also thank Dr. Anton Ishchenko for our fruitful collaboration and inspiring discussions.

I wish to thank Dr. M. Reza and Dr. G. Demetriades from ABB Corporate Research Center, Västerås, Sweden for providing me a three-month position for doing research in their group.

I would like to thank my professors from the University of Patras for the education that I obtained, which was an excellent basis for fulfilling this project. Special thanks go to Dr. E. Pirgioti for her recommendation to join TU Delft.

Regarding the non-academic side of my life, I wish to thank all my friends for the time we spent together. My warmest thanks go to Alicja Lojowska for being a great friend. I enjoyed the good times we had both in and out of office as well as the serious and fun conversations. In addition, I would like to thank Alicja for helping me significantly to design the cover of this thesis.

Last but certainly not least, I address my utmost gratitude to my father Christos, my mother Zoi and my sister Evangelia for their boundless love, support, encouragement and confidence in me during these difficult, but at the same time, exciting four years.

Curriculum Vitae

Ioanna Xyngi was born on April 9, 1983 in Athens, Greece. She attended primary and high school in Aliveri (Evia), Greece. In 2000, she participated in the program ‘The Youth gets to know Europe’ of the General Secretariat of Youth as one of the 450 (out of 90.000 candidates) students with highest marks at the Pan-Hellenic entrance examinations of the Senior Grade B High School. She obtained her dipl-ing with the thesis “Development of an integrated information system for the registration and condition monitoring of HV substation equipment” from the department of Electrical and Computer Engineering of the University of Patras, Greece with an excellent GPA and was ranked 2nd in her generation. During her studies, she had been participating in the scholarship program of the State Scholarship Foundation (IKY) for her continuous ranking among the top four students in her generation. In October 2007, she was awarded with a silver wreath for the achievement of excellent academic record by the Greek Women’s Engineering Association, which is a member of the Technical Chamber of Greece. In April 2007, she joined the Electrical Power System group of the Delft University of Technology as a Ph.D researcher within the framework of the research program ‘Intelligent Power Systems’. From May to July 2010, she took sabbatical leave as a visiting scientist at ABB Corporate Research Center, Västerås, Sweden to conduct research in the field of protection of future power systems supplied with distribution generation.